

**DETERMINING THE ANTI-CANCER PROPERTIES OF ZINC AND
NOVEL QUINOXALINE DERIVATIVES ON LUNG CANCER CELLS**

By

MIXO AUNNY SIBIYA

A RESEARCH DISSERTATION

Submitted in fulfilment of the requirements for the degree of

MASTER OF SCIENCE

in

BIOCHEMISTRY

in the

FACULTY OF SCIENCE AND AGRICULTURE

(School of Molecular and Life Sciences)

at the

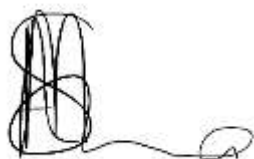
UNIVERSITY OF LIMPOPO

SUPERVISOR: PROF T.M. MATSEBATLELA

2020

DECLARATION

I, Sibiya Mixo Aunny, [REDACTED] hereby declare that this dissertation **“DETERMINING THE ANTI-CANCER PROPERTIES OF ZINC AND NOVEL QUINOXALINE DERIVATIVES ON LUNG CANCER CELLS”** submitted to the University of Limpopo for the degree of Master of Biochemistry has not previously been submitted by me or any other person to this or any institution. I further declare that this is my work and all materials contained herein has been duly acknowledged.



Signature

05 – 07 - 2020

Date

DEDICATION

I dedicate this work to my late grandfather, Elliot Madondoshi Nyakane, who believed in the empirical importance of education and hard work. He used to say that the greatest inheritance he could give his children and grandchildren was education. May this work be a resemblance of the good foundation he has laid for us. I also dedicate this work to my beloved parents, George Buti Sibiya and Dories Makgabo Sibiya, who have showed me reckless love and support towards my dreams and aspirations.

ACKNOWLEDGEMENT

I would like to give my deepest gratitude and appreciation to the following people who have made a contribution to the completion of this work:

- Prof TM Matsebatlela for his patient guidance, enthusiastic encouragement and useful critiques of this research project.
- Prof W Nxumalo and Miss LA Raphoka for synthesising the quinoxaline derivatives.
- My friend and colleague Miss DF Mangokoane and academic brother Mr RT Makola for their constant support, encouragement and assistance with laboratory techniques in order to acquire quality results.
- Dr K Poopedi for her encouragement and assistance with laboratory techniques.
- The NRF for financial support.
- My parents for the spiritual, emotional and financial support they have given.
- My friends Thuto Lowane and Nomvula Maseko for their support and encouragement.
- **Above all, praises to God for with Him everything is possible.**

TABLE OF CONTENTS

DECLARATION.....	i
DEDICATION.....	ii
ACKNOWLEDGEMENT.....	iii
TABLE OF CONTENTS.....	iiiv
LIST OF FIGURES.....	vii
LIST OF ABBREVIATIONS.....	ix
ABSTRACT.....	x
GRAPHICAL ABSTRACT.....	xii
CHAPTER 1: INTRODUCTION.....	1
1.1 Background.....	1
1.2 Zinc.....	5
1.3 Quinoxalines.....	6
1.4 Reactive oxygen species, oxidative stress and antioxidants.....	7
1.5 Role of ROS in apoptosis.....	9
1.6 Cancer and apoptosis.....	10
1.7 Lung cancer.....	14
1.8 Aims and objectives of the study.....	15
CHAPTER 2: METHODS AND MATERIALS.....	16
2.1 Preparation of treatment.....	16
2.2 Antioxidant activity.....	16
2.2.1 Ferric reducing power assay (FRAP).....	16
2.2 DPPH assay.....	16
2.2.1 Quantitative DPPH assay.....	16
2.2.2 Qualitative DPPH assay.....	17
2.3 Cell culture.....	17
2.4 Cytotoxicity and proliferation assay.....	17
2.4.1 MTT assay.....	17
2.4.2 BrdU assay.....	18
2.5 Morphological analysis.....	18
2.6 Cell staining for nuclear morphology analysis.....	19
2.7 Cell cycle analysis.....	19
2.8 Apoptosis analysis using acridine orange and ethidium bromide.....	20
2.9 Annexin V and dead cell apoptosis analysis.....	20

2.10 Oxidative stress analysis	20
2.11 Western blot.....	21
2.12 Statistical analysis	22
CHAPTER 3: RESULTS.....	23
3.1 Determination of the reducing power of quinoxaline derivatives	23
3.2 Determination of free-radical scavenging properties.....	25
3.3 Visualisation of the presence of free-radical scavenging properties	27
3.4 Determination of cell viability on Raw 264.7 cells when induced with quinoxaline derivatives and zinc.	28
3.5 Morphological changes observed on Raw 264.7 cells when induced with quinoxaline derivatives and zinc	30
.....	31
3.6 Determination of cell viability on HeLa cells when induced with quinoxaline derivatives and zinc.	32
3.7 Morphological changes observed on HeLa cells when induced with quinoxaline derivatives and zinc	34
3.8 Determination of cell viability on MCF-7 cells when induced with quinoxaline derivatives and zinc.	36
3.9 Determination of cell viability on A549 cells when induced with quinoxaline derivatives and zinc.	38
3.10 Morphological changes observed on A549 cells when induced with quinoxaline derivatives and zinc	40
3.11 Determination of cell proliferation on A549 cells induced with quinoxaline derivatives (LA-39B, LA-55), zinc and in combination.	42
3.12 Morphological changes observed on A549 cells when induced with quinoxaline derivatives (LA-39B& LA-55), zinc and in combination	44
3.13 Analysis of reduction of oxidative stress levels on Raw 264.7 cells when treated with quinoxaline derivatives (LA-39B & LA-55), zinc and in combination .	46
3.14 Analysis of reduction of oxidative stress levels on A549 cells when treated with quinoxaline derivatives (LA-39B & LA-55), zinc and in combination.....	48
3.15 Analysis of cell cycle arrest on A549 cells when treated with quinoxaline derivatives (LA-39B & LA-55), zinc and in combination	50
3.16. Apoptosis analysis through nuclear staining on A549 cells after treatment with LA-39B and LA-55.....	52
3.17 Morphological analysis of apoptosis on A549 cells when induced with quinoxaline derivatives (LA-39B & LA-55), zinc and in combination	54
3.18 Apoptosis analysis on A549 cells when induced with quinoxaline derivatives (LA-39B & LA-55), zinc and in combination	56

3.19 Bcl-2 and Bax protein ratio expression on A549 cells when treated with quinoxaline derivatives (LA-39B & LA-55), zinc and in combination	58
CHAPTER 4	60
DISCUSSION AND CONCLUSION.....	60
CHAPTER 5	68
REFERENCES.....	68

LIST OF FIGURES

Figure 1.1.i Structure of quinoxaline derivative LA-55A.....	3
Figure 1.1.ii Structure of quinoxaline derivative LA-65C3B.....	3
Figure 1.1.iii Structure of quinoxaline derivative LA-16A.....	4
Figure 1.1.iv Structure of quinoxaline derivative LA-39B.....	4
Figure 1.2 An illustration of the benefits of antioxidants in normal cells and importance of ROS in cancer cells.....	8
Figure 1.3 An illustration of the pivotal role of ROS.....	10
Figure 1.4 Mechanisms contributing to evasion of apoptosis and carcinogenesis...	13
Figure 3.1 Reducing power potential of quinoxaline derivatives.....	24
Figure 3.2 Free radical scavenging properties of quinoxaline derivatives using quantitative DPPH assay.....	26
Figure 3.3 Qualitative display of antioxidant activity of quinoxaline derivatives.....	27
Figure 3.4 Determination of cell viability on Raw 264.7 cells using MTT assay.....	29
Figure 3.5 Morphological analysis on Raw 264.7 cells.....	31
Figure 3.6 Determination of cell viability on HeLa cells using MTT assay.....	33
Figure 3.7 Morphological analysis on HeLa cells.....	35
Figure 3.8 Determination of cell viability on MCF-7 cells using MTT assay.....	37
Figure 3.9 Determination of cell viability on A549 cells using MTT assay.....	39
Figure 3.10 Morphological analysis on A549 cells.....	41
Figure 3.11 Determination of cell viability on cell proliferation on A549 cells using BrdU assay.....	43
Figure 3.12 Morphological analysis on A549 when treated with quinoxaline derivatives, zinc and in combination.....	45
Figure 3.13 Determination of reduction of oxidative stress on Raw 264.7 cells.....	47
Figure 3.14 Determination of reduction of oxidative stress on A549 cells.....	49

Figure 3.15 Cell cycle analysis on A549 cells.....	51
Figure 3.16 Nuclear analysis using Dapi and PI staining on A549 cell.....	53
Figure 3.17 AO/EB fluorescence microscopy on A549 cells.....	55
Figure 3.18 Determination of apoptosis on A549 cells using annexin V/dead cell assay.....	57
Figure 3.19 Analysis of Bcl-2/Bax ratio expression on A549 cells.....	59

LIST OF ABBREVIATIONS

LA-39B	-	3-(quinoxaline-3-yl) prop-2-ynyl methanesulphate
LA-55	-	3-(quinoxaline-3-yl) prop-2-yn-1-ol
LA-65C3	-	2-methyl-4-(quinoxaline-3-yl) but-3-yn-2-ol
LA-16A	-	3-(quinoxaline-3-yl) propionaldehyde
Zn	-	Zinc chloride
Act D	-	Actinomycin D
WHO	-	World Health Organisation
NSCLC	-	Non-small cell lung cancer
A549	-	Adenocarcinomic human alveolar basal epithelial cells cell line
Raw 264.7	-	Murine macrophage cell line
HeLa	-	Cervical cancer cell line
MCF-7	-	Breast cancer cell line
DPPH	-	2,2-diphenyl-1-picrylhydrazyl
MTT	-	3-(4,5-Dimethylthiazol-2-yl)-2,5-diphenyltetrazolium bromide
DMSO	-	Dimethyl sulfoxide
BrdU	-	Bromodeoxyuridine / 5-bromo-2'-deoxyuridine
H ₂ DCFDA	-	2',7'-dichlorodihydrofluorescein diacetate
Dapi	-	4',6-diamidino-2-phenylindole
PI	-	Propidium iodide
AO/EB	-	Acridine Orange/Ethidium Bromide
ROS	-	Reactive Oxygen Species
H ₂ O ₂	-	Hydrogen Peroxide
DR	-	Death Receptor
TNF- α	-	Tumour necrosis alpha
TRAIL	-	TNF-related apoptosis-inducing ligand

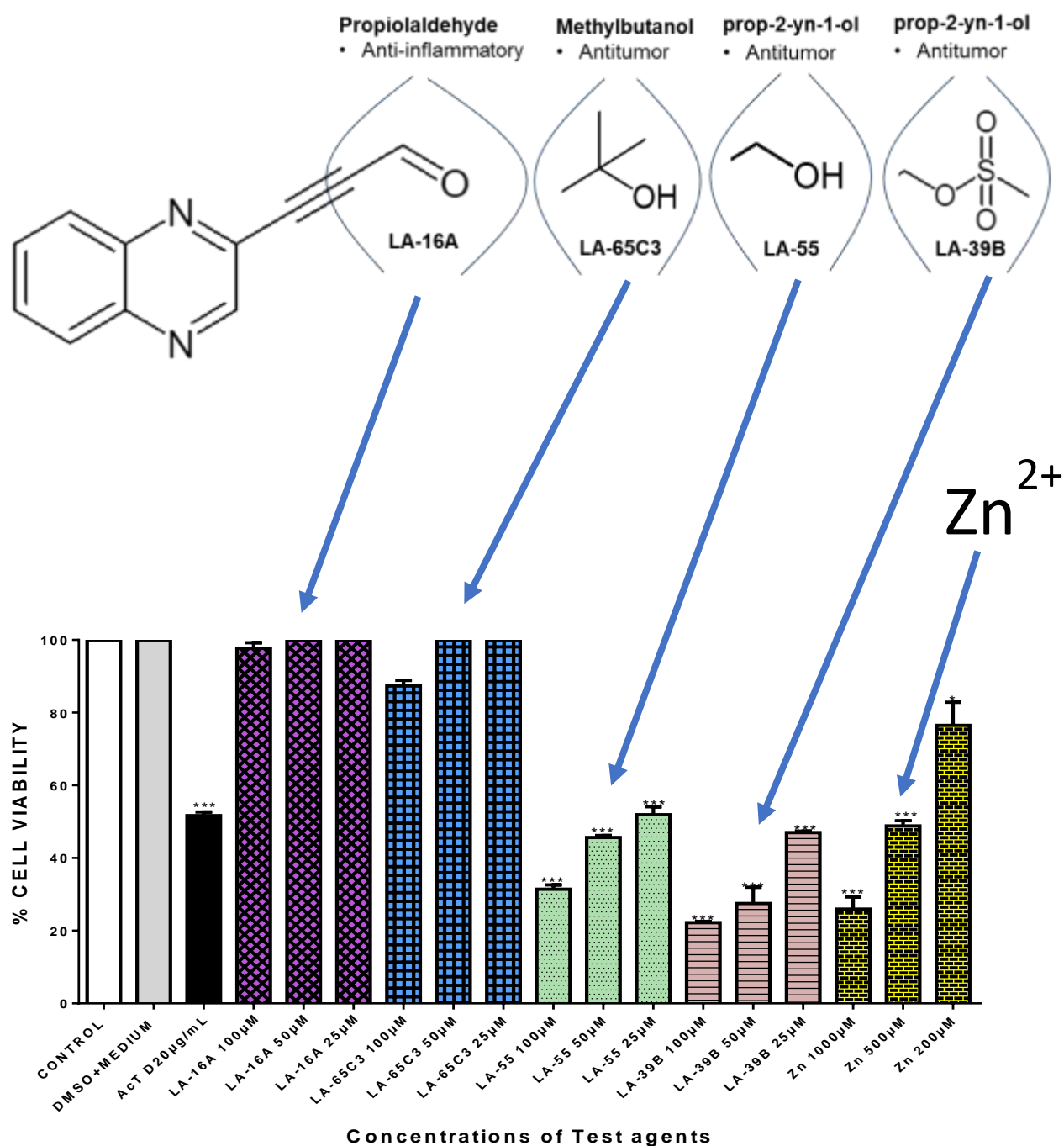
ABSTRACT

Despite major advancements in the development of various chemotherapeutic agents, treatment for lung cancer remains costly, ineffective, toxic to neighbouring normal non-cancerous cells and still hampered by high level of remissions (Wistuba *et al.*, 2018; Tana *et al.*, 2016; Schiller *et al.*, 2002). Synthesis of novel quinoxalines with a wide spectrum of biological activities has recently received considerable attention with promising anticancer drug activity since most of them do not affect non-cancerous cells and are derived from readily available less costly raw materials (Srivastava *et al.*, 2014). Since combination treatment has been shown to augment and improve single drug treatment, trace elements were employed in this study in combination with quinoxalines derivatives (Gomez *et al.*, 2016; Kocdor *et al.*, 2015; Ku *et al.*, 2012; John *et al.*, 2010; Killile and Killilea, 2007). Zinc is an essential element that is integral to many proteins and transcription factors which regulate key cellular functions such as the response to oxidative stress, DNA replication, DNA damage repair, cell cycle progression, and apoptosis (Dhawan and Chadha, 2010). Owing to the importance of these two approaches, the aim of this study was to provide *in vitro* preliminary anticancer activity data on A549 lung cancer cells using combination of zinc and quinoxaline derivatives. An assessment of the quinoxaline derivatives ferric reducing power and DPPH free radical scavenging activity was performed. The cytotoxic and anti-proliferation activity of these derivatives and zinc on cancer cell lines was determined using the MTT assay. The ability of the quinoxaline derivatives and zinc to modulate oxidative stress was evaluated using the H₂DCFDA fluorescence assay. Cell cycle arrest stages were analysed by flow cytometry through propidium iodide cell cycle analyses. The ability of the quinoxaline derivatives to induce apoptosis in cancer cells was assessed using DAPI/PI, Acridine Orange/Ethidium Bromide (AO/EB) and Annexin V-FITC/Dead Cell assays. Western blot was used to investigate the Bcl/Bax expression ratios in A549 lung cancer cells after treatment with quinoxaline derivatives, zinc and in combination.

Of the four quinoxaline derivatives tested, 3-(quinoxaline-3-yl) prop-2-ynyl methanesulphate (LA-39B) and 3-(quinoxaline-3-yl) prop-2-yn-1-ol (LA-55) produced significant anticancer properties against A549 lung cancer cells at minimal concentrations of 25µM. Both quinoxaline derivatives displayed antioxidant properties and did not induce cell death in non-cancerous Raw 267.4 macrophage cells.

Cytotoxicity was observed in A549 lung cancer, HeLa cervical cancer and MCF-7 breast cancer cells *albeit* inhibition was more pronounced in A549 lung cancer cells. Treatment of cancer cells with zinc also resulted in pronounced cytotoxicity at a minimal concentration of 25µM. Although reduced oxidative stress was observed in Raw 264.7 macrophages, in A549 lung cancer cells both compounds were able to increase ROS production which was accompanied by high levels of apoptosis when treated with derivatives and zinc alone but when in combination an improved higher level of apoptosis is observed. The improved anti-cancer activity of this drug combination treatment was further accompanied by lower Bcl/Bax expression ratios with upregulation of Bax in A549 lung cancer cells. The results of the study suggest that 3-(quinoxaline-3-yl) prop-2-ynyl methanesulphate and 3-(quinoxaline-3-yl) prop-2-yn-1-ol are potential candidates drug for treatment of lung cancer. The use of these quinoxaline derivatives in combination with zinc can offer alternative treatment options for lung cancer.

GRAPHICAL ABSTRACT



Four variations of quinoxaline derivatives were synthesized and induced cytotoxicity was observed in A549 lung cancer, HeLa cervical cancer and MCF-7 breast cancer cells *albeit* inhibition was more pronounced in A549 cells. None of the quinoxaline derivatives induced cell death or ROS production in noncancerous Raw 267.4 macrophage cells. Comparing the substitution side chains used on the quinoxaline core, the results of the study suggest that 3-(quinoxaline-3-yl) prop-2-ynyl methanesulphate (LA-39B) and 3-(quinoxaline-3-yl) prop-2-yn-1-ol (LA-55) induce apoptotic cell death in cancer cells.

CHAPTER 1: INTRODUCTION

1.1 Background

Cancer is the second top leading cause of morbidity and mortality with approximately 14 million new cases worldwide in 2012 as reported by the World Health Organization (WHO) (WHO, 2016). These statistics are expected to rise in the next coming two decades especially in the low- and middle-income countries (Ferlay *et al.*, 2012). There also a number of available treatments for lung cancer namely surgery, radiation and chemotherapy. Chemotherapy is the use of toxic drugs as a treatment of advanced cancer as a method of combination cancer cells (Wistuba *et al.*, 2018). This treatment option is coupled with a number of undesirable side effects which is due to the killing of normal body cells which affects the normal functioning of the body (Tana *et al.*, 2016; Schiller *et al.*, 2002). The treatment available remain costly, ineffective with marked relapses and presenting with vast various undesirable side effects which calls for chemistry departments in conjunction with biochemistry department to deliver a drug with minimised toxicity and increased efficacy (Bruni *et al.*, 2016; Oktay *et al.*, 2013; Parkin *et al.*, 2014). This also poses a challenge to discover a drug that will be target specific and use apoptosis instead of necrosis.

Lung cancer has become one of the most common cause of cancer-related deaths globally (Ge *et al.*, 2016; Wang *et al.*, 2016; Gesthalter *et al.*, 2017). Advancements that provide breaking ground for the treatment of NSCLC tumour have been made in terms of the molecular makeup (Wistuba *et al.*, 2018). Another advancement which was made was the classification of the type of cells affected which also adds personalisation of treatment patients with advanced lung cancer (Wistuba *et al.*, 2018).

A break-through in treatment that will target, stimulate and equip the immune system to facilitate inhibition of lung cancer progression is yet to be found. Hence this study is aimed at exploring novel quinoxalines (LA-39B and LA-55), zinc and in combination as a potential remedy for lung cancer treatment. The importance of zinc in cancer treatment was unearthed by its importance in structural stabilisation and activation of p53 (Kaur *et al.*, 2014). Quinoxaline derivatives were discovered to compose of anticancer properties as part of their biological uses (Parkin *et al.*, 2014). Quinoxalines can be manufactured at very low costs and designed to suit the type of cancer or stage

which they have to target. The ability of quinoxalines to be designed as target-specific drugs minimises cytotoxicity and thus limit undesired side effects (Patidar *et al.*, 2011).

Quinoxaline is referred to as a benzopyrazine in chemistry because it is the structure made of a benzene ring and a pyrazine ring (Srivastava *et al.*, 2014). They can also be defined by their nitrogen containing heterocyclic compounds which are capable of triggering antimicrobial activities (Ketter *et al.*, 2009). Quinoxaline derivatives have the ability to bind to the DNA which makes them one of the drugs to explore when it comes to anticancer properties (Patidar *et al.*, 2011). The quinoxaline derivative LA-39B scientific name is 3-(quinoxalin-3-yl) prop-2-ynyl methanesulfonate and LA-55 scientific name 3-(quinoxalin-3-yl) prop-2-yn-1-ol. It is composed of a quinoxaline which has pyrazine granting it the ability to bind to DNA and interfere with replication. It also has an aromatic group with free radical scavenging activity and can also chemically interact with many other substances. Aromatics easily form adduct ions with halogens, participating immensely in the oxidation reactions and oxidative stress. On the onset of lung cancer, there is an increase in oxidative stress which causes, inflammation damage to the cells and causing an imbalance in most of the crucial proteins involved in homeostasis. An imbalance in apoptosis-related genes is affected along with the oxidation and anti-oxidation process may play a central role in the pathogenesis of lung cancer thus providing a therapeutic drug target for lung cancer treatment (Akhtar *et al.*, 2017; Wong, 2011).

Along these lines, a new cohort of targeted quinoxaline derivatives have been synthesised in the local chemistry department at the University of Limpopo and will be screened against lung cancer. In this cohort, various unique variations were made to the quinoxaline benzopyrazine core ring in pursuit of a more effective way of inhibiting lung cancer progression (figures 1.1.i-1.1.iv).

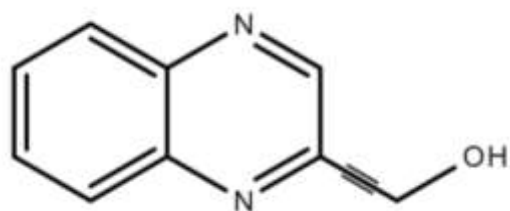


Figure 1.1.i Structure of quinoxaline derivative LA-55

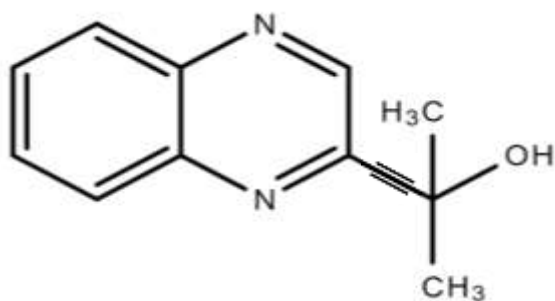


Figure 1.1.ii Structure of quinoxaline derivative LA-65C3

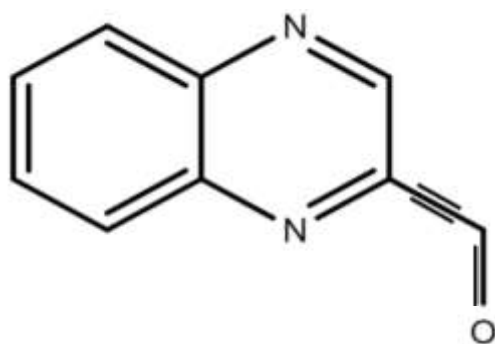


Figure 1.1.iii Structure of quinoxaline derivative LA-16A

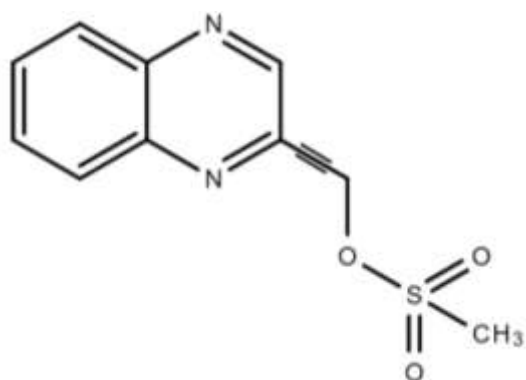


Figure 1.1.iv Structure of quinoxaline derivative LA-39B

To attain a new cohort of candidate anticancer drugs in this study, four slight variations were made on the side chains attached to the benzopyrazine core group. In the first quinoxaline derivative designed (figure 1.1.i), 3-(quinoxalin-3-yl)prop-2-yn-1-ol (LA-55), the prop-2-yn-1-ol side chain was incorporated as in several anticancer agents wherein anti-proliferative effects have been observed (Ketter *et al.*, 2009) by targeting microRNA-21 and reversing phenotypes in cancer cells (Patidar *et al.*, 2011). In the second quinoxaline derivative (figure 1.1.ii), 2-methyl-4-(quinoxalin-3-yl)but-3-yn-2-ol (LA-65C3), the 2-methyl-4-but-3-yn-2-ol group is attached to the benzopyrazine core. The 2-methyl-4-but-3-yn-2-ol group has been shown to inhibit Akt kinase and exhibit antitumor activities (Murthi *et al.*, 2015). In the third quinoxaline derivative (figure 1.1.iii), 3-(quinoxalin-3-yl)propiolaldehyde (LA-16A), a propanal or propiolaldehyde group is attached to the benzopyrazine core group. Propanal groups are known to carry potent anti-inflammatory activities (Velagapudi *et al.*, 2018). In fourth quinoxaline derivative (figure 1.1.iv), 3-(quinoxalin-3-yl)prop-2-ynyl methanesulfonate (LA-39B), a methanesulfonate group is attached. Methanesulfonates are known to cause hyperacetylation of histone deacetylase inhibitors thereby increasing susceptibility to cancer cell death (Rhodes *et al.*, 2008). The four variations made on the side chains attached to the quinoxaline core structure were aimed at searching for more potent forms of the envisaged candidate molecules. The mode of action of each of the quinoxaline derivatives is yet to be determined as these are newly synthesized novel molecules.

1.2 Zinc

Zinc is an essential component that is required in diet, which functions as a catalytic or regulatory component that aids in various structural integrities of many proteins and modulation of protein-protein interaction (Gibson *et al.*, 2016; Gomez *et al.*, 2016 and Maywald and Rink, 2015). It is required in the daily diet at 15mg/day (Gibson *et al.*, 2016). It is viewed significantly non-harmful metal to humans and the body contains an aggregate sum of 2-4g zinc (Haase and Rink, 2010; Beraldo and Gambinob, 2004). Zinc plays a role in the promotion of constant maintenance of the high turnover of immune cells through elevation of cell proliferation and in junction to this, it also plays a role in the apoptotic process (Maywald and Rink, 2015; Dhawan and Chada, 2010).

The importance of zinc is displayed in the apoptotic process where it is considered an essential component. This feature is conveyed by its role in structural stabilization and activation of p53 (Dhawan and Chada, 2010). The decrease in levels of zinc has been associated with the development and progression of prostate cancer and lung cancer (Ku *et al.*, 2012; Song *et al.*, 2009; Gomez *et al.*, 2006). While the increase in intracellular zinc shows an inhibition of prostate cancer cells proliferation, which has been discovered to be due to the induction of apoptosis (Ku *et al.*, 2012; Feng *et al.*, 2002).

Research reveals that the increase in oxidative stress observed when cancer cells were treated with zinc induced apoptosis (Banerjee *et al.*, 2017; Liu *et al.*, 2013; Ott and Gust, 2007). Chemotherapeutic agents' mode of action is primarily through DNA damage, inhibition of cancer cell proliferation and ultimately induction of apoptosis (Moucheron, 2009; Tan *et al.*, 2009; Maheswari *et al.*, 2007). Taxane which as a primary chemotherapeutic agent for non-small cell lung cancer (NSCLC) has not had a satisfactory prognosis thus research is using zinc combination to other potent chemotherapeutic regimens where it has been reported to increase the levels of efficacy (Gomez *et al.*, 2016; Kocdor *et al.*, 2015; Ku *et al.*, 2012; John *et al.*, 2010; Killile and Killilea, 2007).

1.3 Quinoxalines

A quinoxaline is referred to as a benzopyrazine in chemistry because its structure is made of a benzene ring and pyrazine ring (Srivastava *et al.*, 2014). In the pharmacological industry they have become of great interest due to their ability to inhibit metal corrosion which also makes it of interest in the organic and pharmaceutical chemistry industry (El Adnani *et al.*, 2012; Kabanda *et al.*, 2012). Quinoxaline core structure is found in a number of natural pharmaceutical drugs such as vitamins, biomolecules and biological active compounds (Maddila *et al.*, 2015).

The quinoxaline heterocyclic structure comprised of a nitrogen atom which replaces one or more carbon atoms (Srivastava *et al.*, 2014). The 6-membered aromatic heterocyclic compound that contains two nitrogen atoms such as quinoxalines are known for their broad-spectrum biological properties (Jadhavar *et al.*, 2014; Jaso *et al.*, 2005). Amongst its versatile biological activities, it includes anticancer, antimicrobial, antiprotozoal, antiviral, anti-inflammatory, antidepressant, antioxidant,

etc. (Kailasam *et al.*, 2018; Tariq *et al.*, 2018; Galal *et al.*, 2013). The presence of a pyrazine ring grants the quinoxaline the ability to bind to DNA and interfere with replication. It also has an aromatic group with free radical scavenging activity and can also chemically interact with many other substances. Aromatics easily form adduct ions with halogens.

Over the past thirty years, there has been an advent improvement in antitumor agents. Despite this improvement, chemotherapeutic agent available still lacks good prognosis, selectivity and target specificity which is coupled with debating side effects (Kailasam *et al.*, 2018). This remains a driving force for more research to be done in alignment to these loop holes. Quinoxaline derivatives provide infinite possibilities that allows the discovery of chemotherapeutic agents that addresses these loop holes. Research shows that modification of quinoxaline derivatives enriches its biomedical applications (Pereira *et al.*, 2015).

1.4 Reactive oxygen species, oxidative stress and antioxidants

One of the contributing factors to the maintenance of homeostasis is the balance between oxidative stress and antioxidation” (Akhtar *et al.*, 2017). Oxidative stress can be defined as “the damaging outcome of greater oxidants that occur with the cell as compared to antioxidants” (Akhtar *et al.*, 2017). It can also be defined as “the imbalance between the production of free radicals and the ability of the cell to counteract their harmful effects (neutralization via antioxidants)” (Chio and Tuveson, 2017). Reactive oxygen species (ROS) can be broadly defined as oxygen containing molecular species which are highly reactive such as peroxides, superoxide and hydroxyl” (Walton, 2016; Dickinson and Chang 2011). Antioxidants are defined as “any substance that when present at low concentration compared with that of an oxidizable substrate, significantly delays or prevents oxidation of that substrate” (Halliwell and Gutteridge, 1999).

When normal cells undergo oxidative stress due to the increase in ROS levels, the cell becomes prone to carcinogenesis, neurodegeneration, aging, atherosclerosis and diabetes (Haigis and Yankner, 2010; Andersen JK, 2004; Cross *et al.*,1987). High levels of ROS are considered to play a crucial point accountable for malignant cell proliferation and a notable signalling molecule in carcinogenesis (Liou and Storz, 2010). High levels of ROS play a role in the damage of lipids, DNA and proteins

(Walton, 2016). The is down regulation of proteins such as p53 which play a major role in apoptosis (Sablina *et al.*, 2005).

Hence, the maintenance of a healthy biological system is vital. To maintain a healthy biological system, a balance between oxidation and antioxidation has to exist (Akhtar *et al.*, 2017). When the is an imbalance wherein the is less antioxidants, this leads to the increase in ROS levels which causes an irreversible damage to lipids, DNA and proteins (Walton, 2016; Poljsak *et al.*, 2013). This goes to show that endogenous antioxidants alone are not sufficient enough to maintain a healthy system hence a need for exogeneous antioxidants that will aid in the maintenance of a healthy system. As depicted in figure 1.2, in contrast to what is originally known about ROS and oxidative stress, modern cancer therapies use this knowledge in order to combat cancer through the modulation of ROS (Yoshihiro *et al.*, 2014).

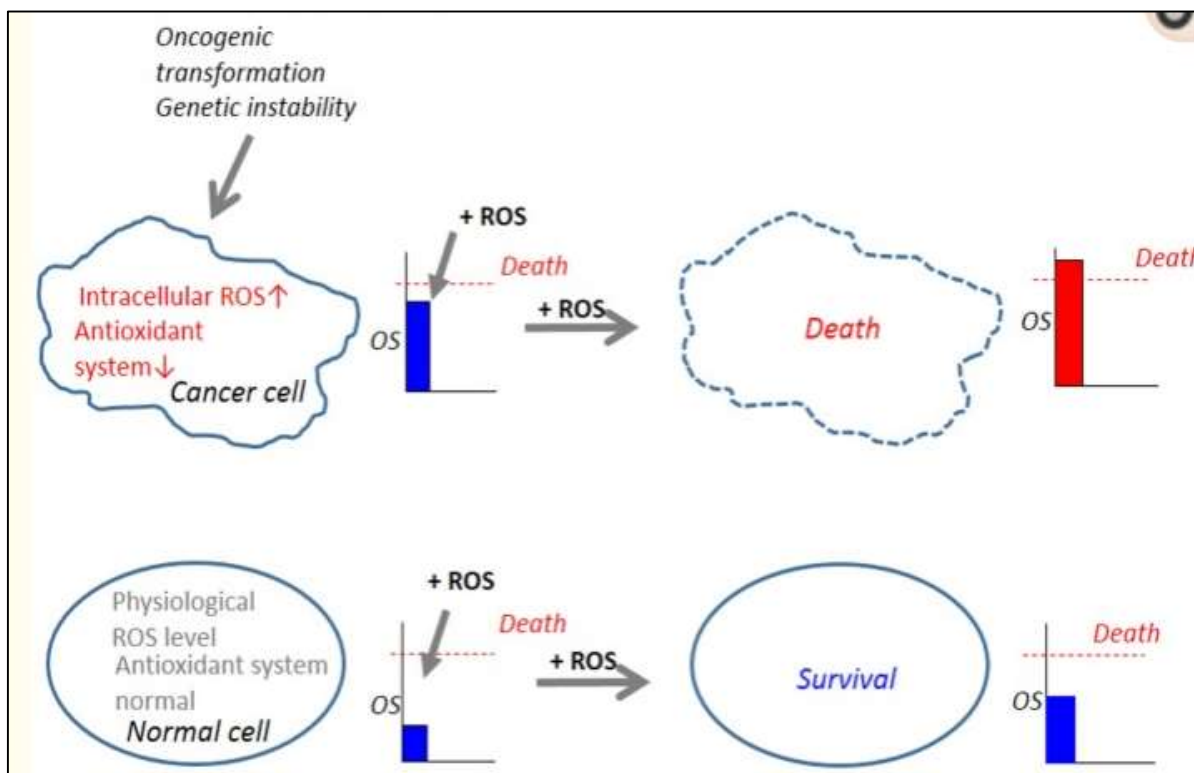


Figure 1.2 An illustration of the benefits of antioxidants in normal cells and importance of ROS in cancer cells. antioxidants lead to the decrease in ROS when maintaining cellular health with consequent cell survival. The increase in ROS in cancer cells lead to the ultimate death (Yoshihiro *et al.*, 2014).

1.5 Role of ROS in apoptosis

Ideal working antitumor agents are presumed to be exceedingly efficient against malignant cells with no toxicity against normal cells. Treatment regimen that are available in the market lack preferential killing towards malignant cells while giving a protective effect towards normal cells. A new angle in research is using the knowledge of the mechanism of ROS in their active metabolism and carcinogenesis that is, most tumour cells display high levels of ROS which activates and deactivates various gene expressions thus causing normal cells vulnerable to carcinogenesis (Magdalena and Tak, 2010) (figure 1.3).

As a way of cleaning out defective cells, apoptosis is the most preferential pathway especially cancerous cells (Tanga *et al.*, 2018; Yen *et al.*, 2015; Raj *et al.*, 2011). Recently there is an ongoing research on drugs that have the ability to modulate ROS in order to initiate apoptosis. As ground work, normal cells may endure with drug-induced ROS stress however the endurance of redox homeostasis on cancerous cells are tremendously lower than in normal cells thus leading to the induction of cell death in cancerous cells (Trachootham *et al.*, 2009). In line to this advantageous ROS modulation factor it shelters a customary strategy for preferential anticancer effect (Raj *et al.*, 2011; Nicco *et al.*, 2005).

ROS damages a number of macromolecules, damages cellular function, and induce apoptosis or necrosis through the involvement of death receptors (DR) ligands (Circu and Aw, 2010). DR ligands such as tumour-necrosis factor alpha (TNF- α) and Fas (known as apoptosis antigens) (Kim *et al.*, 2007; Reinehr *et al.*, 2005; Sato *et al.*, 2004). TRAIL have shown to increase ROS such as H₂O₂ in which some research the results have shown that its direct application may induce apoptosis in some cell lines (Tochigi *et al.*, 2013; Pallepati and Averill-Bates, 2011). These findings add a breaking ground to the importance of ROS as mediators of death ligand-induced apoptosis. In cancer, the p53 gene is one of the most mutated genes which is modulated by ROS and most cancer treatments aim at reactivating this gene in order to up-regulate it and induce apoptosis. A study done on APR-246 has shown that this drug has the ability to reactive p53 through the modulation of ROS which contributed to its anticancer properties (Ali *et al.*, 2016; Mohell *et al.*, 2015; Tessoulin *et al.*, 2014; Gorrini *et al.*, 2013).

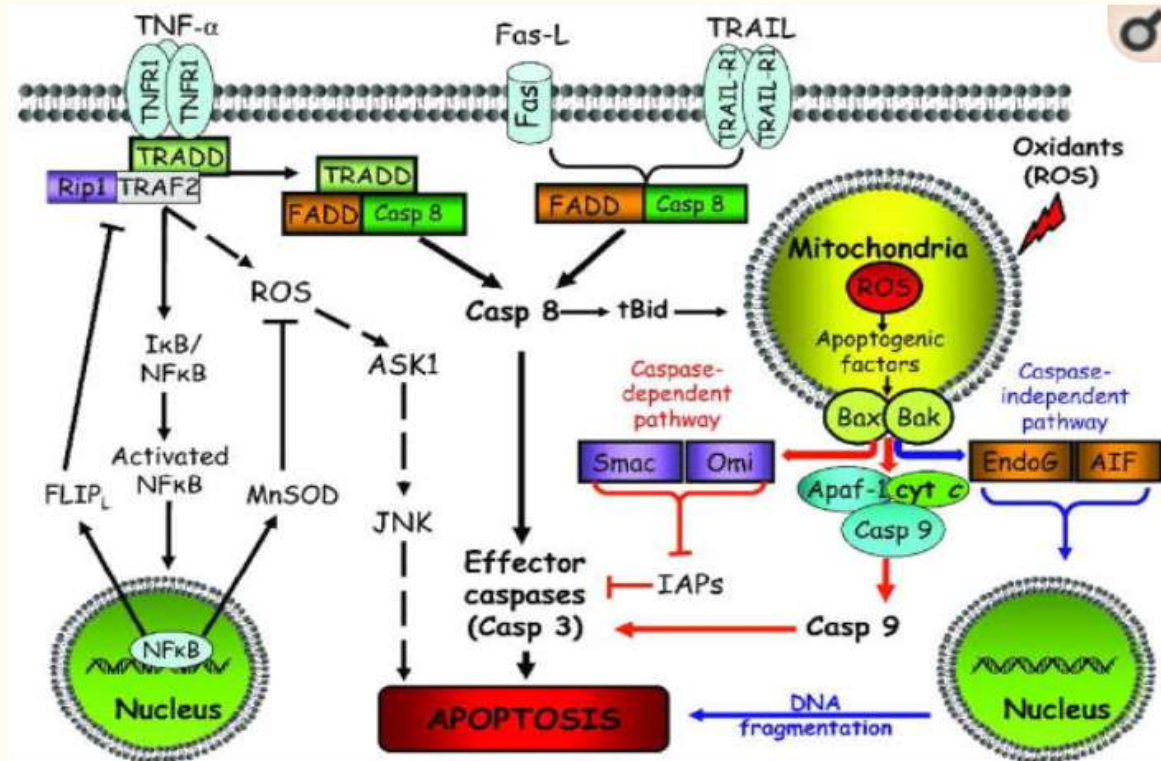


Figure 1.3 An illustration of the pivotal role of ROS. The increase in ROS can lead to the damage of molecules such as lipids, DNA and proteins which ultimately leads to mutation to p53 and activation of TNF- α and Fas which may cause necrosis contributing to the build-up of ROS. The introduction of an ideal drug can be able to neutralize ROS and also activate gene expression that will activate pro-apoptotic genes which promote apoptosis (Magdalena and Tak, 2010).

1.6 Cancer and apoptosis

Carcinogenesis arises from the loss of balance between cell death and cell division, whereby there is a shutdown in the cell death mechanism. Cell death can be achieved through necrosis or apoptosis. Apoptosis is the healthy pathway of cleaning out unhealthy cells, in which the cellular contents are not disposed outside rather contained within the cell while necrosis causes disposal of cellular contents thus

causing inflammation. Apoptosis can be described as “programmed cell death, which is highly regulated and controlled process essential for organisms to remove the damaged, dysfunctional, or excess cell” (Jacobson *et al.*, 1997).

Morphological changes in cells undergoing apoptosis can be observed in the nucleus and cytoplasm which allows recognition by phagocytic cells (Wong, 2011, Kumar *et al.*, 2010). In the early stages of apoptosis, the expression of phosphatidylserine (PS) is observed on the cell membrane which is flipped inside out allowing recognition by phagocytic cells such as macrophages (Hengartner, 2000). Breakdown of the DNA into large 50-300 kilobase pieces is then subsequent (Vaux and Silke, 2003). The breakdown of the DNA can be initiated by an intrinsic (mitochondrial) or extrinsic (DR) pathway (Wong, 2011).

The intrinsic pathway is guided by proteins such as B-cell lymphoma-2 (Bcl-2) family which is composed of both anti-apoptotic (Bcl-2 & Bcl-xL) and pro-apoptotic (Bax, Bad, Bid and Bim) (Johnstone *et al.*, 2002). The anti-apoptotic proteins regulate the apoptosis process by inhibiting the mitochondrial release of cytochrome c, while the pro-apoptotic proteins regulate the process by promoting the release of cytochrome c (Saraste and Pulkki, 2000). Another major protein which is involved is the p53. The Bcl-2 family and p53 function through the control of the mitochondria which is known as the power house of the cells; Wang, 2001; Hengartner, 2000). The Bcl-2 family regulates the release of cytochrome c which will bind to Apaf1 and form activated caspase 9 complex which also functions through the mitochondrial apoptosis (Ashkenazi A, 2015).

The pivotal role of Bcl-2 family which contains the pro- and anti-apoptotic proteins is crucial in the regulation of apoptosis in the intrinsic pathway (Minn *et al.*, 1997). The loss of balance between these two proteins in the Bcl-2 family has been shown to result in disease development. Raffo *et al* discovered that high expression of Bcl-2 resulted in the inhibition of apoptosis in neuroblastoma, glioblastoma and breast carcinoma cells (Raffo *et al.*, 1995).

This high expression of Bcl-2 has also been reported in multi-drug resistant cancer cells through the inhibition of apoptosis (Minn *et al.*, 1995). In colorectal cancer, a mutation in the Bax gene was reported which resulted in under expression and failure to promote apoptosis leading to its resistance to anticancer treatment (Miquel *et al.*,

2005). In chronic lymphatic leukaemia (CLL), Pepper *et al* reported an imbalance in the Bcl-2/Bax ratio in patient when B-lymphocytes were cultured the results showed that the Bcl-2/Bax ratio was inversely proportional related to the drug induced apoptosis (Pepper *et al.*, 1997).

One of the well documented tumour suppressor proteins is p53 which is encoded by the TP53 gene and earned its name because of its molecular weight of 53KDa (Levine *et al.*, 1991). The inheritance of this mutant gene leads to a condition known as Li-Fraumeni syndrome (Varley, 2003). Mutation of this gene has been identified in a number of malignancies, lung cancer included (Hainaut and Pfeifer, 2016). P53 is one of the crucial proteins which play a role in the maintenance of homeostasis through the regulation of apoptosis thus impact carcinogenesis (Berkers *et al.*, 2013). In the maintenance of homeostasis, p53 works alongside with the pro-apoptotic Bcl-2 family such as Bax. It interacts with these proteins directly in the cytoplasm or on the outer membrane of the mitochondria in order to regulate their response to stimuli (Labuschagne *et al.*, 2018).

The pro-apoptotic family Bcl-2 family is also able to regulate p53 which was reported in a study done on Pin-1 where the enhanced functioning of p53 depended on Bax activation for its translocation to the mitochondria for the triggering of apoptosis (Castrogiovanni *et al.*, 2018; Follis *et al.*, 2015). When cellular stress is detected, p53 initiates an assessment on the G₁-S phase checkpoint to prevent the cell from proceeding with mitosis, which then initiates a transient to cell-cycle arrest (Berkers *et al.*, 2013). The promotion of anti-apoptotic proteins in the Bcl-2 family and p53 while inhibiting the pro-apoptotic Bcl-2 family, makes it a target for anti-cancer treatment (figure 1.4).

The balance between the two determines the activation of apoptosis (Saraste and Pulkki, 2000). The extrinsic pathway involves the commonly known DR which are TNF receptor and Fas (CD95). These DR have intracellular mediators/ domains which they activate to initiate cell death. The TNF has TNF-receptor-associated domain (TRADD) while the Fas has Fas-associated death domain (FADD). Once the DR binds to their domains they form a protein complex known as death- inducing signalling complex (DISC) (O'Brien and Kirby, 2008). The DISC then activates pro-caspase 8 which then initiates apoptosis process (Schneider and Tschopp, 2000).

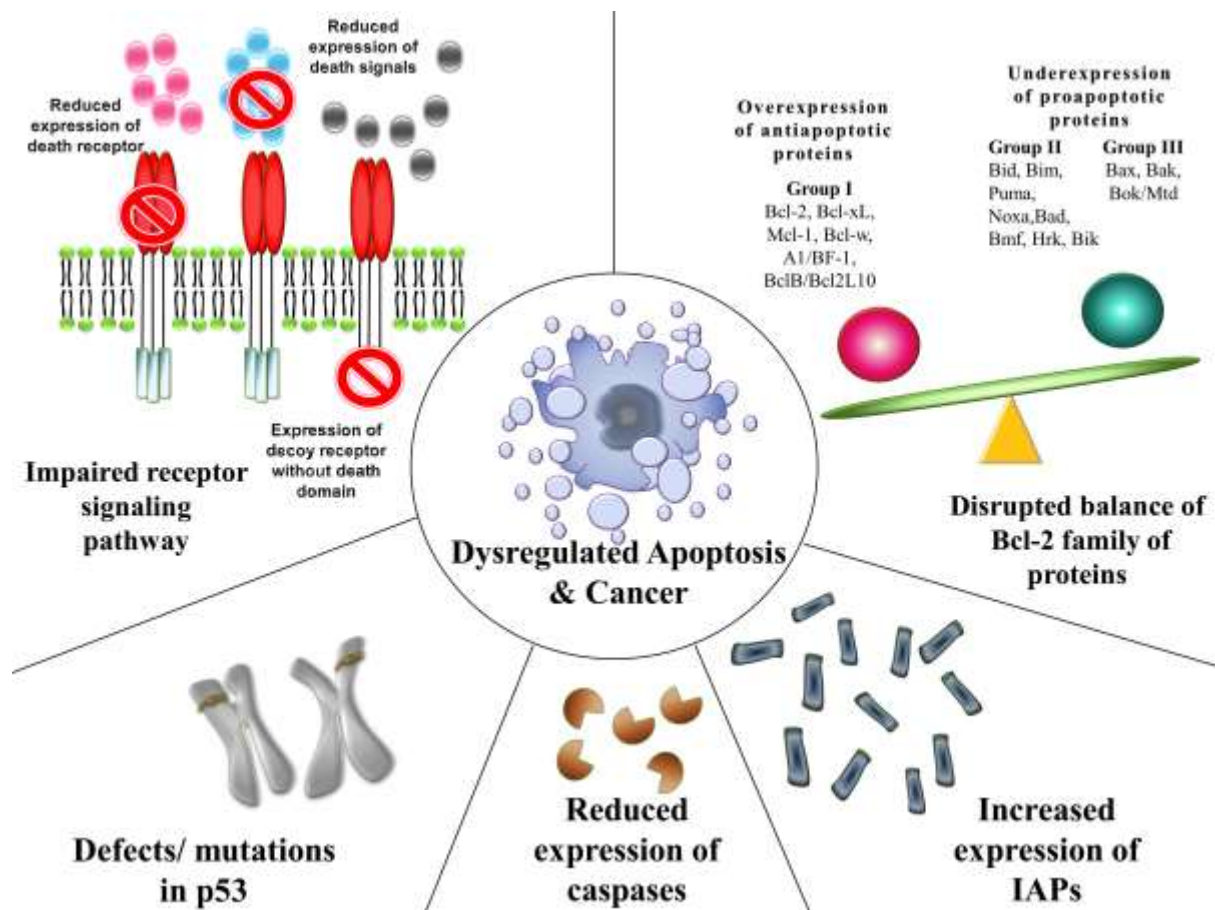


Figure 1.4 Mechanisms contributing to evasion of apoptosis and carcinogenesis (Wong, 2011).

Defects may occur in the DR and their ligands involved in signalling and this would affect the transmission of messages that have to initiate cascade activities required to activate apoptosis (Lavrik *et al.*, 2005). Defects may involve downregulation of the receptors or dysfunction of receptors involving the mode of action of apoptosis (Wong, 2011). Downregulation of the expression of CD95 was reported in treatment-resistant leukaemia and neuroblastoma cells (Fulda *et al.*, 1998; Friesen *et al.*, 1997). The role of the poor expression of DR and defective expression of decoy receptors on the membrane has been reported in various cancers. Reesink-Peter *et al.* has reported that the loss of Fas and dysregulation of FasL and tumour necrosis factor-related had an effect on apoptosis-inducing ligands and were observed in cervical intraepithelial neoplasia which led to its carcinogenesis (Reesink-Peters *et al.*, 2005).

1.7 Lung cancer

Of all cancers, lung cancer has become one of the most common cause of cancer-related deaths globally (Ge *et al.*, 2016; Wang *et al.*, 2016; Gesthalter *et al.*, 2017). Advancements that provide breaking ground for the treatment of NSCLC tumour have been made in terms of the molecular makeup (Wistuba *et al.*, 2018). Another advancement which was made was the classification of the type of cells affected which also adds personalisation of treatment patients with advanced lung cancer (Wistuba *et al.*, 2018).

Lung cancer is categorised in terms of its histological features, which are non-small cell lung cancer (NSCLC) which accounts for 85% of lung cancer cases and small-cell lung cancer (SCLC) which accounts for 15% of lung cancer cases (Weili *et al.*, 2016). NSCLC is further divided into squamous cell carcinoma, adenocarcinoma and large cell carcinoma (Petersen, 2011). Lung cancer is commonly associated with smoking although a significant proportion (15%) occurs in amongst never smokers, who commonly acquire adenocarcinoma histology (Wistuba *et al.*, 2018).

Lung tumorigenesis occurs through a number of steps where normal cells evolve from the accumulation of various genetic and epigenetic abnormalities (Petersen, 2011). Biomarkers for NSCLC has been identified mainly as epidermal growth factor receptor (EGFR) mutations and anaplastic lymphoma kinase (ALK) rearrangement which commonly present themselves as “echinoderm microtubule-associated protein-like 4-anaplastic lymphoma kinase”(EML4-ALK) combination oncogenes (Gerber, 2008). Amongst other mutant genes in NSCLC is the mutation is the p53 in which the is dysregulation (Jaaks and Bernasconi, 2017).

An increase in the levels of ROS has been identified in the progression of lung cancer and associated with tumour development and metastasis (da Motta *et al.*, 2014). A study done by Gupta *et al* discovered that oxidative stress improved the efficiency of the treatment and survival of lung cancer patients (Jaaks and Bernasconi, 2017). This discovery makes it a target for lung cancer treatment in which a treatment which possesses the potency to modulate ROS in NSCLC will enhance its prognosis.

1.8 Aims and objectives of the study

Aim

This study aims at exploring the potential anticancer properties of novel quinoxaline derivatives and zinc on various cancer cell lines and non-cancerous Raw 264.7 cells.

Objectives

The objectives of this study were to determine:

- I. Antioxidant properties of quinoxaline derivatives using ferric reducing power assay and DPPH free-radical scavenging activity assay.
- II. The effect of quinoxaline derivatives and zinc on viability and morphology of HeLa, MCF-7, A549 and Raw 264.7 cells using MTT assay and light microscopy.
- III. The ability of quinoxaline derivatives and zinc to inhibit cell proliferation using the BrdU incorporation assay.
- IV. Modulation of oxidative stress by quinoxaline derivatives in cancer cells and Raw 264.7 cells.
- V. Nuclear integrity through fluorescence staining using Dapi and PI after treatment of cells with quinoxaline derivatives and zinc.
- VI. Ability of quinoxaline derivatives and zinc to inhibit cell cycle progression using the Muse™ flow cytometry assay.
- VII. Induction of apoptosis in cancer cells using the annexin V/dead cell assay and acridine orange/ethidium bromide assay after treating cells with a combination of quinoxaline derivatives and zinc.
- VIII. Regulation of apoptotic proteins (Bax & Bcl-2) using western-blot after treating cells with quinoxaline derivatives and zinc.

CHAPTER 2: METHODS AND MATERIALS

2.1 Preparation of treatment

Quinoxaline derivatives were obtained from the University of Limpopo, chemistry department. They were dissolved in dimethyl sulfoxide (DMSO Hybri Max[®] purchased from Sigma) to various stock concentrations depending on amount obtained. They were further diluted in culture medium to various concentrations. Zinc chloride was purchased from Rochelle Chemicals It was dissolved in distilled water to a final stock concentration of 500mM. It was further diluted in cell culture medium to various concentrations.

2.2 Antioxidant activity

2.2.1 Ferric reducing power assay (FRAP)

This assay is principled on the ability of antioxidant containing compound to react with Potassium Ferricyanide to form Ferrocyanide. This will then react with ferric chloride to form ferrous complex that has absorption maximum at 700nm. Antioxidant activity of quinoxalines was assessed following the ferric reducing power assay protocol. Briefly, 100µL of quinoxaline derivatives and ascorbic acid at different concentrations were prepared. Water was used as a blank. Phosphate buffer (250µL) and potassium ferricyanide (250µL) were added to the 100µL of quinoxaline derivatives, ascorbic acid and water, then incubated for 20 minutes at 50°C. trichloroactetic acid (250µL) was added to the mixture then vortex mixed for 30 seconds. From the mixture, 250µL was aliquoted into a new test tube and freshly prepared ferric chloride (250µL) was added. Absorbance was measured at 700nm using a GloMax-Multi microplate reader (Promega, USA). To calculate the percentage of reducing power the following formula was used:

$$\% \text{ increase in reducing power} = \frac{A_{test}}{A_{blank}} - 1 \times 100$$

2.2 DPPH assay

2.2.1 Quantitative DPPH assay

The principle of the assay is based on the ability of antioxidant containing compounds to scavenge free radicals from DPPH thus converting purple coloured DPPH to yellow colour. The absorbance is then measured at 517nm which is in the range for the purple colour. Briefly, 300µL of various concentrations of quinoxaline derivatives were prepared at various concentrations. Ascorbic acid was used as a standard with

correlating concentrations to quinoxalines and water as a blank/control and 100µL of 0.4mM DPPH in methanol was then added then incubated for 30 min in the dark. Absorbance was then measured at 517nm using GloMax-Multi microplate reader (Promega, USA). To calculate the percentage of inhibition the following formula was used:

$$\% \text{ Inhibition} = \frac{A_{blank} - A_{test}}{A_{blank}} \times 100$$

2.2.2 Qualitative DPPH assay

This assay is based on the ability of compounds with antioxidant activity to scavenge free-radical molecules from DPPH (2,2-diphenyl-1-picrylhydrazyl) which is observed by development of colour on purple background. Briefly, 10µL of quinoxaline derivatives, ascorbic acid as a standard and water as blank\control were dot blotted on Merk silica gel F₂₅₄ plates. They were allowed to dry then sprayed with 0.4mM DPPH solution in methanol.

2.3 Cell culture

Raw 264.7 macrophage cells, lung cancer A549 cells, breast cancer cells MCF-7 and cervical cancer HeLa cells were obtained from ATCC. The cells were maintained at 37°C, in a humidified 95% air and 5% CO₂ environment in cell culture flasks. Raw 264.7 cells and A549 cells were proliferated in RPMI-1640 culture medium supplemented with 10% FBS, 2 mM L-glutamine and 1x penicillin, streptomycin and neomycin mixture (PSN). Cervical cancer HeLa and breast cancer MCF-7 cells were obtained from ATCC. The cells were maintained under the same conditions but proliferated in DMEM medium supplemented with 10% FBS, 2 mM L-glutamine and 1x penicillin, streptomycin and neomycin mixture (PSN). Cell density was determined by diluting cells with 10x trypan blue dye then counted using a Life technologies countess II FL.

2.4 Cytotoxicity and proliferation assay

2.4.1 MTT assay

Cell viability was determined using MTT [3-(4,5-Dimethylthiazol-2-yl)-2,5-diphenyltetrazolium bromide] assay which is principled on the ability of mitochondrial succinyl dehydrogenase of viable cells to convert soluble yellow tetrazolium salt into an insoluble formazan product (Plumb *et al.*, 1989). Briefly, cells (Raw 264.7, A549,

Hela or MCF-7) were seeded at a density of 1×10^6 in a 96 well-plate and incubated overnight. Cell were then treated with various concentrations of quinoxaline derivatives (25 μ M, 50 μ M, 100 μ M and 200 μ M), zinc chloride (200 μ M, 500 μ M and 1000 μ M), 0.5% DMSO in culture medium and 20 μ g/ml actinomycin-D (ActD) (Sigma Aldrich, USA) for 24 hrs. Prior to the addition of MTT reagent, cell imaging was conducted. MTT of 5mg (Sigma Aldrich, USA) was added and again for 4 hrs. Upon incubation, medium was aspirated then 100 μ L DMSO was added and incubated in the dark for 30 min. Absorbance was the measured at 570nm using GloMax-Multi microplate reader (Promega, USA).

2.4.2 BrdU assay

This ELISA assay is based on the ability of viable, proliferating cells to incorporate BrdU in which the antibody will also be incorporated. The substrate will then bind to the antibody to produce a blue colour which dead cells are unable to (Lehner *et al.*, 2011). Cell proliferation ELISA, BrdU [colorimetric] (Roche) kit was used. Briefly, cells were seeded at a density of 1×10^6 in a 96 well-plate overnight. They were then treated with the test compounds namely, quinoxaline derivatives at 25 μ M, zinc 500 μ M, combination (quinoxaline derivatives 25 μ M + zinc 500 μ M), 0.5% DMSO in medium and Actinomycin D (20 μ g/mL) with a final volume of 100 μ L for 24 hrs. BrdU labelling solution (10 μ L) was added and incubated for 2-24 hrs. Labelling solution was then discarded and fix Denat (100 μ L) was added and incubated for 30 min at 15 $^{\circ}$ C -25 $^{\circ}$ C. Solution was aspirated and anti-BrdU POD (100 μ L) was added and incubated for 90 min at 15 $^{\circ}$ C -25 $^{\circ}$ C. The solution was then removed and the cells were washed 3 times with wash solution (100 μ L), then the substrate was added and incubated for 3-5 min at 15 $^{\circ}$ C -25 $^{\circ}$ C for colour development then stopped the reaction with 1M HCl. Absorbance was then measured at 450-690nm using GloMax-Multi microplate reader (Promega, USA).

2.5 Morphological analysis

The assay is based on the analysis of shape cells, integrity of nucleus and cell population in comparison to untreated cells. Briefly, cells were seeded at a density of 1×10^6 on coverslips in 6 well plates overnight. Cells were then treated for 24 hours with quinoxaline derivatives at 25 μ M, zinc at 500 μ M combination (quinoxaline derivatives 25 μ M + zinc 500 μ M) and actinomycin D at 20 μ g/mL. Plates were

centrifuged at 5000rpm for 5 min then washed with PBS. Cells were then fixed with 2.7% paraformaldehyde for 30 min and centrifuged for 5 min at 5000rpm. Coverslips were then mounted onto slides and viewed under the microscope using the Nikon Ti-E inverted microscope.

2.6 Cell staining for nuclear morphology analysis

This assay is principled on the ability of DAPI to stain the DNA of both live and dead cells but fluoresces more on condensed chromatin while PI stains only dead cells and fluoresces more with cells undergoing late apoptosis/necrosis (Tarnowski *et al.*, 1991). Briefly, cells were seeded at a density of 1×10^6 on coverslips in 6 well plates overnight. Cells were then treated for 24 hours with quinoxaline derivatives at 25 μ M, zinc at 500 μ M combination (quinoxaline derivatives 25 μ M + zinc 500 μ M) and actinomycin D at 20 μ g/mL. Plates were centrifuged at 5000rpm for 5 min then washed with PBS. Cells were then fixed with 2.7% paraformaldehyde for 30 min and centrifuged for 5 min at 5000rpm. Cells were stained with PI 10 μ g/mL for 5 min, centrifuged and washed then stained with DAPI 5 μ g/mL for 5 min and washed again after centrifuging. Coverslips were then mounted onto slides and viewed under the microscope using the Nikon Ti-E inverted microscope.

2.7 Cell cycle analysis

This test is principled on staining DNA with PI (propidium iodide) which is impermeable to viable cells with an intact membrane but permeable to dead cells with compromised membrane. Cells are then classified as to which phase of the cell cycle according to the DNA content (Lee E-J *et al.*, 2012). Briefly, cells were seeded in 12 well plates at a density of 1×10^6 for 12 hours then synchronized by starvation for 12 hrs. They were then treated with quinoxaline derivatives at 25 μ M, zinc 500 μ M, combination (quinoxaline derivatives 25 μ M + zinc 500 μ M), and Actinomycin D 20 μ g/mL for 24 hrs. Cells were then centrifuged at 5000rpm for 5 min then resuspended in 75% ethanol for fixing and incubated at -20°C overnight. Cells were centrifuged at 5000rpm for 5 min then resuspended in PBS and centrifuged again at 5000rpm for 5 min. Cells were then stained with PI (10mg/mL in PBS with 0.1% Triton-X 100) and counter stained with H₂DCFDA for 30min in the dark. Muse™ Cell Analyser was then used to quantify the DNA content at different cell cycle phases.

2.8 Apoptosis analysis using acridine orange and ethidium bromide

This assay is based on staining cells with acridine orange (AO) which stains the DNA and RNA of live cells and ethidium bromide (EB) which stains exposed DNA and RNA of dead/necrotic cells (Mallavadhani *et al.*, 2014). The combination of the two dyes resembles apoptosis. Briefly, cells were seeded at a density of 1×10^6 on coverslips in 6 well plates overnight. Cells were then treated for 24 hours with quinoxaline derivatives at $25 \mu\text{M}$, zinc at $500 \mu\text{M}$ combination (quinoxaline derivatives $25 \mu\text{M}$ + zinc $500 \mu\text{M}$) and actinomycin D at $20 \mu\text{g/mL}$. Plates were centrifuged at 5000rpm for 5 min then washed with PBS. Cells were then fixed with 2.7% paraformaldehyde for 30 min and centrifuged for 5 min at 5000 rpm. Cells were stained with acridine orange $100 \mu\text{g/mL}$ for 5 min, centrifuged and washed then stained with ethidium bromide $100 \mu\text{g/mL}$ for 5 min and washed again after centrifuging. Coverslips were then mounted onto slides and viewed under the microscope using the Nikon Ti-E inverted microscope.

2.9 Annexin V and dead cell apoptosis analysis

This assay is principled on Annexin V and PI stain which is based on the staining of cells undergoing early apoptosis with annexin V which binds to phosphatidylserine which is being expressed on an impermeable membrane, while with late apoptosis, PI will be able to bind to the DNA due to permeability of the membrane (Khan *et al.*, 2012). Muse[®] Annexin V and Dead Cell Assay kit was used according to manufacturer's instruction. Briefly, cells were seeded in 12 well plates at a density of 6×10^6 for 24 hours. They were then treated with quinoxaline derivatives at $25 \mu\text{M}$, zinc $500 \mu\text{M}$, combination (quinoxaline derivatives $25 \mu\text{M}$ + zinc $500 \mu\text{M}$), and Actinomycin D $20 \mu\text{g/mL}$ for 24 hrs. Cell were detached, centrifuged and resuspended in 1% FBS. Muse[™] Annexin V and Dead Cell Reagent was then added to the suspension and incubated for 20 min in the dark. Analysis was then done using Muse[™] Cell Analyzer.

2.10 Oxidative stress analysis

This flow cytometric assay is principled on fluorogenic H₂DCFDA dye which is principled on the cell permeant H₂DCFDA which measures superoxide radicals which fluoresce when oxidized by these reactive oxygen species (ROS) to DCF (Saleh *et al.*, 2015). Briefly, cells were seeded in 12 well plates at a density of 6×10^6 for 24 hours. Oxidative stress was stimulated with Lipopolysaccharides ($10 \mu\text{g/mL}$) on Raw 264.7 for 24 hours and on A549 cells hydrogen peroxide (1mM) for 1 hour prior to analysis

of addition of H₂DCFDA. They were then treated with quinoxaline derivatives at 25µM, zinc 500µM, combination (quinoxaline derivatives 25µM + zinc 500µM), and Actinomycin D 20µg/mL for 24 hours. Cells were detached, centrifuged and resuspended in culture medium with H₂DCFDA for 30 min at 37°C in the dark. Analysis was then done using Muse™ Cell Analyzer.

2.11 Western blot

This is a qualitative assay used in the detection of characterised proteins. Examination of the expression of apoptotic proteins cells were seeded at 1x10⁶ for 24 hrs. They were then treated with quinoxaline derivatives at 25µM, zinc 500µM, combination (quinoxaline derivatives 25µM + zinc 500µM), and Actinomycin D 20µg/mL for 24 hours. Cells were washed once with 1x PBS, thereafter cells lysis was accomplished with 500µL lysis buffer [10 mM Tris-HCl, pH 6.8, 1 % SDS, 100 mM sodium chloride, 1 mM EDTA, 1% NP 40, protease inhibitor], the cells were vortexed for 10 sec and incubated on ice for 30 minutes. The supernatant was collected by centrifugation at 15 000 x g for 20 minutes at 4°C and then protein concentration was determined using BCA protein assay at 562 nm. For SDS PAGE 50µg proteins was mixed with the sample buffer [1 mM Tris buffer pH 6.8, 20 % SDS, 20 % glycerol, 0.05 % β-mercaptoethanol, 0.002 % bromophenol blue] and then separated by 12 % SDS-PAGE then transferred to a polyvinylidene fluoride (PVDF) membrane using a semi-dry blotting system (Bio-Rad).

The membranes were blocked with Tris buffered saline (TBS) [150 mM NaCl, 50 mM Tris, 0.1 % Tween, pH 7.5] containing 3 % fat free dried milk. The membranes were washed with wash buffer [0.05 % TBS- Tween] and then incubated each time with one of the 1:500 dilutions of anti- Bax, and Bcl-2 primary antibodies for 1 hr at RT. After incubation, the membranes were washed with wash buffer and the primary will be bound by corresponding peroxidase-conjugated secondary antibodies at 1:10 000 dilutions for 1hr at RT. The membranes were washed with wash buffer and the immunoreactive proteins was detected using the super signal west pico-chemiluminescent substrate (Thermo Scientific, Rockford, USA) visualised and photographed using the ChemiDoc XRS+ software (Bio-RAD, USA).

2.12 Statistical analysis

Statistical analysis was performed in order to determine significant differences between samples. Differences were considered significant at, * $p < 0.05$; ** $p < 0.01$; *** $p < 0.001$. The analysis of variants test (ANOVA), Tukey-Kramer was used to compare samples using Graph Pad InStat™ 3 software. Mean fluorescence intensities were analysed using Image J software. ChemiDoc XRS software was used to analyse western blot results.

CHAPTER 3: RESULTS

3.1 Determination of the reducing power of quinoxaline derivatives

The antioxidant property of quinoxaline derivatives was determined using ferric reducing power assay which measured the extent of donation of electrons from antioxidants to convert ferric chloride to ferrous chloride. The ability of antioxidants to donate electrons is an important step in neutralization of free radicals. Various concentrations of quinoxaline derivatives (0.25mM- 2mM) were prepared. Ascorbic acid was used as a standard with concentrations correlating to quinoxalines and water used as a control/blank. Reducing power is displayed as percentage against the control without any addition of antioxidant molecule (Figure 3.1A). Of the four quinoxaline derivatives assayed, LA-39B displayed the highest reducing power with the lowest concentration on 0.25mM LA-39B exhibiting about 6.05% reducing power and the highest concentration of 2mM LA-39B having a reducing power of 26.95% compared to the water blank. The increase in reducing power displayed by LA-39B was directly proportional to the concentrations used. Following LA-39B was LA-55 which showed reducing power of up to 12.8% at a concentration of 2mM. The increase in reducing power displayed by LA-55 was also directly proportional to the concentrations used.

Reducing power of up to 10.15% was displayed by LA-65C3 at 2mM. Reducing power increased from 6.35% to 10.15% in a concentration-dependent manner. The least reducing power was observed with LA-16A which showed very minimal changes of only up to 3.2% reducing power. As expected, ascorbic acid displayed the highest reducing power of up to 56.9% compared to control. As summarised in Figure 3.1B, comparing reducing power of quinoxaline derivatives at their highest concentration on 2mM against water. Ascorbic acid shows the highest reducing power at 56.9%, followed by LA-39B at 26.95%, which was followed by LA-55 at 12.8%, then LA-65C3 at 10.15%, and the least reducing power displayed by LA-16A at 3.2%. From the results observed, the strength of reducing power could be arranged in the order: ascorbic acid>LA-39B>LA-55>LA-65C3>LA-16A.

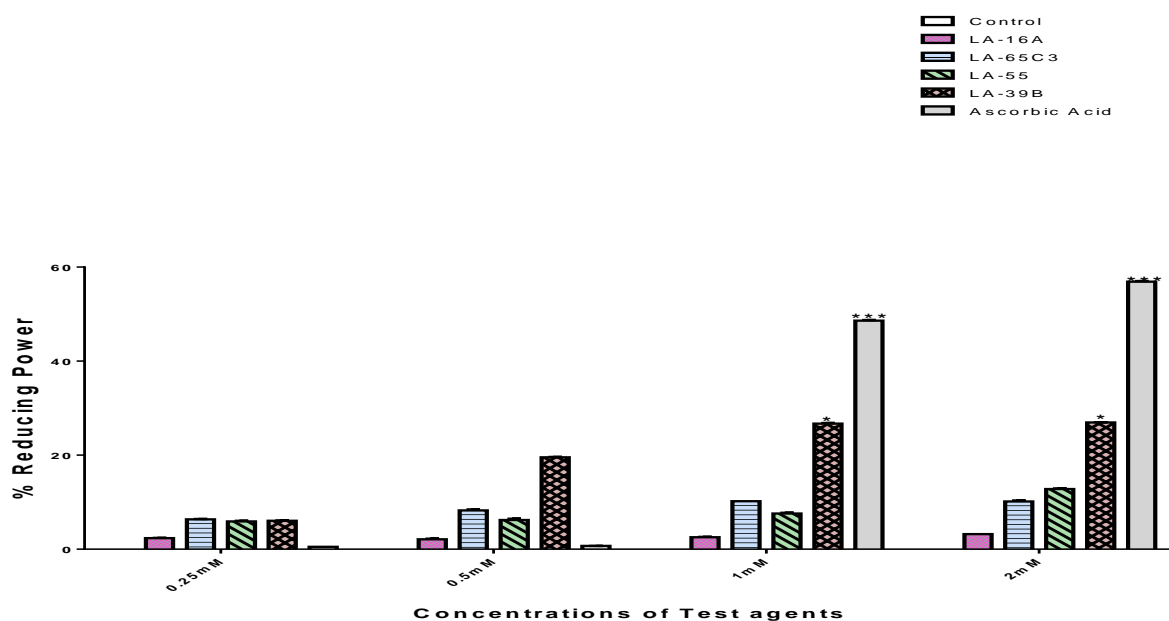
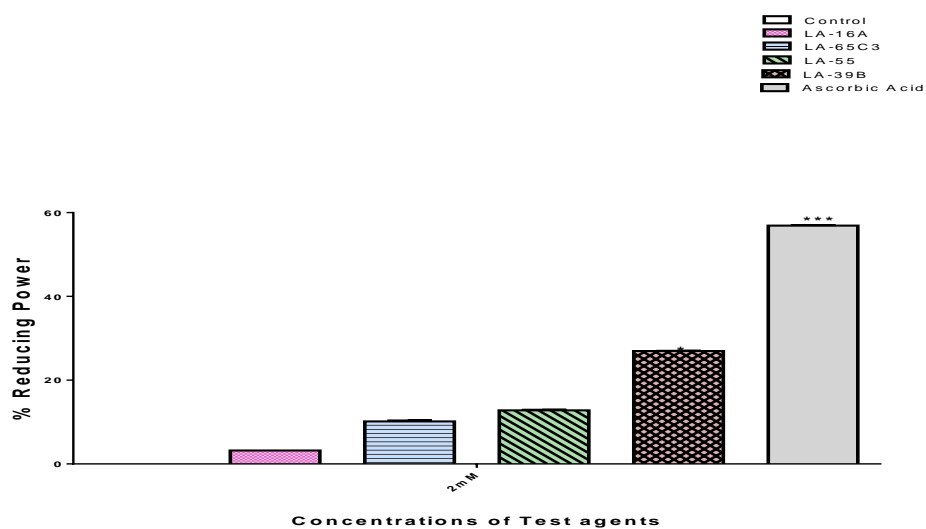
A**B**

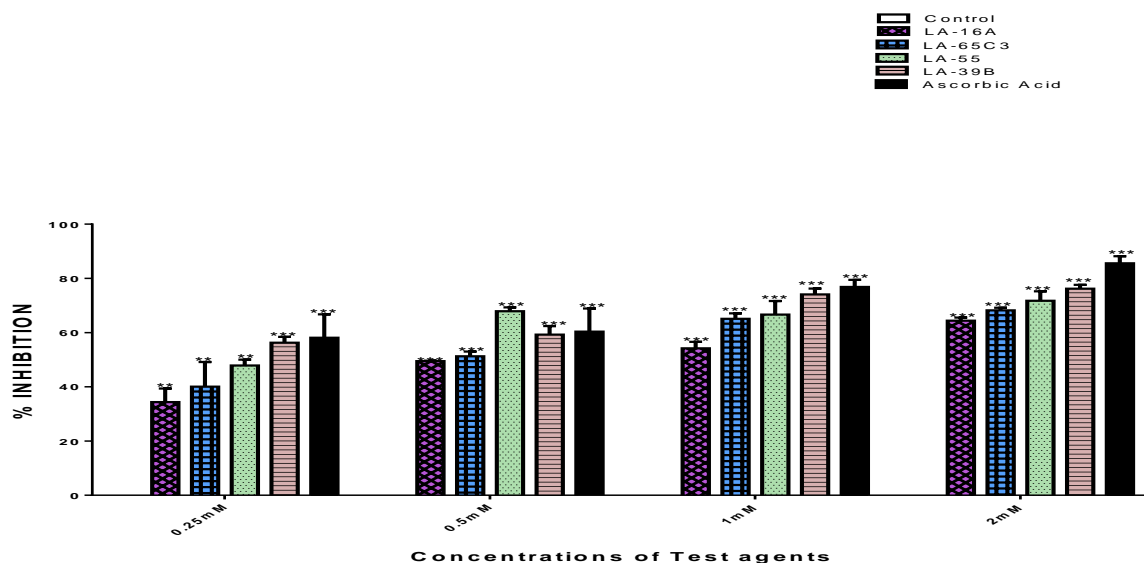
Figure 3.1 Reducing power potential of quinoxaline derivatives. Antioxidant property of quinoxaline derivatives LA-39B, LA55, LA-65C3 and LA-16A were assayed at various concentrations (0.25-2mM), using ascorbic acid as a standard and water as control. Each value represents the mean \pm SD of three experiments performed in triplicates independently. (* $p < 0.05$ and *** $p < 0.001$).

3.2 Determination of free-radical scavenging properties

The presence of free-radical scavenging property was quantified using DPPH assay, which is based on the scavenging of free-radical molecules from DPPH which is then analysed through the measurement of absorbance at 517nm which detects DPPH and decrease in absorbance represents scavenging property. Various concentrations of quinoxaline derivatives (0.25mM-2mM) were prepared. Ascorbic acid was used as standard with correlating concentrations and water as a control which had no free-radical scavenging property. Free-radical scavenging property was displayed as percentages against the control [Figure 3.2A]. Of the four quinoxaline derivatives tested LA-39B showed the highest scavenging percentage, with the lowest concentration 0.25mM had 56.25% and the highest concentration 2mM at 76.2% when compared to the control. The increase in scavenging percentage of free-radicals shown by LA-39B was directly proportional to the concentrations used. LA-55 was second highest with 71.75% at 2mM and 47.85% at 0.25mM. The increase in scavenging properties shown by LA-55 is also directly proportional to the concentration used.

LA-65C3 was the third of the four quinoxaline derivatives with 68.2% scavenging activity at 2mM when compared to the control. The scavenging percentage increased from 40.05% at 0.25mM to 68.2% 2mM which shows a concentration-dependent pattern. The compound with the least scavenging properties was LA-16A which had 64.4% at 2mM. The scavenging activity increased from 34.35% at 0.25mM to 64.4% at 2mM which also represents a concentration-dependent manner. As expected, ascorbic acid displayed the highest scavenging activity of up to 85.55% when compared to the control. As summarised in Figure 3.2B, comparing the scavenging activity of quinoxaline derivatives at their highest concentration of 2mM against the control. Which shows ascorbic acid having the highest scavenging percentage at 85.55%, followed by LA-39B at 76.2%, which was then followed by LA-55 at 71.75%, then LA-65C3 at 68.2% and the lastly LA-16A at 64.4%. From the results observed the scavenging percentages can be arranged in this order, ascorbic acid>LA-39B>LA-55>LA-65C3>LA-16A.

A



B

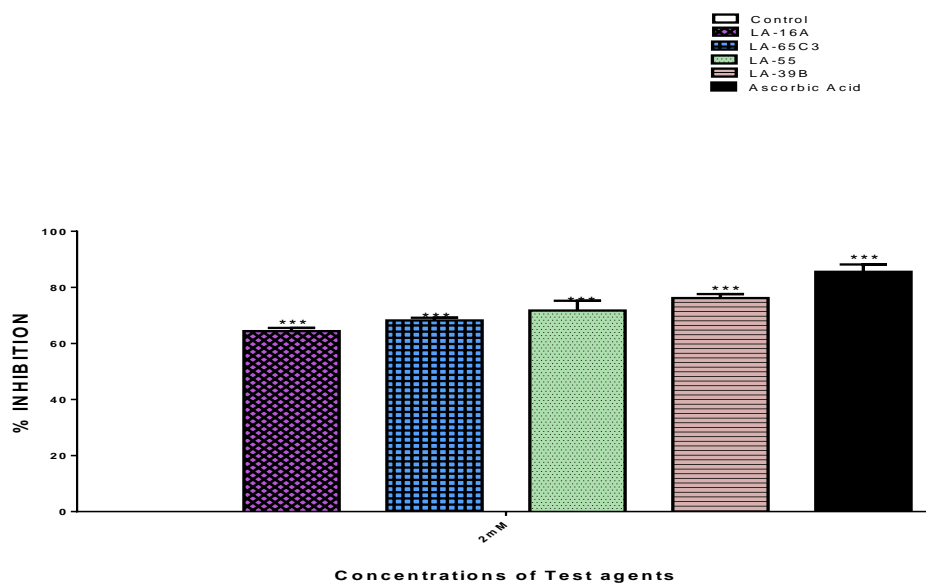


Figure 3.2 Free radical scavenging properties of quinoxaline derivatives using quantitative DPPH assay. Antioxidant property of quinoxaline derivatives LA-39B, LA55, LA-65C3 and LA-16A were assayed at various concentrations (0.25-2mM), using ascorbic acid as a standard and water as control. Each value represents the mean \pm SD of three experiments performed in triplicates independently. (* $p < 0.05$ and *** $p < 0.001$)

3.3 Visualisation of the presence of free-radical scavenging properties

The presence of free -radical scavenging activity was visualised through the use of qualitative DPPH antioxidant assay which is based on the ability of antioxidant to scavenge free-radical molecules from DPPH which is observed as colour development from purple to yellow. A concentration of 2 mM was prepared for quinoxaline derivatives and ascorbic acid was used a standard. Water was then used a control. Scavenging property was observed as development of a yellow colour against the control which had no scavenging property [Figure 3.3]. In all four quinoxaline derivatives a pale-yellow colour was observed in comparison to water where the was no colour development. As expected, ascorbic acid displayed a more intense a yellow colour which showed high scavenging property.

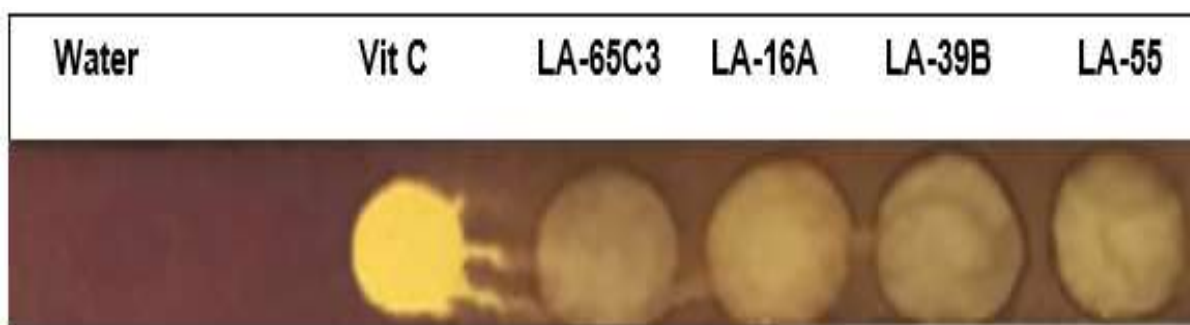


Figure 3.3 Qualitative display of antioxidant activity of quinoxaline derivatives.

A chromatography of a dot-blot of thin layer chromatography (TLC) plate sprayed with 0.4mM DPPH solution in methanol after blotting quinoxaline derivatives, ascorbic acid (Vit C) used as a standard and water as a blank. Change in colour displayed antioxidant activity.

3.4 Determination of cell viability on Raw 264.7 cells when induced with quinoxaline derivatives and zinc.

The effect on cell viability of Raw 264.7 cells when treated with quinoxaline derivatives and zinc on was determined by the use of mitochondrial-dependent conversion of yellow MTT [3-(4,5-dimethylthiazol-2-yl) 2,5-diphenyltetrazoliumbromide] to blue formazan. Various concentrations of quinoxaline derivatives (25 μ M-100 μ M), zinc (200 μ M-1000 μ M) were prepared. Actinomycin D (20 μ g/mL) was used as positive control (standard), DMSO (0.05%) in culture medium was used as a negative control to ensure that DMSO is not responsible for the decrease in cell viability and untreated cells were used as a control. Cell viability was displayed as percentage against untreated control (Figure 3.4A). Of the four quinoxaline derivatives assayed, LA-39B displayed the lowest cell viability percentage at 35.39% on 100 μ M with the lowest concentration of 25 μ M with 96.50% when compared to the untreated control. The decrease in cell viability displayed by LA-39B was inversely proportional to the concentration used. Following LA-39B was LA-55 which showed cell viability of 41.95% on 100 μ M, with lowest concentration of 25 μ M with 90.02% when compared to untreated control. The decrease in cell viability displayed by LA-55 was also inversely proportional to the concentration used. Cell viability of 86.68% was displayed by LA-65C3 on 100 μ M, which decreased from 100% on 25 μ M to 87.35% on 100 μ M which is also inversely proportional pattern Lastly, LA-16A had cell viability of 84.96% on 100 μ M and 100% on 25 μ M, which also shows an inversely proportional fashion.

Zinc also had an inversely proportional pattern, where cell viability decreased from 62.60% on 200 μ M to 35.67% on 1000 μ M. As expected, actinomycin D was effective and had cell viability percentage of 50.40% at 20 μ g/mL and DMSO in culture medium had no significant effect with 98.86% cell viability when both compared to untreated control. As summarised in Figure 3.4B, comparing cell viability of quinoxaline derivatives at their lowest concentration of 25 μ M against untreated control. The lowest cell viability was 90.02% induced by LA-55, followed by LA-39B 96.50%, then LA-16A and LA-65C3 which had no effect at all with 100% cell viability. Zinc had an inhibitory concentration of closest to 50% at 500 μ M.

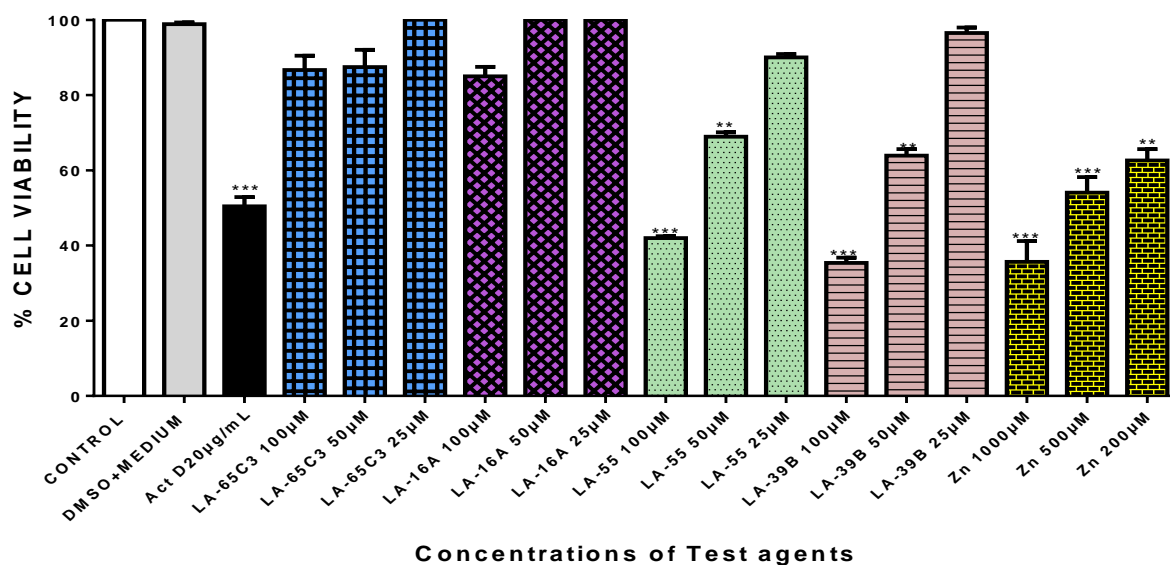
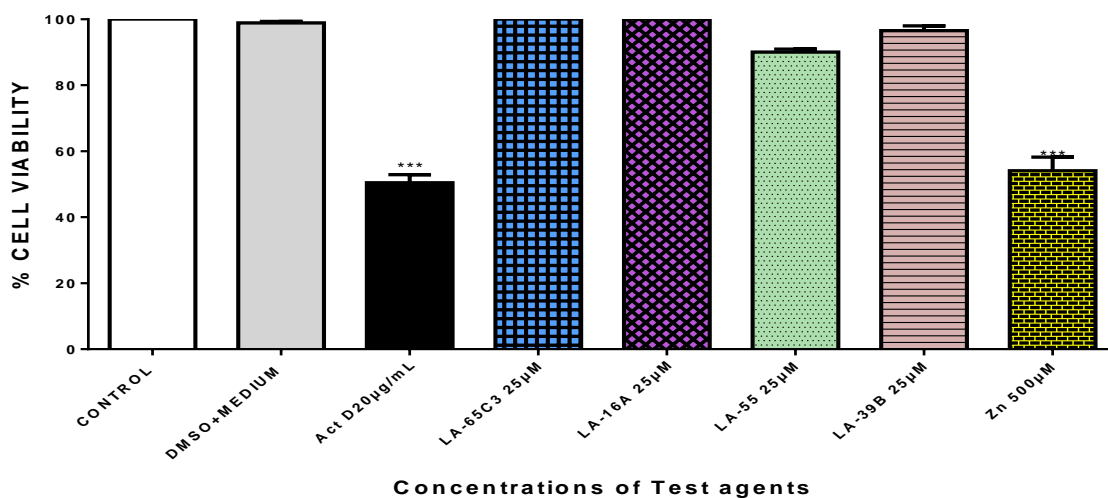
A**B**

Figure 3.4 Determination of cell viability on Raw 264.7 cells using MTT assay.

Cell viability of Raw 264.7 cells when in treated with quinoxaline derivatives LA-39B, LA55, LA-65C3 and LA-16A at various concentrations (25-100µM) and zinc at various concentrations (200-1000µM) were assayed, using actinomycin D(20µg/mL) as a standard and untreated cell as control. Each value represents the mean \pm SD of three experiments performed in triplicates independently. (* $p < 0.05$ and *** $p < 0.001$)

3.5 Morphological changes observed on Raw 264.7 cells when induced with quinoxaline derivatives and zinc

The effect on morphological integrity of Raw 264.7 cells when treated with quinoxaline derivatives and zinc was determined by treating cells for 24 hours then capture the images. Quinoxaline derivatives (25 μ M) and zinc (500 μ M) were prepared. Actinomycin D (20 μ g/mL) was used as positive control (standard) and untreated cells were used as a control. Morphological changes were observed in reference to untreated cells [Figure 3.5]. All four quinoxaline derivatives did not have any distinct effect on the morphology when comparing it to the untreated control. While zinc was characterised by a distinct decrease in the cell population which was characterised by round shaped cells with a glistening surface. And as expected, actinomycin D was effective and was characterised by decrease in cell population, round to irregular shaped cells with rough surface. In summary, only zinc showed cytotoxicity on Raw 264.7 cells while the quinoxaline derivatives had no effect.

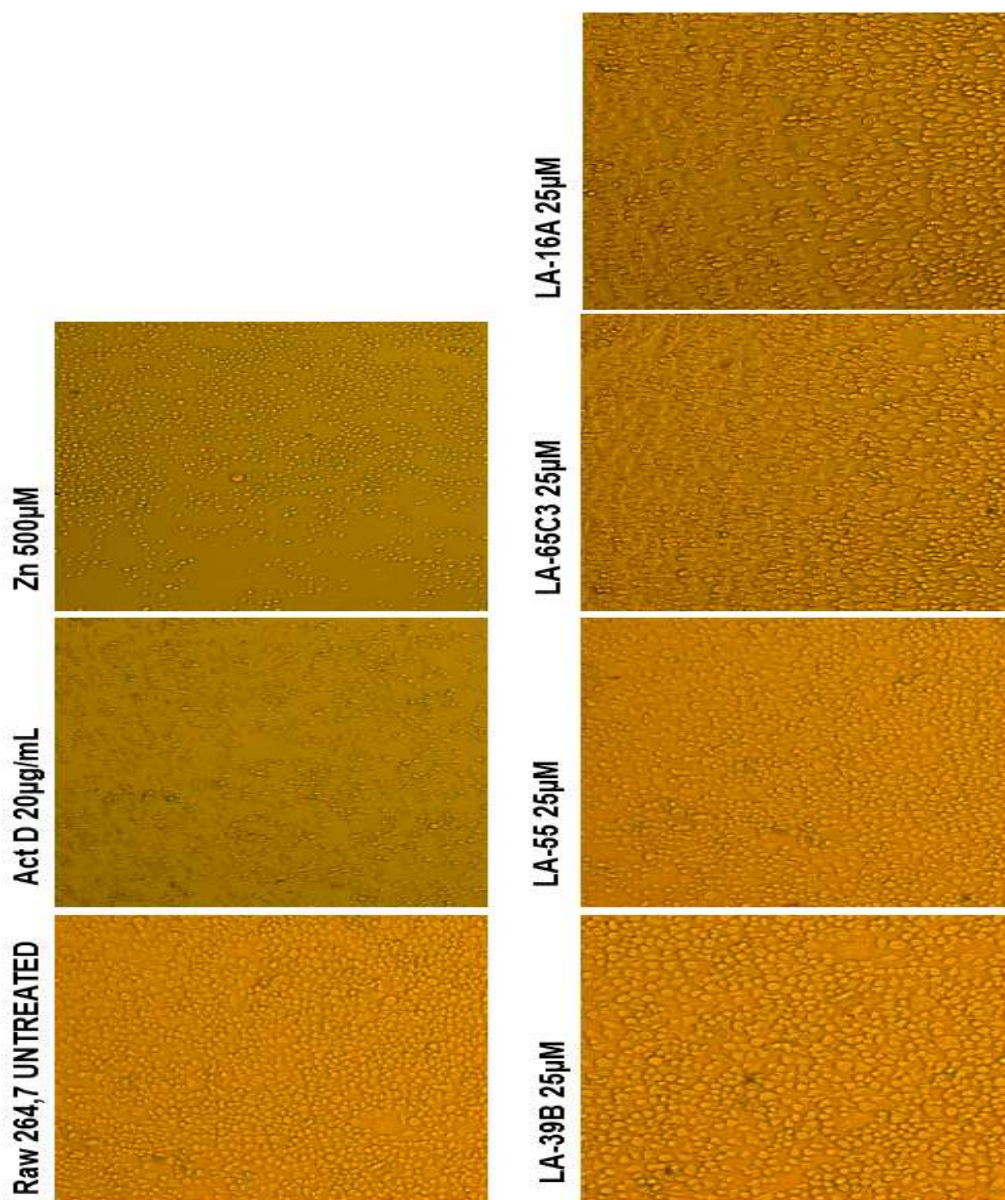


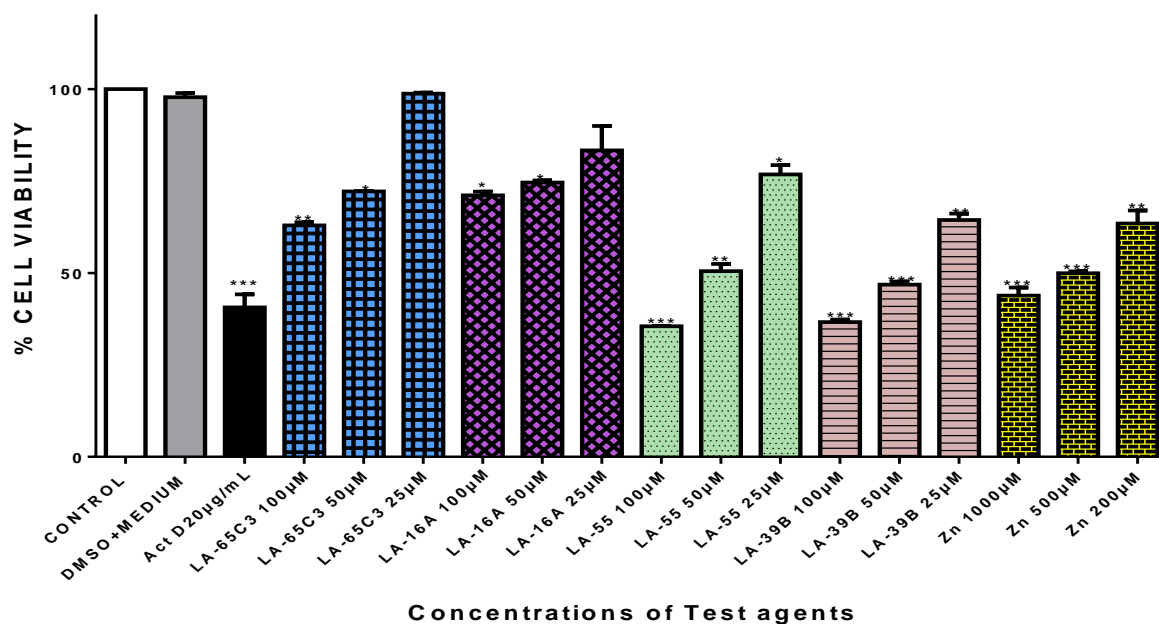
Figure 3.5 Morphological analysis on Raw 264.7 cells. Morphology of Raw 264.7 cells when treated with quinoxaline derivatives LA-39B, LA55, LA-65C3 and LA-16A at 25 µM and zinc at 500µM were assayed, using actinomycin D (20µg/mL) as a standard and untreated cell as control. Images were captured using Nikon Ti-E inverted microscope.

3.6 Determination of cell viability on HeLa cells when induced with quinoxaline derivatives and zinc.

The effect on cell viability of HeLa cells when treated with quinoxaline derivatives and zinc on was determined by the use of mitochondrial-dependent conversion of yellow MTT [3-(4,5-dimethylthiazol-2-yl) 2,5-diphenyltetrazoliumbromide] to blue formazan. Various concentrations of quinoxaline derivatives (25 μ M-100 μ M) and zinc (200 μ M-1000 μ M) were prepared. Actinomycin D (20 μ g/mL) was used as positive control (standard), DMSO (0.05%) in culture medium was used as a negative control to ensure that DMSO is not responsible for the decrease in cell viability and untreated cells were used as a control. Cell viability was displayed as percentage against untreated control (Figure 3.6A). Of the four quinoxaline derivatives assayed, LA-39B displayed the lowest cell viability percentage at 36.65% on 100 μ M with the lowest concentration of 25 μ M with 64.41% when compared to the untreated control. The decrease in cell viability displayed by LA-39B was inversely proportional to the concentration used. Following LA-39B was LA-55 which showed cell viability of 35.53% on 100 μ M, with lowest concentration of 25 μ M with 76.82% when compared to untreated control. The decrease in cell viability displayed by LA-55 was also inversely proportional to the concentration used. Cell viability of 62.98% was displayed by LA-65C3 on 100 μ M, which decreased from 98.8% on 25 μ M to 62.98% on 100 μ M which is also an inversely proportional pattern. Lastly, LA-16A had cell viability of 71.10% on 100 μ M and 83.36% on 25 μ M, which also shows an inversely proportional fashion.

Zinc also had an inversely proportional pattern, where cell viability decreased from 63.49% on 200 μ M to 43.85% on 1000 μ M. As expected, actinomycin D was effective and had cell viability percentage of 40.66% at 20 μ g/mL and DMSO in culture medium had no significant effect with 97.85% cell viability when both compared to untreated control. As summarised in figure 3.6B, comparing cell viability of quinoxaline derivatives at their lowest concentration of 25 μ M against untreated control. The lowest cell viability was 64.41% induced by LA-39B, followed by LA-55 76.82%, then LA-16A 83.36% then lastly LA-65C3 with no significant effect at 98.81%. Zinc had an inhibitory concentration of 50% on 500 μ M.

A



B

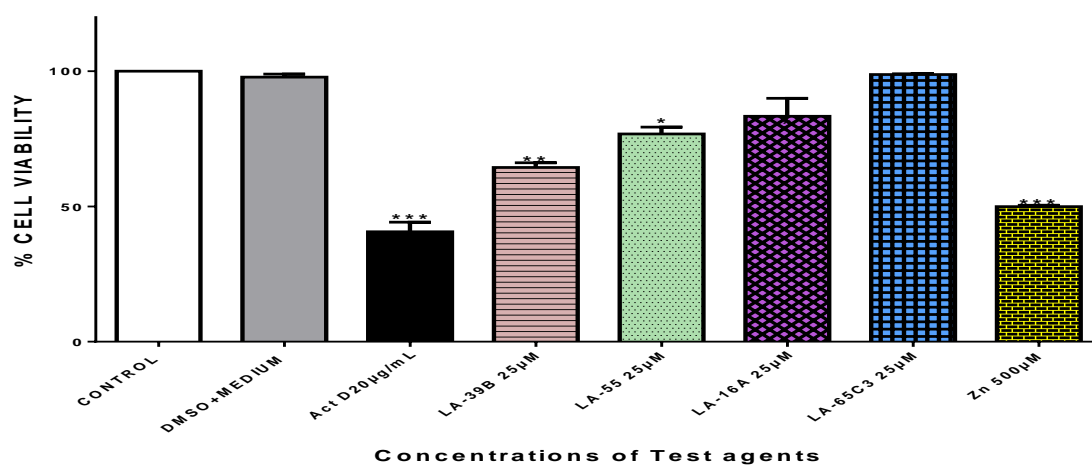


Figure 3.6 Determination of cell viability on HeLa cells using MTT assay. Cell viability of HeLa cells when treated with quinoxaline derivatives LA-39B, LA55, LA-65C3 and LA-16A at various concentrations (25-100µM) and zinc at various concentrations (200-1000µM) were assayed, using actinomycin D(20µg/mL) as a standard and untreated cell as control. Each value represents the mean ± SD of three experiments performed in triplicates independently. ((*p<0.05 and ***p<0.001)

3.7 Morphological changes observed on HeLa cells when induced with quinoxaline derivatives and zinc

The effect on morphological integrity of HeLa cells when treated with quinoxaline derivatives and zinc was determined by treating cells for 24 hours then capture the images. Quinoxaline derivatives (25 μ M) and zinc (500 μ M) were prepared. Actinomycin D (20 μ g/mL) was used as positive control (standard) and untreated cells were used as a control. Morphological changes were observed in reference to untreated cells [Figure 3.7]. Of the four quinoxaline derivatives tested, LA-39B displayed major changes especially the decrease in cell population which were characterised by round to irregular shaped cells with a rough surface and clumping of the nucleus. Following LA-39B is LA-55 which also had a decrease in the cell population and morphology was characterised by irregular shaped with cells with a rough surface and clumping of the nucleus. Both LA-65C3 and LA-16A had no morphological changes.

Zinc was also characterised by a distinct decrease in the cell population which was characterised by round shaped cells with a glistening surface. And as expected, actinomycin D was effective and was characterised by decrease in cell population, round to irregular shaped cells with rough surface. In summary, of the four quinoxaline derivatives, LA-39B and LA-55 are the ones that induced morphological changes on HeLa cells while LA-65C3 and LA-16A had no effect. Zinc was also able to induce morphological changes.

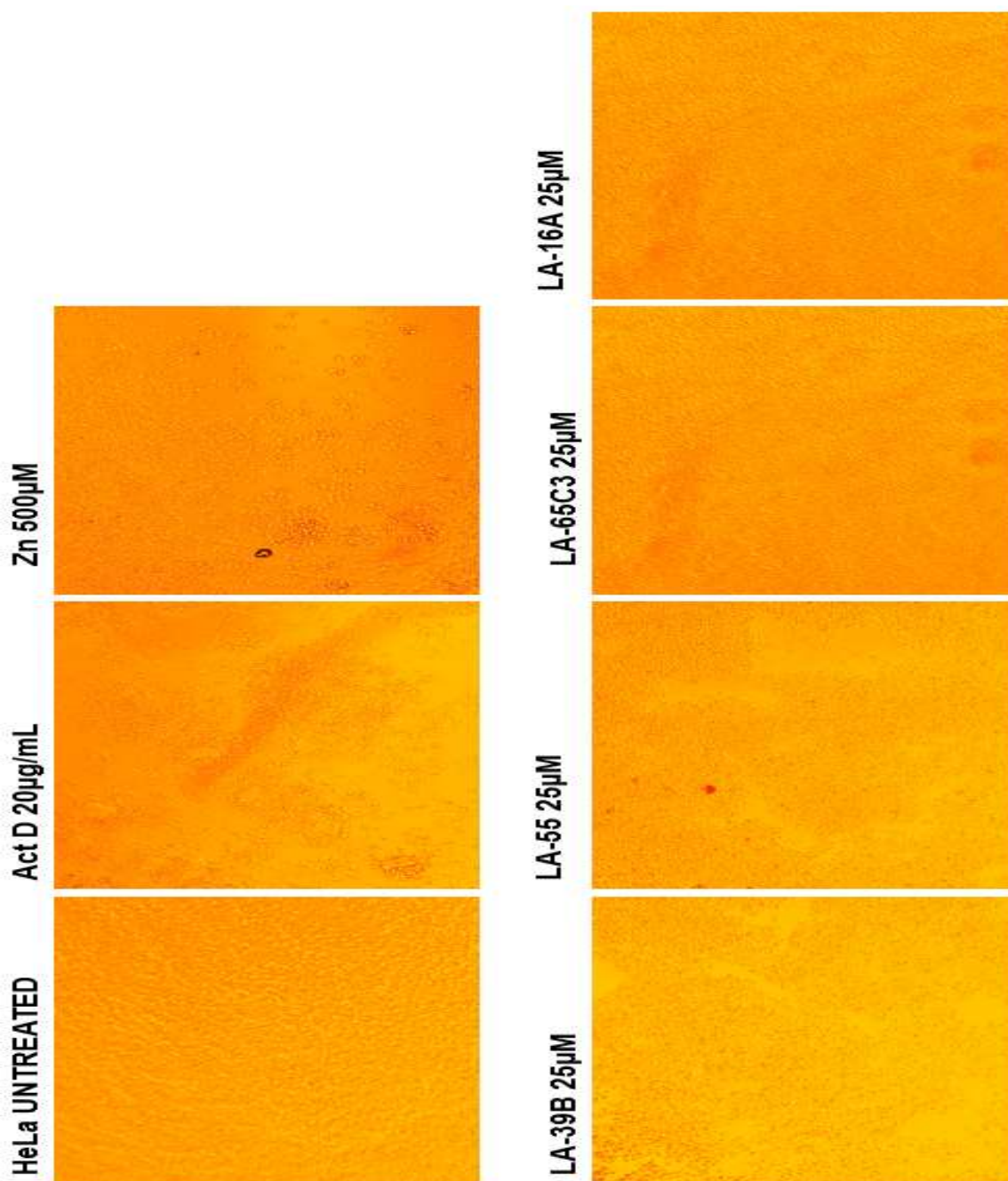


Figure 3.7 Morphological analysis on HeLa cells. Morphology of HeLa cells when treated with quinoxaline derivatives LA-39B, LA55, LA-65C3 and LA-16A at 25µM and zinc at 500µM were assayed, using actinomycin D(20µg/mL) as a standard and untreated cell as control. Images were captured using Nikon Ti-E inverted microscope.

3.8 Determination of cell viability on MCF-7 cells when induced with quinoxaline derivatives and zinc.

The effect on cell viability of MCF-7 cells when treated with quinoxaline derivatives and zinc on was determined by the use of mitochondrial-dependent conversion of yellow MTT [3-(4,5-dimethylthiazol-2-yl) 2,5-diphenyltetrazoliumbromide] to blue formazan. Various concentrations of quinoxaline derivatives (25 μ M-100 μ M) and zinc (200 μ M-1000 μ M) were prepared. Actinomycin D (20 μ g/mL) was used as positive control (standard), DMSO (0.05%) in culture medium was used as a negative control to ensure that DMSO is not responsible for the decrease in cell viability and untreated cells were used as a control. Cell viability was displayed as percentage against untreated control (Figure 3.8A). Of the four quinoxaline derivatives assayed, LA-55 displayed the lowest cell viability percentage at 57.1% on 100 μ M with the lowest concentration of 25 μ M with 83.71% when compared to the untreated control. The decrease in cell viability displayed by LA-55 was inversely proportional to the concentration used. Following LA-55 was LA-39B which showed cell viability of 56.71% on 100 μ M, with lowest concentration of 25 μ M with 93.24% when compared to untreated control. The decrease in cell viability displayed by LA-93B was also inversely proportional to the concentration used. Cell viability of 94.99% was displayed by LA-65C3 on 100 μ M, which decreased from 100% on 25 μ M to 94.99% on 100 μ M which is also an inversely proportional pattern. Lastly, LA-16A had no effect at all where cell viability remained at 100% when compared to the untreated control.

Zinc also had an inversely proportional pattern, where cell viability decreased from 65.05% on 200 μ M to 41.26% on 1000 μ M. As expected, actinomycin D was effective and had cell viability percentage of 52.96% at 20 μ g/mL and DMSO in culture medium had no significant effect with 98.97% cell viability when both compared to untreated control. As summarised in Figure 3.8B, comparing cell viability of quinoxaline derivatives at their lowest concentration of 25 μ M against untreated control. The lowest cell viability was 83.71% induced by LA-55, followed by LA-39B 76.82%, then LA-16A and LA-65C3 which had no effect at all with 100% cell viability. Zinc had an inhibitory concentration of closest to 50% at 500 μ M.

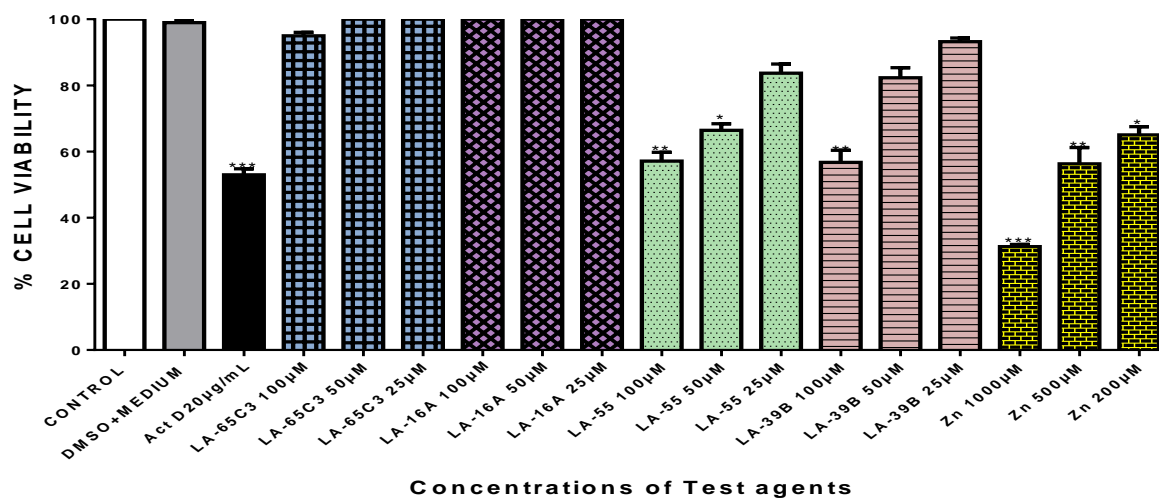
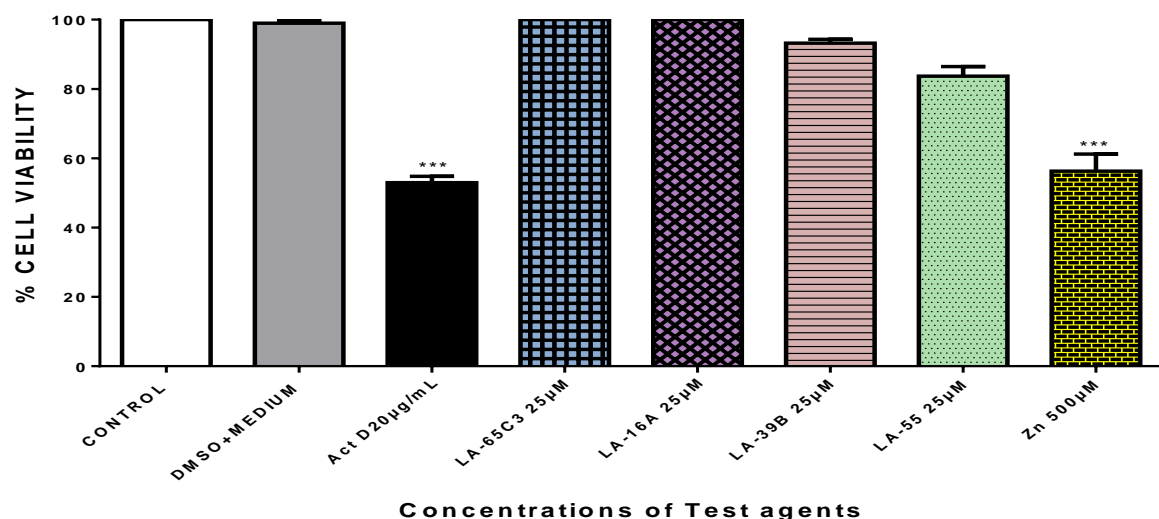
A**B**

Figure 3.8 Determination of cell viability on MCF-7 cells using MTT assay. Cell viability of MCF-7 cells when treated with quinoxaline derivatives LA-39B, LA55, LA-65C3 and LA-16A at various concentrations (25-100µM) and zinc at various concentrations (200-1000µM) were assayed, using actinomycin D(20µg/mL) as a standard and untreated cell as control. Each value represents the mean ± SD of three experiments performed in triplicates independently (*p<0.05 and ***p<0.001)

3.9 Determination of cell viability on A549 cells when induced with quinoxaline derivatives and zinc.

The effect on cell viability of A549 cells when treated with quinoxaline derivatives and zinc on was determined by the use of mitochondrial-dependent conversion of yellow MTT [3-(4,5-dimethylthiazol-2-yl) 2,5-diphenyltetrazoliumbromide] to blue formazan. Various concentrations of quinoxaline derivatives (25 μ M-100 μ M) and zinc (200 μ M-1000 μ M) were prepared. Actinomycin D (20 μ g/mL) was used as positive control (standard), DMSO (0.05%) in culture medium was used as a negative control to ensure that DMSO is not responsible for the decrease in cell viability and untreated cells were used as a control. Cell viability was displayed as percentage against untreated control (Figure 3.9A). Of the four quinoxaline derivatives assayed, LA-39B displayed the lowest cell viability percentage at 22.23% on 100 μ M with the lowest concentration of 25 μ M with 46.97% when compared to the untreated control. The decrease in cell viability displayed by LA-39B was inversely proportional to the concentration used. Following LA-39B was LA-55 which showed cell viability of 31.41% on 100 μ M, with lowest concentration of 25 μ M with 51.91% when compared to untreated control. The decrease in cell viability displayed by LA-55 was also inversely proportional to the concentration used. Cell viability of 87.35% was displayed by LA-65C3 on 100 μ M, which decreased from 100% on 25 μ M to 87.35% on 100 μ M which is also an inversely proportional pattern. Lastly, LA-16A had cell viability of 97.66% on 100 μ M and 100% on 25 μ M, which also shows an inversely proportional fashion.

Zinc also had an inversely proportional pattern, where cell viability decreased from 76.5% on 200 μ M to 25.95% on 1000 μ M. As expected, actinomycin D was effective and had cell viability percentage of 51.65% at 20 μ g/mL and DMSO in culture medium had no effect with 100% cell viability when both compared to untreated control. As summarised in Figure 3.9B, comparing cell viability of quinoxaline derivatives at their lowest concentration of 25 μ M against untreated control. The lowest cell viability was 46.97% induced by LA-39B, followed by LA-55 51.91%, then LA-16A and LA-65C3 which had no effect at all with 100% cell viability. Zinc had an inhibitory concentration of closest to 50% at 500 μ M.

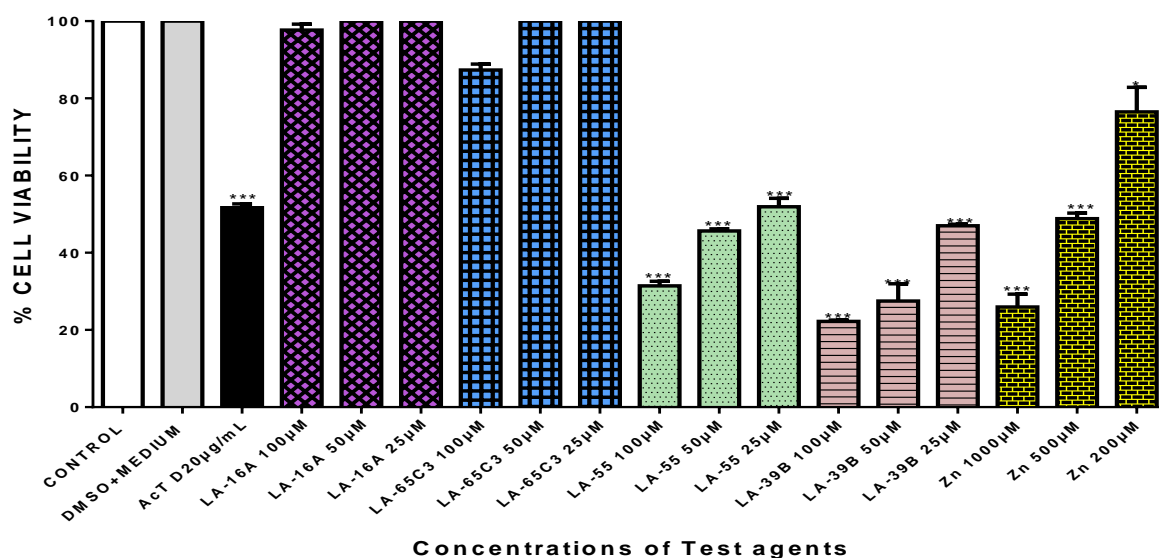
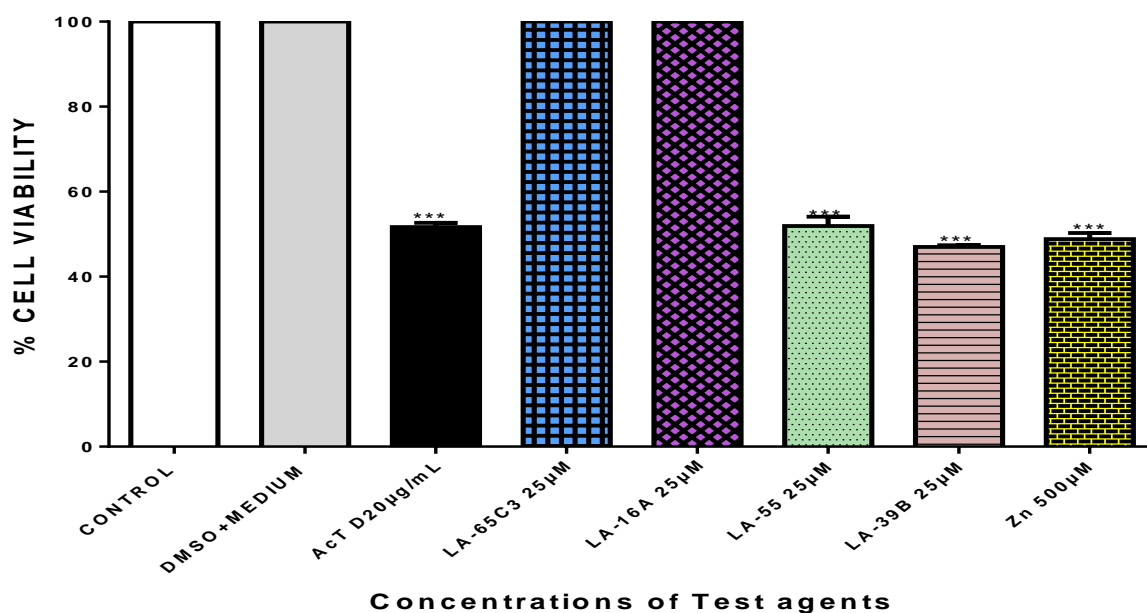
A**B**

Figure 3.9 Determination of cell viability on A549 cells using MTT assay. Cell viability of A549 cells when treated with quinoxaline derivatives LA-39B, LA55, LA-65C3 and LA-16A at various concentrations (25-100µM) and zinc at various concentrations (200-1000µM) were assayed, using actinomycin D (20µg/mL) as a standard and untreated cell as control. Each value represents the mean \pm SD of three experiments performed in triplicates independently (* $p < 0.05$ and *** $p < 0.001$)

3.10 Morphological changes observed on A549 cells when induced with quinoxaline derivatives and zinc

The effect on morphological integrity of A549 cells when treated with quinoxaline derivatives and zinc on was determined by treating cells for 24 hours then capture the images. Quinoxaline derivatives (25 μ M) and zinc (500 μ M) were prepared. Actinomycin D (20 μ g/mL) was used as positive control (standard) and untreated cells were used as a control. Morphological changes were observed in reference to untreated cells [Figure 3.10]. LA-39B and LA-55 were both characterized by decrease in cell population, cell shrinkage and irregular shape with a condensed nucleus. Both LA-65C3 and LA-16A had no morphological changes.

Zinc was also characterised by a distinct decrease in the cell population which was characterised by swelling of the cell with a condensed nucleus. And as expected, actinomycin D was effective and was characterised by decrease in cell population, round shaped cells and condensed nucleus. In summary, of the four quinoxaline derivatives, LA-39B and LA-55 are the ones that induced morphological changes on HeLa cells while LA-65C3 and LA-16A had no effect. Zinc was also able to induce morphological changes.

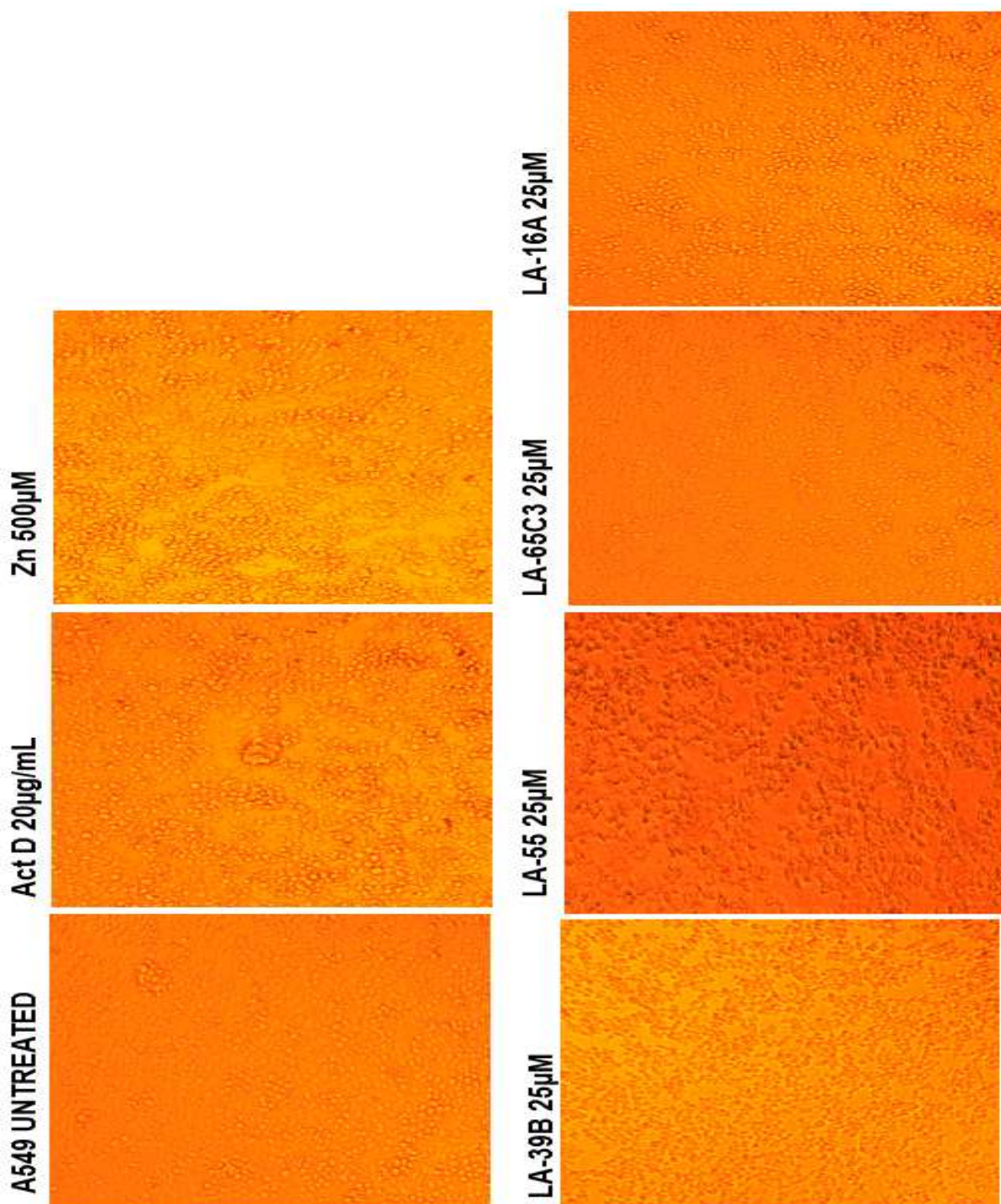


Figure 3.10 Morphological analysis on A549 cells. Morphology of A549 cells when treated with quinoxaline derivatives LA-39B, LA55, LA-65C3 and LA-16A at 25µM and zinc at 500µM were assayed, using actinomycin D (20µg/mL) as a standard and untreated cell as control. Images were captured using Nikon Ti-E inverted microscope.

3.11 Determination of cell proliferation on A549 cells induced with quinoxaline derivatives (LA-39B, LA-55), zinc and in combination.

The effect on cell proliferation of A549 cells when treated with quinoxaline derivatives (LA-39B & LA-55), zinc and in combination (LA-39B+zinc & LA-55+zinc) was determined via the BrdU ELISA assay which is principled on the incorporation of BrdU substrate on viable cells in which an antibody will bind to produce a blue colour. Quinoxaline derivatives (LA-39B & LA-55) of 25 μ M and zinc 500 μ M were prepared. Actinomycin D (20 μ g/mL) was used as positive control (standard) and untreated cells as control. Cell proliferation is displayed as percentage against untreated control (Figure 3.11). LA-39B had cell proliferation percentage of 53.63% on 25 μ M and when in combination with zinc had a slight increase to 55.66% when compared to untreated control. From the results it shows that when LA-39B is used in combination with zinc, there is a slight increase on cell proliferation percentage compared to when the cells are treated with LA-39B alone. LA-55 had cell proliferation percentage of 55.2% and when in combination with zinc had a very slight increase to 55.94% when compared to untreated control. From the results it also shows that when LA-55 is in combination with zinc, there is a slight increase on cell proliferation percentage compared to when the cells are treated with LA-55 alone. When zinc was tested alone, it had a cell proliferation percentage of 57.30% when compared to untreated control. As expected, actinomycin D was effective and had cell viability percentage of 52.77% at 20 μ g/mL when compared to untreated control.

A549 BrdU ASSAY

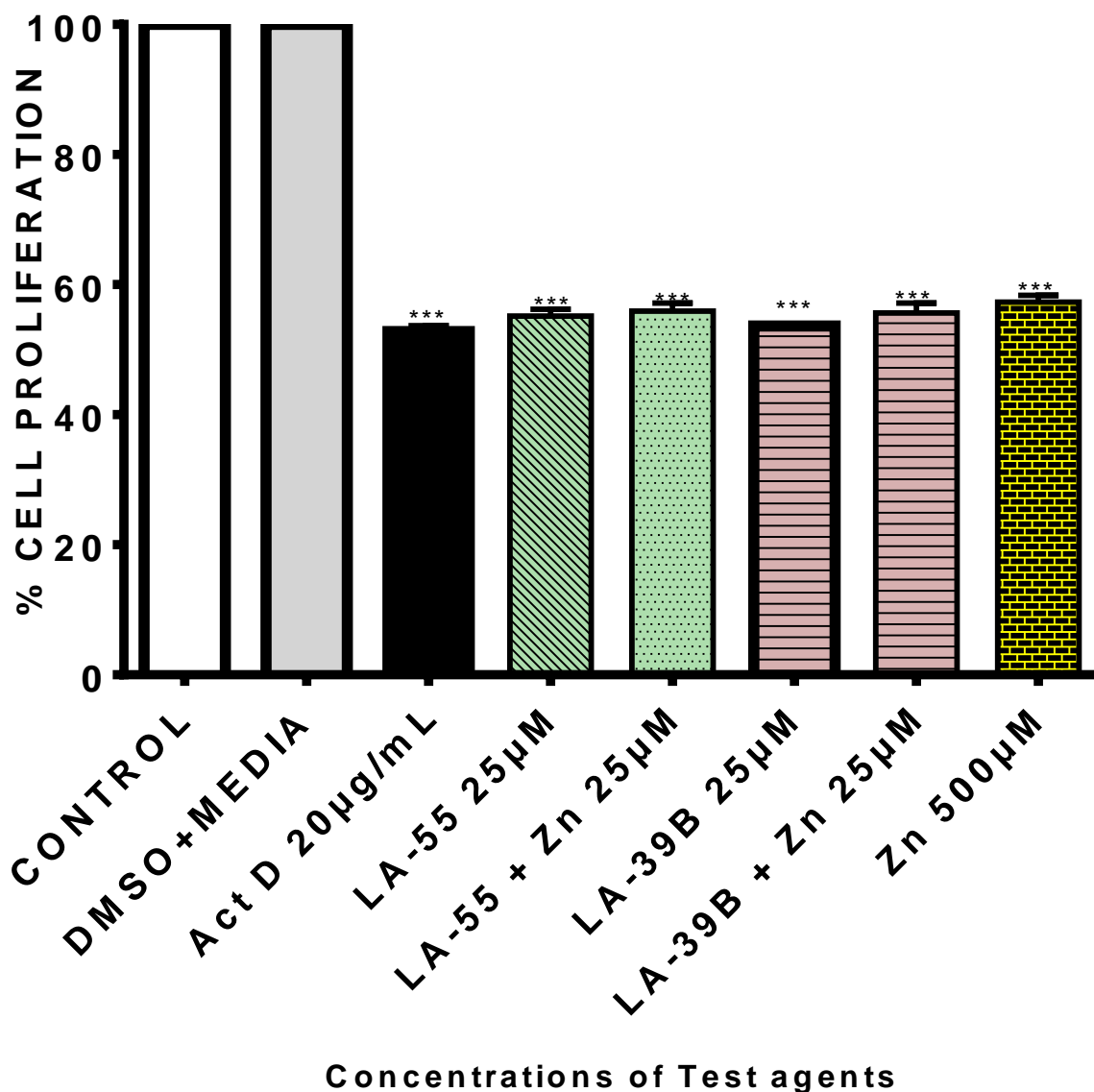


Figure 3.11 Determination of cell viability on cell proliferation on A549 cells using BrdU assay. Cell viability of A549 cells when treated with quinoxaline derivatives LA-39B and LA55 on 25µM, zinc on 500µM and in combination were assayed, using actinomycin D (20µg/mL) as a standard and untreated cell as control. Each value represents the mean \pm SD of three experiments performed in triplicates independently (* $p < 0.05$ and *** $p < 0.001$)

3.12 Morphological changes observed on A549 cells when induced with quinoxaline derivatives (LA-39B& LA-55), zinc and in combination

The effect on morphological integrity of A549 cells when treated with quinoxaline derivatives (LA-39B & LA-55), zinc and in combination (LA-39B+zinc & LA-55+zinc) was determined by treating cells for 24 hours then capture the images. Quinoxaline derivatives (25 μ M) and zinc (500 μ M) were prepared. Actinomycin D (20 μ g/mL) was used as positive control (standard) and untreated cells were used as a control. Morphological changes were observed in reference to untreated cells [Figure 3.12]. LA-39B characterized by decrease in cell population, cell shrinkage and irregular shape with a condensed nucleus and when in combination with zinc the is enhanced decrease in the cell population. LA-55 is characterized by decrease in cell population, cell shrinkage and irregular shape with a condensed nucleus and when in combination with zinc the is also an enhancement in the decrease of cell population while the morphology remains the same as to when treated with LA-55 alone.

Zinc was also characterised by a distinct decrease in the cell population which was characterised by swelling of the cell with a condensed nucleus. And as expected, actinomycin D was effective and was characterised by decrease in cell population, round shaped cells and condensed nucleus. In summary, the is an enhancement to the decrease in cell population when quinoxaline derivatives are used in combination.

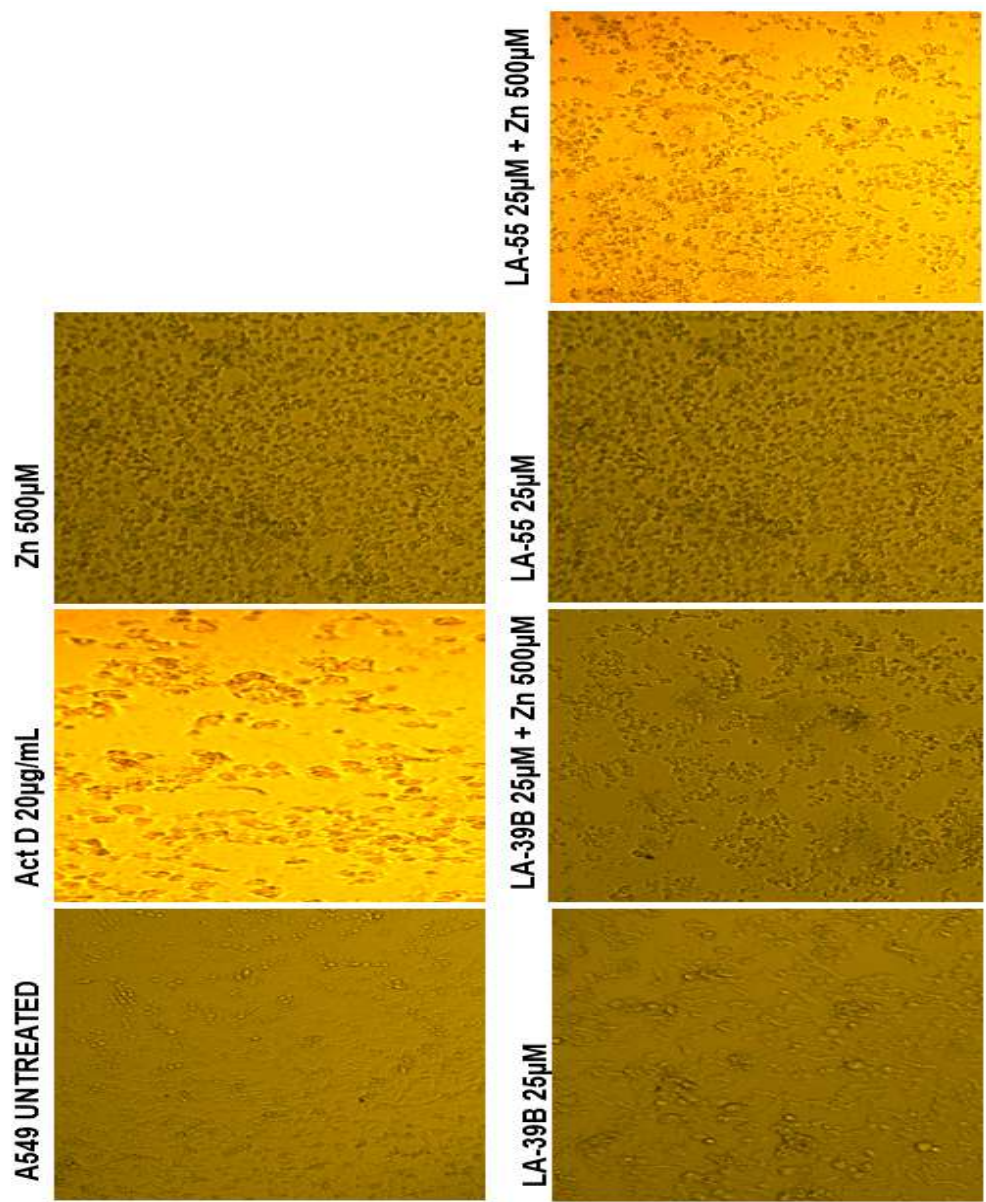


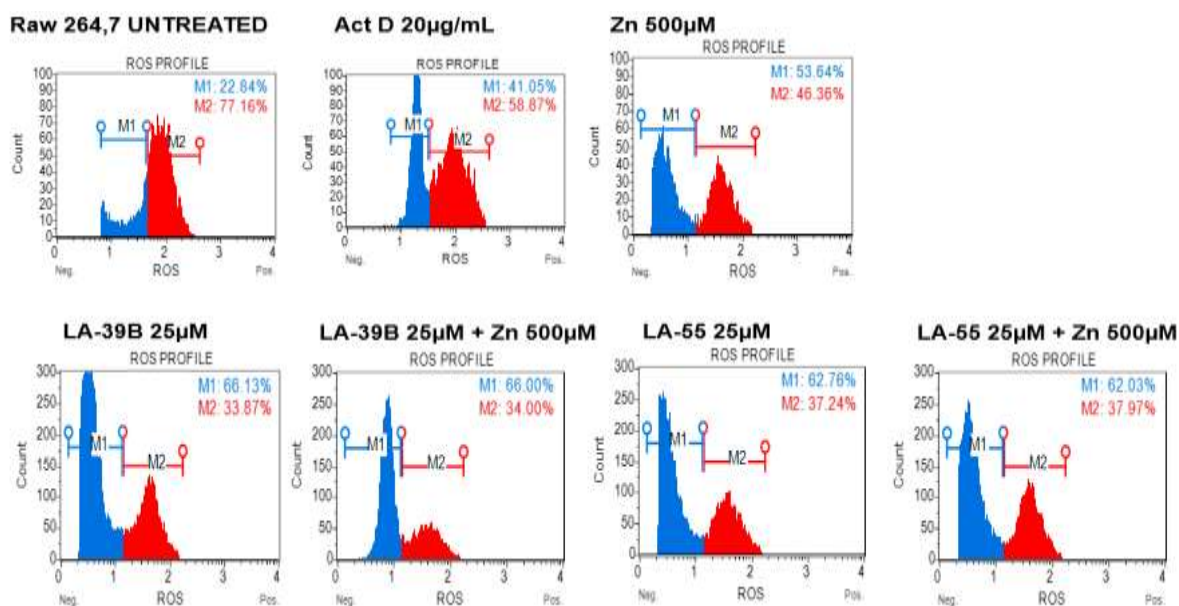
Figure 3.12 Morphological analysis on A549 when treated with quinoxaline derivatives, zinc and in combination. Morphology of A549 cells when treated with quinoxaline derivatives (LA-39B & LA55) on 25µM, zinc on 500µM and in combination were assayed, using actinomycin D (20µg/mL) as a standard and untreated cell as control. Images were captured using Nikon Ti-E inverted microscope.

3.13 Analysis of reduction of oxidative stress levels on Raw 264.7 cells when treated with quinoxaline derivatives (LA-39B & LA-55), zinc and in combination

Oxidative stress levels on Raw 264.7 cells when treated with quinoxaline derivatives (LA-39B & LA-55), zinc and in combination (LA-39B+zinc & LA-55+zinc) was determined through flow cytometric analysis of H₂DCFDA which is principled on the cell permeant H₂DCFDA which measures superoxide radicals which fluoresce when oxidized by these reactive oxygen species (ROS). Quinoxaline derivatives (LA-39B & LA-55) of 25µM and zinc (500µM) were prepared. Actinomycin D (20µg/mL) was used as positive control (standard) and untreated cells were used as a control. Oxidative stress levels are displayed as ROS profile where M1 shows a population of live cells with a blue colour and M2 shows a profile of cells exhibiting ROS with a red colour [Figure 3.13A]. LA-39B was able to reduce oxidative stress with a ROS profile showing M2 with 33.87% as compared to the control with an M2 percentage of 77.16% which shows high level of oxidative stress. When in combination with zinc, there is no significant difference with an M2 percentage of 34.00% as compared to LA-39B alone but has a significant difference when compared to the control.

LA-55 was also able to reduce oxidative stress with a ROS profile showing M2 with 37.24% as compared to the control. When in combination with zinc, there is no significant difference with an M2 percentage of 37.97% as compared to LA-55 alone but has a significant difference when compared to the control. Zinc also reduce oxidative stress with a ROS profile showing M2 with 46.36% as compared to the control. In summary, figure 3.13B shows a graphical representation of ROS profile with two cell populations of control, actinomycin D, LA-39B, LA-55, zinc and in combination.

A



B

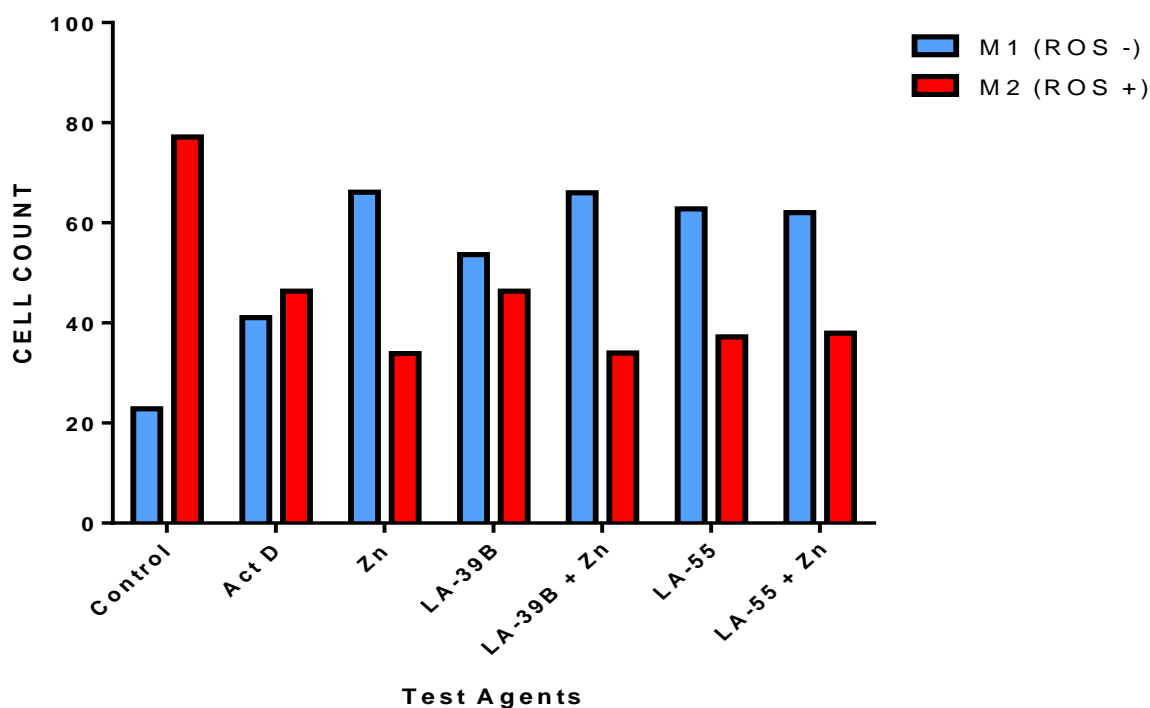


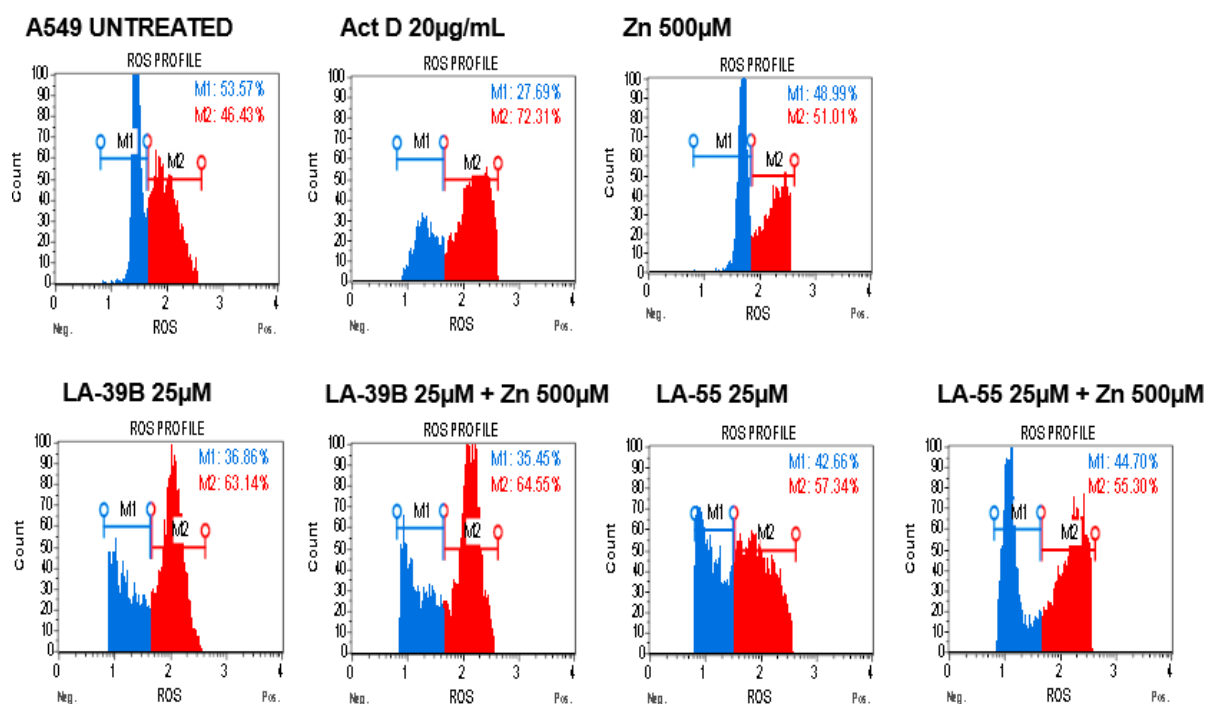
Figure 3.13 Determination of reduction of oxidative stress on Raw 264.7 cells. Oxidative stress on Raw 264.7 cells when treated with quinoxaline derivatives (LA-39B & LA55) on 25µM, zinc on 500µM and in combination were assayed, using actinomycin D as a standard and untreated cell as control. Flow cytometric analysis was done using Muse Analyzer.

3.14 Analysis of reduction of oxidative stress levels on A549 cells when treated with quinoxaline derivatives (LA-39B & LA-55), zinc and in combination

Oxidative stress levels on A549 cells when treated with quinoxaline derivatives (LA-39B & LA-55), zinc and in combination (LA-39B+zinc & LA-55+zinc) was determined through flow cytometric analysis of H₂DCFDA which is principled on the cell permeant H₂DCFDA which measures superoxide radicals which fluoresce when oxidized by these reactive oxygen species (ROS). Quinoxaline derivatives (LA-39B & LA-55) of 25µM and zinc (500µM) were prepared. Actinomycin D (20µg/mL) was used as positive control (standard) and untreated cells were used as a control. Oxidative stress levels are displayed as ROS profile where M1 shows a population of live cells with a blue colour and M2 shows a profile of cells exhibiting ROS with a red colour [Figure 3.14A]. LA-39B in showed an increase oxidative stress with a ROS profile showing M2 with 63.14% as compared to the control with an M2 percentage of 46.43%. When in combination with zinc, the is no significant difference with an M2 percentage of 64.55% as compared to LA-39B alone but has a significant difference when compared to the control.

LA-55 was also showed an increase oxidative stress with a ROS profile showing M2 with 57.34% as compared to the control. When in combination with zinc, the is no significant difference with an M2 percentage of 55.30% as compared to LA-55 alone but has a significant difference when compared to the control. Zinc also showed an increase oxidative stress with a ROS profile showing M2 with 51.01% as compared to the control. In summary, figure 3.14B shows a graphical representation of ROS profile at with two cell populations of control, actinomycin D, LA-39B, LA-55, zinc and in combination.

A



B

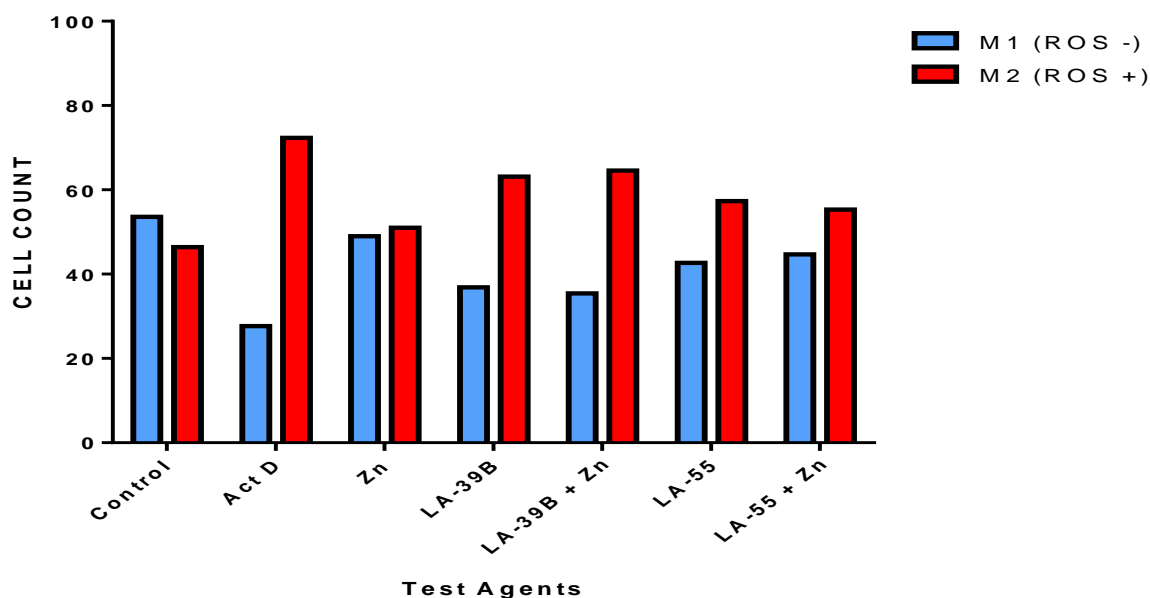


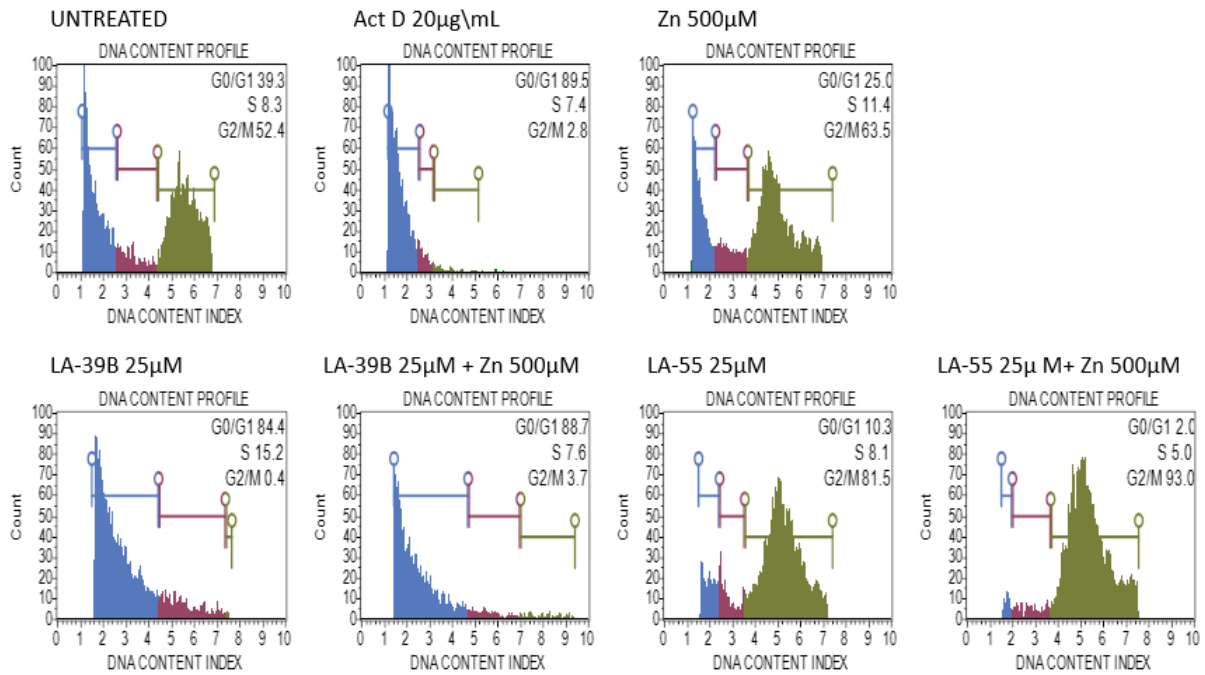
Figure 3.14 Determination of reduction of oxidative stress on A549 cells. Oxidative stress on A549 cells when treated with quinoxaline derivatives (LA-39B & LA55) on 25µM, zinc on 500µM and in combination were assayed, using actinomycin D as a standard and untreated cell as control(B). Flow cytometric was done using Muse Analyzer. A comparative summary of the assay outcome in also illustrated (B).

3.15 Analysis of cell cycle arrest on A549 cells when treated with quinoxaline derivatives (LA-39B & LA-55), zinc and in combination

The effect on cell cycle arrest on A549 cells when treated with quinoxaline derivatives (LA-39B & LA-55), zinc and in combination (LA-39B+zinc & LA-55+zinc) was determined through cell cycle analysis which is principled on staining DNA with PI (propidium iodide) which is impermeable to viable cells with an intact membrane but permeable to dead cells with compromised membrane. Quinoxaline derivatives (LA-39B & LA-55) of 25 μ M and zinc (500 μ M) were prepared. Actinomycin D (20 μ g/mL) was used as positive control (standard) and untreated cells were used as a control. Cell cycle arrest is displayed as DNA content index at different cell cycle phases [Figure 3.15A]. LA-39B arrested more cells at the G₀/G₁ phase with a DNA content index of 84.4% and S phase with a DNA content index of 15.2%, when compared to the untreated control. When LA-39B is in combination with zinc, there is an increase in the number of cells arrested in the G₀/G₁ phase with a DNA content index of 88.7%, with a decrease in the DNA content index of the S phase moving slightly to the G₂/M phase.

LA-55 arrested more cells in the G₂/M phase with a DNA content index of 81.4% with few cells in the G₀/G₁ phase and S phase when compared to the untreated control. When LA-55 is in combination with zinc, there is an increase in the number of cells arrested in the G₂/M phase with a DNA content index of 93.0% with a decrease in the DNA content index of cells in the G₀/G₁ and S phase when compared to the control. Zinc arrested more cells in the G₂/M phase with a DNA content index of 63.5% with a decrease in the DNA content index of cells in the S and G₀/G₁ phase when compared to untreated control. As expected, actinomycin D arrested cells in the G₀/G₁ phase with a DNA content index of 89.5% with few cells in the S and G₂/M phase when compared to the untreated control. In summary, figure 3.15B shows a graphical representation of the DNA content index of control, actinomycin D, quinoxaline derivatives, zinc and in combination.

A



B

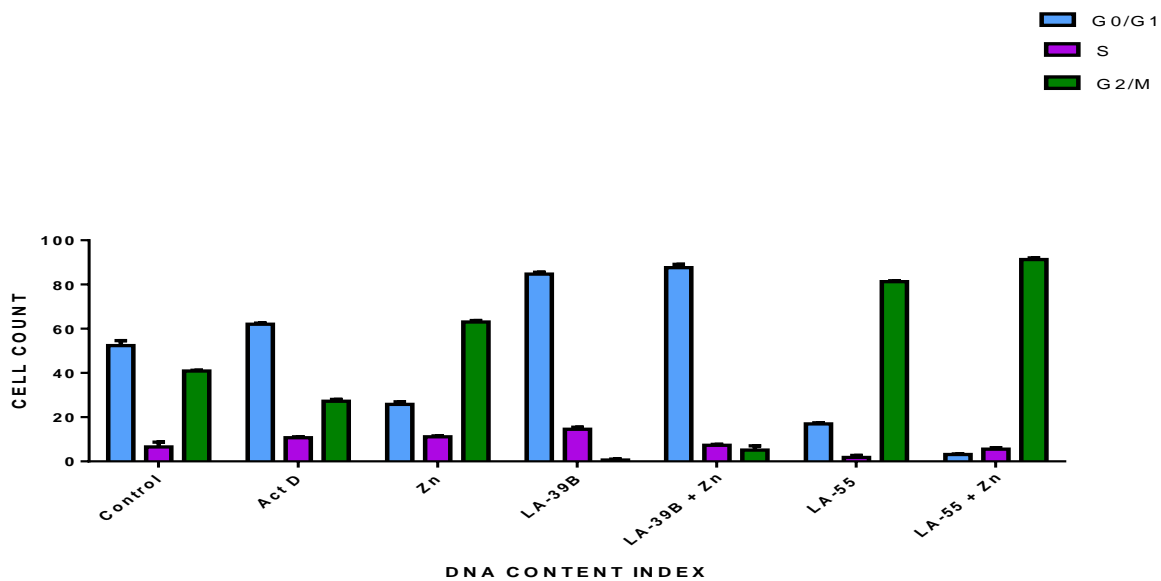


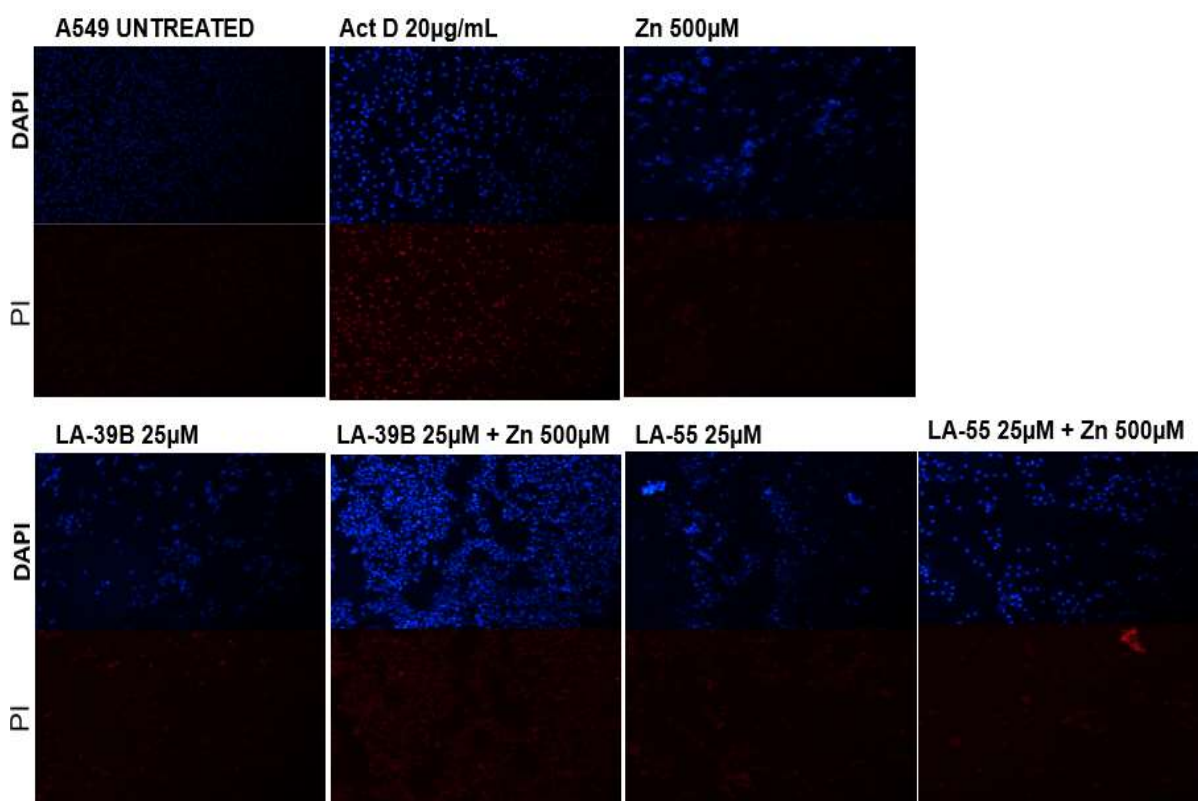
Figure 3.15 Cell cycle analysis on A549 cells. Cell cycle arrest on A549 cells when treated with quinoxaline derivatives (LA-39B & LA55) on 25µM, zinc on 500µM and in combination were assayed, using actinomycin D (20µg/mL) as a standard and untreated cell as control. Muse Analyzer™ was used to analyse the DNA index.

3.16. Apoptosis analysis through nuclear staining on A549 cells after treatment with LA-39B and LA-55

Fluorescence intensity of the DNA of A549 cells when treated with quinoxaline derivatives (LA-39B & LA-55), zinc and in combination (LA-39B+zinc & LA-55+zinc) was determined through staining the cells with fluorescent dyes (DAPI & PI) which is principled on the ability of DAPI to stain the DNA of both live and dead cells but fluoresces more on condensed chromatin while PI stains only dead cells and fluoresces more with cells undergoing late apoptosis'/necrosis. Quinoxaline derivatives (LA-39B & LA-55) of 25 μ M and zinc (500 μ M) were prepared. Actinomycin D (20 μ g/mL) was used as positive control (standard) and untreated cells were used as a control. Fluorescence of DAPI is displayed as a blue colour while PI is represented as a red colour [Figure 3.17A]. LA-39B had increased fluorescence with a mean intensity of 7.193 as compared to control with mean intensity of 4.716 when stained with DAPI. When stained with PI it also had it still had increased fluorescence with a mean intensity of 3.243 as compared to the control with mean intensity of 2.183. When LA-39B is in combination with zinc the is an increase in the fluorescence with a mean intensity of 20.212 as compared to the control and LA-39B alone when stained with DAPI. When stained with PI the is still an increase in the fluorescence with a mean intensity of 5.449 as compared to control and LA-39B alone.

LA-55 had increased fluorescence with a mean intensity of 7.073 as compared to control when stained with DAPI. When stained with PI it also had it still had increased fluorescence with a mean intensity of 3.537 as compared to the control. When LA-55 is in combination with zinc the is an increase in the fluorescence with a mean intensity of 8.277 as compared to the control and LA-55 alone when stained with DAPI. When stained with PI the is still an increase in the fluorescence with a mean intensity of 3.738 as compared to control and LA-55 alone. Zinc had increased fluorescence with a mean intensity of 6.626 as compared to control when stained with DAPI. When stained with PI it also had it still had increased fluorescence with a mean intensity of 3.503 as compared to the control. As expected, actinomycin D had increased fluorescence with a mean intensity of 9.709 as compared to control when stained with DAPI. When stained with PI it also had it still had increased fluorescence with a mean intensity of 4.901 as compared to the control. In summary, figure 3.16B show the graphical representation of the mean fluorescence intensities of both DAPI and PI.

A



B

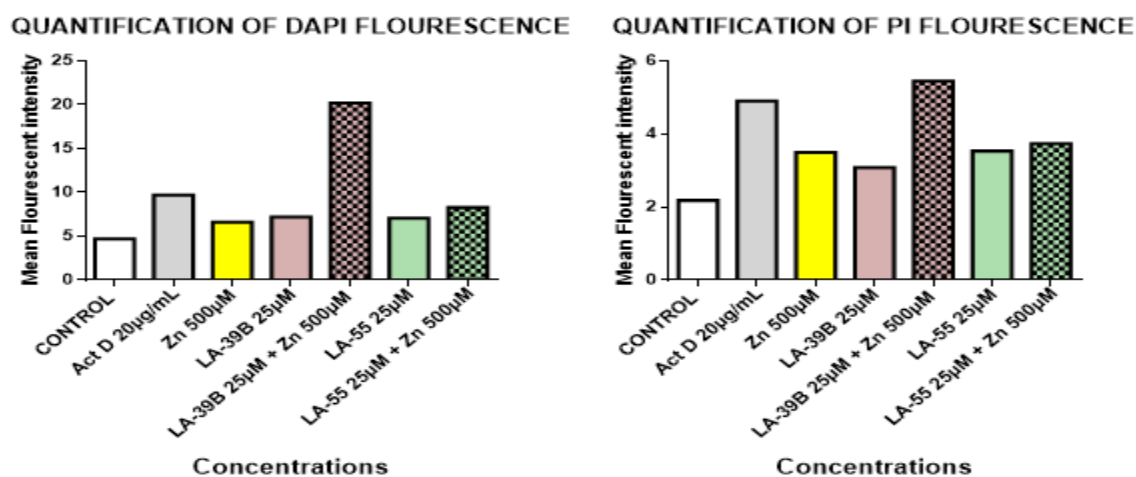


Figure 3.16 Nuclear analysis using DAPI and PI staining on A549 cells. Fluorescence of A549 cells when treated with quinoxaline derivatives (LA-39B & LA55) on 25µM, zinc on 500µM and in combination were assayed, using actinomycin D (20µg/mL) as a standard and untreated cell as control. Images were captured using Nikon Ti-E inverted microscope.

3.17 Morphological analysis of apoptosis on A549 cells when induced with quinoxaline derivatives (LA-39B & LA-55), zinc and in combination

The ability to induce apoptosis on A549 cells when treated with quinoxaline derivatives (LA-39B & LA-55), zinc and in combination (LA-39B+zinc & LA-55+zinc) was determined through dual staining with acridine orange (AO) which stains the DNA and RNA of live cells and ethidium bromide (EB) which stains exposed DNA and RNA of dead/necrotic cells. The combination of the two dyes resembles apoptosis. Quinoxaline derivatives (LA-39B & LA-55) of 25 μ M and zinc (500 μ M) were prepared. Actinomycin D (20 μ g/mL) was used as positive control (standard) and untreated cells were used as a control. Fluorescence of AO is displayed in a green colour, EB in red and the combination of the two dyes (AO/EB) in orange [Figure 3.17]. LA-39B showed signs of apoptosis in which an orange colour fluoresced as compared to the control which fluoresced a green colour. When in combination with zinc there was an increase in the number of cells undergoing apoptosis displaying an orange as compared to the control and LA-39B alone.

LA-55 was also able to induce apoptosis in which an orange colour on cells as compared to control. When in combination with zinc there is a significant increase in the number of cells undergoing apoptosis, which are displaying an orange colour as compared to the control and LA-55 alone. Zinc also induces apoptosis in which an orange colour is observed as compared to the control. As expected, actinomycin D showed signs of apoptosis in which an orange colour is observed. In summary, the quinoxaline derivatives, zinc and in combination display signs of apoptosis.

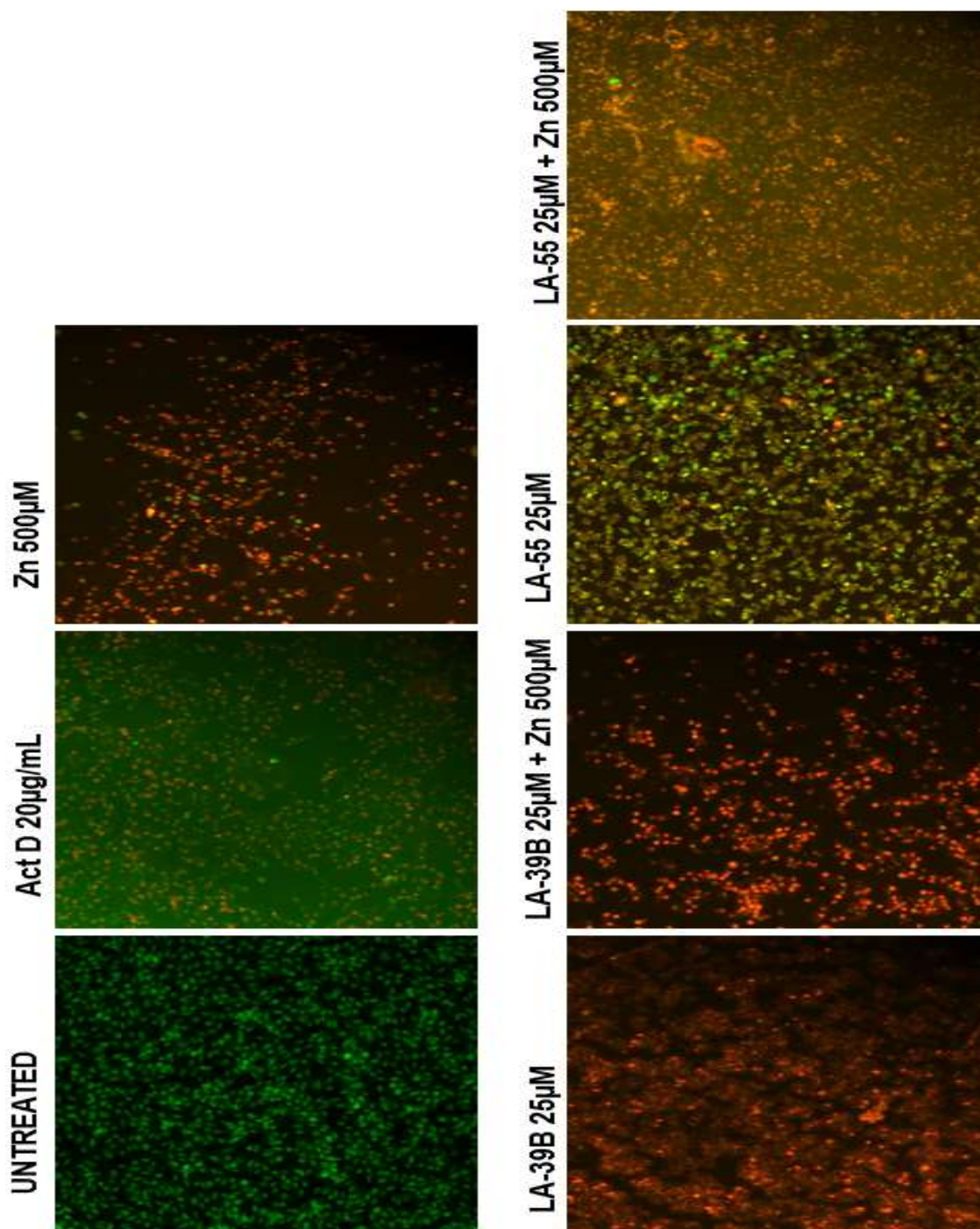


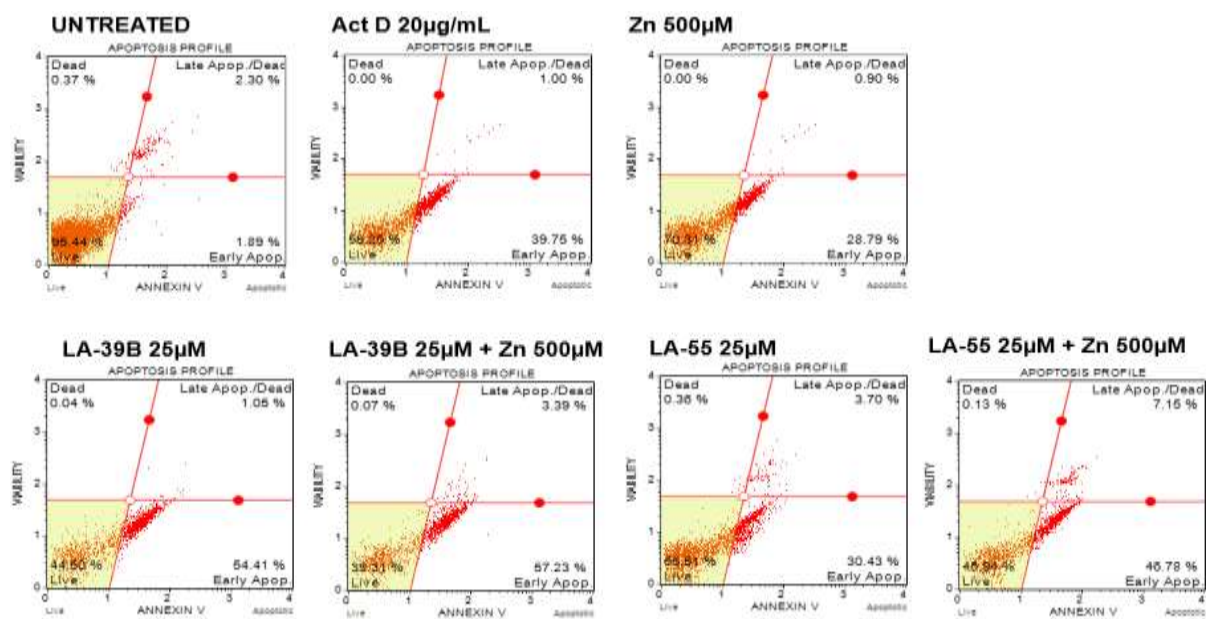
Figure 3.17 AO/EB fluorescence microscopy on A549 cells. Fluorescence of A549 cells when treated with quinoxaline derivatives (LA-39B & LA55) on 25µM, zinc on 500µM and in combination were assayed, using actinomycin D (20µg/mL) as a standard and untreated cell as control. Images were captured using Nikon Ti-E inverted microscope.

3.18 Apoptosis analysis on A549 cells when induced with quinoxaline derivatives (LA-39B & LA-55), zinc and in combination

Apoptosis profile on A549 cells when treated with quinoxaline derivatives (LA-39B & LA-55), zinc and in combination (LA-39B+zinc & LA-55+zinc) was determined through annexin V and PI stain which is based on the staining of cells undergoing early apoptosis with annexin V which binds to phosphatidylserine which is being expressed on an impermeable membrane, while with late apoptosis, PI will be able to bind to the DNA due to permeability of the membrane. Quinoxaline derivatives (LA-39B & LA-55) of 25 μ M and zinc (500 μ M) were prepared. Actinomycin D (20 μ g/mL) was used as positive control (standard) and untreated cells were used as a control. Apoptosis profile is displayed in a quadratic format showing stages of apoptosis [Figure 3.19A]. LA-39B induced early apoptosis with an apoptosis profile of 54.41% as compared to the control which had an apoptosis of 1.89% on early apoptosis. When in combination with zinc, there is an increase in the number of cells undergoing early apoptosis with an apoptosis profile of 57.23% as compared to the control and LA-39B alone.

LA-55 also induced early apoptosis with an apoptosis profile of 30.43% as compared to the control and had a significant increase in the number of cells undergoing early apoptosis when in combination with zinc with an apoptosis profile of 46.78% as compared to control. Zinc induced early apoptosis with an apoptosis profile of 28.79% as compared to the control. As expected, actinomycin D induced early apoptosis with an apoptotic profile of 39.75%. In summary, figure 3.18B shows a graphical representation of apoptosis profile at different stages of control, actinomycin D, LA-39B, LA-55, zinc and in combination.

A



B

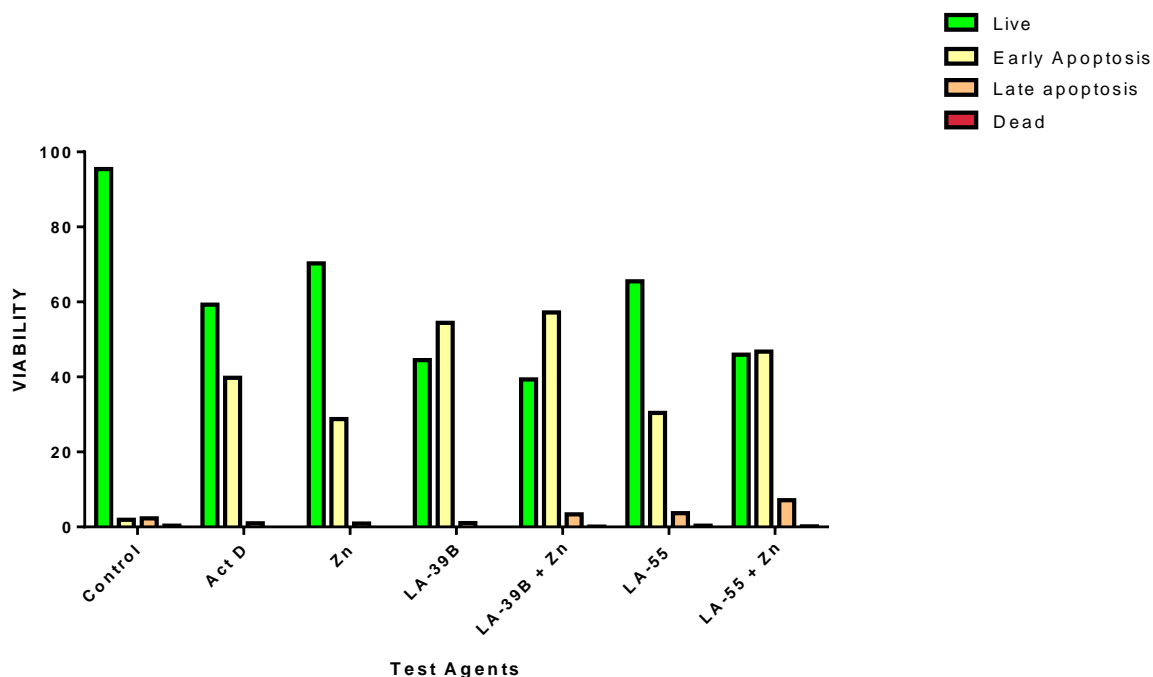


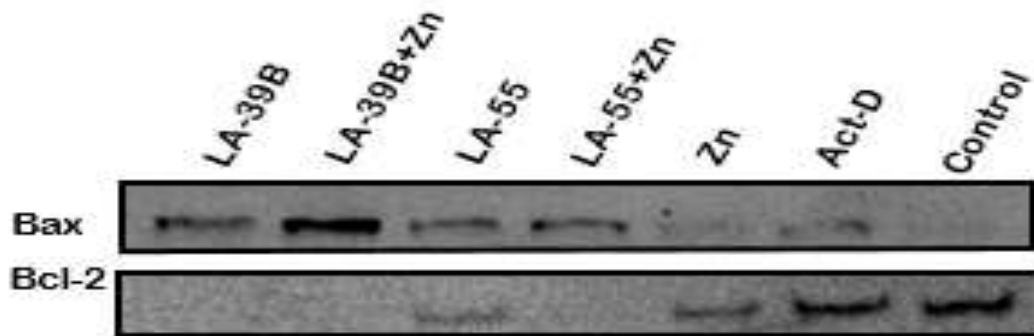
Figure 3.18 Determination of apoptosis on A549 cells using annexin V/dead cell assay. Apoptosis on A549 cells when treated with quinoxaline derivatives (LA-39B & LA55) on 25µM, zinc on 500µM and in combination were assayed, using actinomycin D as a standard and untreated cell as control. Flow cytometric analysis was done using Muse Analyzer.

3.19 Bcl-2 and Bax protein ratio expression on A549 cells when treated with quinoxaline derivatives (LA-39B & LA-55), zinc and in combination

The expression of Bcl-2 and Bax protein on A549 cells when treated with quinoxaline derivatives (LA-39B & LA-55), zinc and in combination (LA-39B+zinc & LA-55+zinc) was determined using western blot which displays the expression of protein represented as bands. The band thickness or volume represented the level of expression, the thicker the band the higher the expression of the protein which will be made in reference to the control [figure 3.19A]. When cells were treated with LA-39B, the expression of Bax is high with no expression of Bcl-2 when compared to the control which had expression of Bcl-2 and no expression of Bax. When LA-39B was used in combination, there was higher expression of Bax with no expression of Bcl-2 when compared to the control. When cells were treated with LA-55, there was high expression of Bax than the expression of Bcl-2 when compared to the control. In combination treatment of LA-55 and zinc, there was higher expression of Bax with no expression of Bcl-2 when compared to the control.

Zinc treatment displayed higher Bcl-2 expression than the expression of Bax when compared to the control that had highest expression of Bcl-2 with no expression of Bax. Actinomycin D, expressed high Bcl-2 than Bax when compared to the control which had no expression of Bax. In summary, Figure 3.19B shows the graphical representation of the band volume of with different treatment agents along with the controls.

A



B

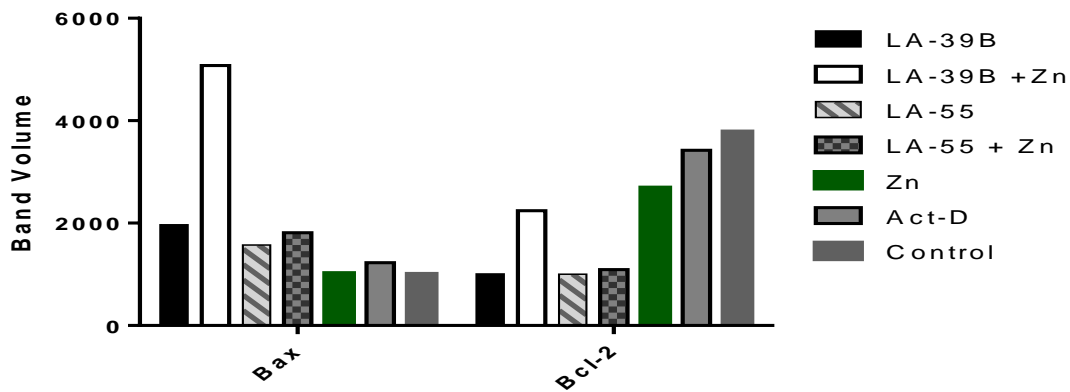


Figure 3.19 Analysis of Bcl-2/Bax ratio expression on A549 cells. In order to determine the expression of the above depicted proteins A549 cells were treated with LA-39B, LA-39B+Zn, Zn, LA-55, LA-55+Zn and Act-D for 24 hrs. This was then followed by isolation of proteins then western blotting assay. The pictures were captured with ChemiDoc XRS+ (Bio-RAD, USA). The blot picture shows the expressed Bax and Bcl-2 (A). The ChemiDoc XRS+ software was used to measure band volume and then the plots were developed with Graph pad prism 6 software to show the expression difference of the Bax to Bcl-2 A549 cells (B). The Bax Bcl-2 ratio show apoptosis at a molecular level. Over expression of Bcl-2 mean viability while Bax mean apoptosis. Apoptosis is demonstrated by reciprocal expression of bax to bcl-2.

CHAPTER 4: DISCUSSION AND CONCLUSION

Despite major advancements in the management of cancer through chemotherapy, the progressive pledge in research of discovering new treatment with improved efficacy remains of crucial importance (Noolvi *et al.*, 2011; Al-Rashood *et al.*, 2006). The use of quinoxaline hybrids has been employed as a mechanism of attempting to discover treatment that will have selectivity (Noolvi *et al.*, 2011). The use of radiation along with chemotherapy are some of the effective treatment plans implemented in the control of cancer progression. These treatment options lead to an increase in intracellular ROS levels especially in non-cancerous cells but in contrast these high levels of ROS contribute to the killing of cancer cells (Vijaya *et al.*, 2018; Moding *et al.*, 2013; Indran *et al.*, 2011). The imbalance in ROS levels due to certain treatments has been associated with side effects such as heart failure (Carvalho *et al.*, 2014). Hence the present study aimed at exploring treatment that will not only promote killing and inhibition of cancer cells proliferation but also be able to offer a protective effect on normal cells.

A body of experiments showed that quinoxaline derivatives possess antioxidant properties which could contribute to their protective measure on normal cells; hence, Raw 264.7 macrophages were used as normal non-cancerous cells in the current study. Advancement in cancer treatment is discovering a drug that will have preferential killing and selectively induce apoptotic cell death while sparing non-cancerous cells. Amongst the hybrids of quinoxalines which were used in the present study, quinoxaline derivatives LA-39B and LA-55 exhibited more antioxidant activity compared to quinoxaline derivatives LA-65C3 and LA-16A [figure 3.1B and figure 3.2B] which were evaluated using ferric reducing power and DPPH. Their possession of antioxidant activity can be accounted for by the reaction between the free radicals and the nitrogen atom of the quinoxaline structure which gives them stability through their ability to donate the hydrogen atom (Mani *et al.*, 2018; Sankaran *et al.*, 2010; Zhang, 2005).

The selective cytotoxic ability of quinoxalines was tested on Raw 264.7 macrophage cell line using the MTT viability assay wherein cells were challenged with selected quinoxaline derivatives for 24 hours. The results showed no significant cytotoxicity [figure 3.4B and 3.5] of quinoxaline derivatives on Raw 264.7 macrophages whereas

an extremely significant cytotoxic effect was observed on A549 lung cancer cells [figure 3.9B and 3.10] when treated with quinoxaline derivatives LA-39B and LA-55. The alteration of the quinoxaline derivatives side chain has been shown to improve effectiveness along with specificity to certain cell lines in a dose dependent pattern (Huanga *et al.*, 2018; Tu *et al.*, 2011; Wei *et al.*, 2000). Noolvi *et al* reported that quinoxaline analogy displays significant signs of selectivity with regards to different cell lines (Noolvi *et al.*, 2011).

In the present study, the uniqueness of the side chains attached to the quinoxaline core ring structure seemed to confere unique and significant characteristics to the quinoxaline derivative with LA-55 and LA-39B exhibiting much higher anti-cancer activities. The prop-2-nl-1-o1 side chain and the methanesulfonate group attached to the quinoxaline core in the LA-55 and LA-39B structures, respectively, seemed to be responsible for the observed anticancer activities. Prop-2-nl-1-ol has been incorporated in anticancer agents in which anti-proliferative effect has been observed. (E)-2-arylmethylideneidolin-3-ol is a compound which incoporates Prop-2-nl-1-ol and has been reported to have properties oh inhibition of proliferation of cancer cells (Murthi *et al.*, 2015). Sardon *et al* reported that from a series of novel Aurora A kinase inhibitor drug agents they tested, the quinoxaline derivative which induced anti-proliferative activity on cancer cells did not necessarily target the protein of interest (Sardon *et al.*, 2009). Methanesulfonate is used in conjunction to an alcohol group and has been approved as a chemotherapeutic agent. One of the approved drugs is methyl methanesulfonate which was reported to cause advent and reversible hyperacetylation in proteins found in the cytoplasm and nucleus which are associated with cancer cell death (Lee *et al.*, 2007). It is therefore probable that these unique side chains added to LA-55 and LA-39B could be responsible for the induction of cancer cell death in the various cell lines tested.

The antioxidant activity which gives the ability to scavenge free radicals was observed in the H₂DCFDA assay performed on Raw 264.7 cells which displayed an increase in the number of live cells with a decrease in the number of cells with free radicals after treatment with quinoxaline derivative LA-39B and LA-55 [figure 3.13A and 3.13B]. Since most chemotherapeutic drugs are accompanied by undesirable side effects

there is a great need for treatment that can suppress side effects through the use of antioxidant supplements (Vijaya *et al.*, 2018). It can be suggested that an ideal treatment would be one that carries both properties of tumour suppressing activity along with antioxidant properties. High levels of ROS within non-cancerous are considered to play a crucial role in their transformation to malignant cells (Sablina *et al.*, 2005; Liou and Storz, 2010). An imbalance between ROS and antioxidants leads to an irreversible damage of lipids, DNA and proteins (Roy *et al.*, 2015; Bedard and Krause, 2007).

In contrast to the effect of high levels of ROS in non-cancerous cells, high levels of ROS in cancer cells can be used as an advantage to push cells to the edge of cell death. A rationale has been made that non-cancerous cells may have the capability to tolerate drug-induced ROS production and resultant oxidative stress up to a certain threshold whereby homeostasis is still maintained along with cell survival but the threshold of cancer cells is extremely low and these induced ROS levels leads to their death (Roy *et al.*, 2015). When ROS levels was tested on a cancer cell line (A549) [figure 3.14A and figure 3.14B], an increase in the levels ROS was observed when treated with quinoxaline derivative LA-39B and LA-55. When the quinoxaline derivatives were used in combination with zinc there was an increase in ROS levels with subsequent corresponding decrease in live cells. Selective ROS modulation gives a strategy for anticancer treatment (Quintavalle *et al.*, 2011; Bedard and Krause, 2007). ROS modulation can also contribute to the control of normal cell physiology along with inflammation disorders (Mani *et al.*, 2018). It can also contribute to the induction of apoptosis; for example, 4 β -hydroxywithanolide E and tunifolide B were previously shown to modulate ROS through the induction and apoptosis (Fang, 2011; Waris and Ahsan, 2006).

A number of studies are being conducted wherein quinoxaline are used as templates. Hajri *et al* synthesized a series of new quinoxaline derivatives in which they were evaluated for antitumor activity against NSCLS (A549) and glioblastoma (U87-MG) cell lines (Hajri *et al.*, 2016). The change in position of the 3-ethyl group which was attached to the quinoxaline base structure resulted in a decrease in the antiproliferative activity while the para substituted quinoxaline derivative had an increase in its antiproliferative activity (Tariq *et al.*, 2018). In this current study, a novel cohort of quinoxaline derivatives was synthesized where the position of the side chains

of the quinoxalines could be associated to the observed differences in antitumor activity. The difference between LA-39B and LA-16A is the addition of a sulphur atom to the structure of LA-39B which resulted in its high antiproliferative activity against HeLa and MCF-7 cells at 100 μ M. In A549 cells, LA-39B induced inhibition of up to 50% at only 25 μ M. The same trend was observed between LA-55 and LA-65C3, in which they differ in terms of the position of the alcohol group, when the OH- is on carbon atom 3 (LA-55) there was improved antiproliferative activity in HeLa and MCF-7 cells at 100 μ M and significant efficacy on A549 cells at low concentrations of 25 μ M. Tseng *et al* also proved it in their study that the position of the side chain had an effect on the antiproliferative activity of the quinoxaline derivative (Tseng *et al.*, 2016).

In an attempt to improve efficacy, combining quinoxaline derivatives with trace elements also forms the core of the current study. Zinc has been identified as one of the crucial trace elements that plays a role in a number of protein and transcriptional factors that regulate the cell's optimum functioning (Jagadeesan and Sivanantham, 2012). Research shows that zinc has the potential to induce apoptosis in a number of cells such as prostate epithelial cells, neuron and glial cells, ovarian cells, oesophageal epithelial cells, choriocarcinoma cells and hepatoma cells (Franklin and Costello, 2009). Due to anticancer properties exhibited by zinc, research aims at finding strategies that will enhance its cellular uptake and functioning (Limbach *et al.*, 2007). In the present study, zinc was found to be cytotoxic and had the potential to inhibit cell proliferation in HeLa [figure 3.6 and 3.7], MCF-7 [figure 3.8] and A549 [figure 3.9 and 3.10] but not Raw 264.7 cells [figure 3.4 and 3.5]. These findings support what has been reported about its properties and its importance in cancer treatment. When zinc was used in combination with quinoxaline derivatives, there was an enhancement of its anticancer activity [figure 3.11 and 3.12]. This may be due to improved cellular uptake and function. An increase in ROS levels was observed when Raw 264.7 [figure 3.13] and A549 [figure 3.14] cells were treated with zinc and combination of zinc and quinoxaline derivatives (LA-39B and LA-55). Previous research supports the results found in terms of the increase in ROS levels observed when cells were treated with zinc (Chen *et al.*, 2008). Other researchers also observed an increase in oxidative stress due to an increase in ROS production as a result of challenging cells with zinc (Wu and Zhang, 2018; Guo *et al.*, 2008). The increase in ROS has been reported to lead to apoptotic cell death in various studies. Increased ROS generation has been

reported to be a killing mechanism associated with zinc's anticancer properties (Wu and Zhang, 2018).

Upon observation of cell growth inhibition, cell cycle analysis was performed. A number of studies previously performed on quinoxaline derivatives reported an induction of cell cycle arrest at different cell cycle phases. In this current study, the results obtained supported previous findings since cell cycle arrest was observed when cancer cells were challenged with quinoxaline derivatives of interest (Malumbres and Barbacid, 2009). Quinoxaline derivative LA-39B induced cell cycle arrest at G₀/G₁ phase, while LA-55 induced cell cycle arrest at in the G₂/M phase. G₀/G₁ phase is a cell progression checkpoint, in which a cell goes through a restriction point to progress to the synthesis (S) phase. Damage in the DNA leads to the activation of ATM/ATR and Chk1/2 kinase to inhibit the activity of CDK which leads to cell cycle arrest to allow DNA repair or cell death (Malumbres and Barbacid, 2009).

The G₂/M phase is a checkpoint which is responsible for stopping cells with damaged DNA from proceeding with mitosis. Damaged DNA activates a number of kinases that activate Chk1/2 and p53 (Wohlbold and Fisher, 2009). Induction of cell cycle arrest at S phase was also previously recorded when the cells were treated with quinoxaline derivative (Mani *et al.*, 2018). In this current study, cells treated with zinc exhibited cell cycle arrest at the G₂/M phase. When the cells were treated with a combination of quinoxalines and zinc there was an enhancement of the activity of the quinoxaline, whereby with quinoxaline derivative LA-39B, *more cells were arrested* in the G₀/G₁ phase and with quinoxaline derivative LA-55, more cells were arrested in the G₂/M phase. In a study conducted by Huang *et al*, quinoxaline derivatives induced cell cycle arrest at the G₁ phase followed by a decrease in cell population in the G₂/M and S phase (Huanga *et al.*, 2018). These results give a breaking ground in terms of the mode of death employed by the drugs in relation to the cell cycle checkpoints. Elevated ROS levels have been reported to induce DNA damage and activate cell cycle checkpoint arrest (Guachalla and Rudolph, 2010).

Cell death can occur by either necrosis which is caused by external injury or apoptosis which is programmed cell suicide by internal or external stimuli (Wong, 2011). Apoptosis is characterised by morphological changes that also occur in the nucleus that include chromatin condensation which is followed by nuclear fragmentation and

swelling of the cell (Wong, 2011; Kroemer *et al.*, 2005). To achieve this, treatment agents have to attempt to trigger and stimulate pro-apoptotic proteins either internally or externally in order to initiate morphological changes that occur during apoptosis. Nuclear analysis was conducted in this study through staining the cells with DAPI/PI [figure 3.16A]. The results obtained showed nuclear condensation of the A549 cells when they were treated with quinoxaline derivatives (LA-39B and LA-55) and zinc through fluorescence of the DAPI stain. When cells were treated with combination of quinoxaline and zinc there was an increase in the number of cells exhibiting DAPI intense bright fluorescence. DAPI fluorescence displays chromatin condensation or nuclear damage which is achieved through its attachment to the A-T rich segments of the DNA (Mani *et al.*, 2018). As DAPI can pass through an intact cell membrane, it can be used to stain both live and fixed cells, though it passes through the membrane less efficiently in live cells and therefore the effectiveness of the stain is lower. It stains damaged nuclear DNA easily giving it a high fluorescent intensity (Mani *et al.*, 2018). A study conducted by Mani *et al.* reported cell death via apoptosis upon observations made using the DAPI nuclear staining assay after treatment of cells with quinoxaline derivatives (Mani *et al.*, 2018). In a study done by Wu and Zhanga, fluorescence-based staining was used to report cell death via apoptosis when cells displayed intense fluorescence of Hoechst 22242 stain which functions in a similar manner as DAPI (Wu and Zhang, 2018).

In the current study, cells did not display any significant PI fluorescence after treatment with quinoxaline derivatives. This is a positive sign that quinoxaline derivatives, zinc and combination treatment induced apoptotic cell death rather than necrosis. It is known that PI is only permeable to dead cells in order to gain access to the intracellular DNA. In a study conducted by Huang *et al.*, treatment of cells using quinoxalines induced necrosis after nuclear analysis through DAPI/PI stain wherein a high fluorescent intensity of PI was observed (Huang *et al.*, 2014). It was further illustrated that after 24 hours cells displayed cell membrane defects which was due to the entry of the PI stain (Huang *et al.*, 2014). Cells displaying PI fluorescence are regarded to be undergoing late apoptosis/necrosis owing to damage in their plasma membrane (Coleman *et al.*, 2001; Bredesen, 1995).

To further analyse morphological changes due to apoptosis, AO/EB assay was employed wherein results obtained supported what was observed with DAPI/PI assay.

When cells were treated with quinoxaline derivatives (LA-39B and LA-55) and zinc, signs of cells undergoing early apoptosis were observed. Combination of quinoxaline derivatives with zinc resulted in an increase in the number of cells undergoing early apoptosis [figure 3.17]. AO/EB stain helps differentiate live from early apoptotic cells and early apoptotic cells to those in late apoptosis or undergoing necrosis. AO is a cell permeable stain which stains the nucleus with a green fluorescence while EB stains dead cells with a disrupted plasma membrane gaining access to the nuclei and giving a red fluorescence. The combination of the two stains give cells an orange fluorescence due to partial entry of the EB resembling early apoptosis (Mallavadhani *et al.*, 2014). A study conducted by Mani *et al.*, also employed this method to assess inhibition of cell growth through apoptosis or necrosis (Mani *et al.*, 2018).

To verify the morphological results observed through the use of DAPI/PI and AO/EB methods upon treatment with quinoxaline derivatives (LA-39B and LA-55) and zinc the annexin V/dead cell assay was carried out. Wu and Zhanga reported that zinc oxide nanoparticles induced apoptosis through the use of annexin V/PI assay (Wu and Zhang, 2018). A study done by Ku *et al.* reported that zinc sulphate induced early apoptosis through the use of annexin V assay (Ku *et al.*, 2012). Results obtained from this current study displayed the induction of early apoptosis with an increase in the number of cells when treated with combination of quinoxalines and zinc. The results obtained from treatment of cells with zinc are supported by the results found from the study conducted by Ku *et al.*, 2012.

Treatment agents that can repair the apoptotic signalling pathway have become of great interest to cancer researcher. After observation of signs of apoptosis, an investigation of the proteins involved in the activation of apoptosis were undertaken. Western blot method was employed to measure expression levels of pro-apoptotic (Bax) and anti-apoptotic (Bcl-2) proteins and results obtained showed down-regulation of Bcl-2 with upregulation of Bax expression [figure 3.19]. When the cells were treated with quinoxaline derivatives LA-39B and LA-55, an upregulation of Bax was observed although treatment of cells with zinc resulted in upregulation of Bcl-2 with minimal expression of Bax. The same trend was observed with previous assays wherein enhancement in activity of quinoxaline derivatives was observed when cells were treated in combination with zinc and *expression of Bax was elevated*. Pepper *et al.* reported an increase in Bcl-2/Bax ratio in patients with CLL but upon treatment the

number of cells that were undergoing apoptosis was inversely proportional to the Bcl-2/Bax ratio (Pepper *et al.*, 1997). This observation supports the results obtained in the current study wherein an increase in the number of cells undergoing apoptosis was observed in combination treatments and this was accompanied by the upregulation of Bax with downregulation of Bcl-2.

In conclusion, the results obtained from this work suggests that novel quinoxaline derivatives LA-39B and LA-55 are potent adenocarcinoma treatment agents which can be used in combination with zinc to enhance their anticancer activity. The mode of action of these agents in combination with zinc can be associated with modulation of ROS levels wherein an increase in ROS levels leads to apoptosis along with the activation and upregulation of Bax protein and simultaneous downregulation of Bcl-2. These newly developed cohort of quinoxaline derivatives drugs may present new affordable alternatives with potential abilities for use in lung cancer treatment.

CHAPTER 5: REFERENCES

Akhtar MJ , Ahamed M , Alhadlaq HA and Alshamsan A, 2017. Mechanism of ROS scavenging and antioxidant signalling by redox metallic and fullerene nanomaterials: Potential implications in ROS associated degenerative disorders. *Biochimica et Biophysica Acta*, Volume 1861, pp. 802-813.

Poljsak B, Šuput D and Milisav , 2013. IAchieving the Balance between ROS and Antioxidants: When to Use the Synthetic Antioxidants. *Oxidative Medicine and Cellular Longevity*, Volume 2013, p. 11.

Tana C-S, Chob B-C and Soo RA, 2016. Next-generation epidermal growth factor receptor tyrosine kinase inhibitors in epidermal growth factor receptor -mutant non-small cell lung cancer. *Lung Cancer*, Volume 93, pp. 59-68.

Wong RSY, 2011. Apoptosis in cancer: from pathogenesis to treatment. *Journal of Experimental & Clinical Cancer Research*, Volume 30, p. 87.

Ali D, Mohammad DK, Mujahed H, Jonson-Videsäter K, Nore B, Paul C and Lehmann S, 2016. Anti-leukaemic effects induced by APR-246 are dependent on induction of oxidative stress and the NFE2L2/HMOX1 axis that can be targeted by PI3K and mTOR inhibitors in acute myeloid leukaemia cells. *British Journal of Haematology*, Volume 174, pp. 117-126.

Al-Rashood ST, Aboldahab IA, Nagi MN, Abouzeid LA, Abdel-Aziz AA, Abdel-Hamide SG, Youssef KM, Al-Obaid AM and El-Subbagh H, 2006. Synthesis, dihydrofolate reductase inhibition, antitumor testing, and molecular modeling study of some new 4(3H)-quinazolinone analogs.. *Bioorganic & Medicinal Chemistry*, Volume 14, pp. 8606-8621.

Andersen JK, 2004. Oxidative stress in neurodegeneration: cause or consequence?. *Nature Medicine*, Volume 10, pp. S18-S25.

Ashkenazi A, 2015. Targeting the extrinsic apoptotic pathway in cancer: lessons learned and future directions.. *Journal of Clinical Investigation*, Volume 125, pp. 487-489.

Banerjee A, Banerjee K, Sinha A, Das S, Majumder S, Majumdar S and Choudhuri SK, 2017. zinc Schiff base complex inhibits cancer progression both in vivo and in vitro by inducing apoptosis. *Environmental Toxicology and Pharmacology*, Volume 56, pp. 383-392.

Bedard K and Krause KH, 2007. The NOX family of ROS-generating NADPH oxidases: physiology and pathophysiology. *Physiological Reviews*, Volume 87, p. 245–313.

Beraldo H and Gambino D, 2004. The wide pharmacological versatility of semicarbazones, thiosemicarbazones and their metal complexes. *Mini-Reviews in Medicinal Chemistry*, Volume 4, pp. 31-39.

Berkers CR, Maddocks ODK, Cheung EC, Mor I and Vousden KH, 2013. Metabolic Regulation by p53 Family Members. *Cell Metabolism*, Volume 18, pp. 617-633.

Bredesen DE, 1995. Neural apoptosis. *Annals of Neurology*, Volume 38, p. 839–851.

Bruni L, Diaz M, Castellsague X, Ferrer E, Bosch FX and Sanjose S, 2010. Human Papillomavirus prevalence in 5 continents: meta-analysis of 1 million women with normal cytological findings. *Journal of Infectious Diseases*, Volume 202, pp. 1789-1799.

Carvalho FS, Burgeiro A, Garcia R, Moreno AJ, Carvalho RA and Oliveira PJ, 2014. Doxorubicin-induced cardiotoxicity: from bioenergetic failure and cell death to. *Medicinal Research Reviews*, Volume 34, p. 106–135.

Castrogiovanni C, Waterschoot B, De Backer O and Dumont P, 2018. Serine 392 phosphorylation modulates p53 mitochondrial translocation and transcription-independent apoptosis. *Cell Death and Differentiation*, Volume 25, pp. 190-203.

Chen HH, Song IS, Hossain A, Choi MK, Yamane Y, Liang ZD, Lu J, Wu LY, Siddik ZH, Klomp LW, Savaraj N and Kuo MT, 2008. Elevated glutathione levels confer cellular sensitization to cisplatin toxicity by up-regulation of copper transporter hCtr1. *Molecular Pharmacology*, Volume 74, p. 697–704.

Chio IIC and Tuveson DA, 2017. ROS in Cancer: The Burning Question. *Trends in Molecular Medicine*, Volume 23, pp. 411-429.

Circu ML and Aw TY, 2010. Reactive oxygen species, cellular redox systems, and apoptosis.. *Free Radical Biology and Medicine*, Volume 48, pp. 749-762.

Coleman ML, Sahai EA, Yeo M, Bosch M, Dewar A and Olson MF, 2001. Membrane blebbing during apoptosis results from caspase-mediated activation of ROCK I. *Nature Cell Biology* , Volume 3, pp. 339-45.

Cross CE, Halliwell B, Borish ET, Pryor WA, Ames BN, Saul RL, McCord JM and Harman D, 1987. Oxygen radicals and human disease. *Annals of Internal Medicine*, Volume 107, pp. 526-545.

da Motta LL, Müller CB, De Bastiani MA, Behr GA, França FS, da Rocha RF, Minotto JB, Meurer RT, Fernandes MC, Roehe A, Markoski MM, Andrade CF, Castro MAA and Klamt F, 2014. Imbalance in redox status is associated with tumor aggressiveness and poor outcome in lung adenocarcinoma patients. *Journal of Cancer Research and Clinical Oncology*, Volume 140, pp. 461-470.

Dhawan DK and Chada VD, 2010. Zinc: A promising agent in dietary chemoprevention of cancer. *Indian Journal of Medical research*, Volume 132, pp. 676-682.

Dickinson BC and Chang CJ, 2011. Chemistry and biology of reactive oxygen species in signaling or stress responses. *Nature Chemical Biology* , Volume 7, pp. 504-511.

El Adnani Z, Sfaira MMM, Benzakour M, Benjelloun A, Ebn Touhami M, Hammouti B and Taleb M, 2012. Investigation of Newly Pyridazine Derivatives as Corrosion Inhibitors in Molar hydrochloric Acid. Part III: Computational Calculations. *International Journal of ELECTROCHEMICAL SCIENCE* , Volume 7, pp. 3982-3996.

Fang FC, 2011. Antimicrobial actions of reactive oxygen species. *mBio*, Volume 2, pp. e00141-00411.

Feng P, Li TL and Guan ZX, 2002. Direct effect of zinc on mitochondrial apoptosis in prostate cells. *Prostate*, Volume 52, pp. 311-318.

Ferlay J, Soerjomataram I, Dikshit R, Eser S, Mathers C, Rebelo M, Parkin DM, Forman D and Bray F, 2015. Cervical cancer Incidences, Mortality and Preveence Worldwide: Sources, methods and major patterns in GLOBOCAN 2012. *International Journal of Cancer*, Volume 136, pp. E359-E386.

- Follis AV, Llambi F, Merritt P, Chipuk JE, Green DR and Kriwacki RW, 2015. Pin1-induced proline isomerization in cytosolic p53 mediates BAX activation and apoptosis. *Molecular Cell*, Volume 59, pp. 677-684.
- Franklin RB and Costello LC, 2009. The important role of the apoptotic effects of zinc in the development of cancers. *Journal of Cellular Biochemistry*, Volume 106, p. 750–757.
- Friesen C, Fulda S and Debatin KM, 1997. Deficient activation of the CD95 (APO-1/Fas) system in drug resistant cells. *Leukaemia*, Volume 11, pp. 1833-1841.
- Fulda S, Los M, Friesen C and Debatin KM, 1998. Chemosensitivity of solid tumour cells in vitro is related to activation of the CD95 system. *International Journal of Cancer*, Volume 76, pp. 105-114.
- Galal SA, Abdelsamie AS, Soliman SM, Mortie J, Wolber G, Ali MM, Tokuda H, Suzuki N, Lida A, Ramadan RA and El Diwani HI, 2013. Design, synthesis and structure-activity relationship of novel quinoxaline derivatives as cancer chemopreventive agent by inhibition of tyrosine kinase receptor. *European Journal of Medicinal Chemistry*, Volume 69, pp. 115-124.
- Ge G, Wang A, Yang J, Chen Y, Yang J, Li Y and Xue Y, 2016. Interleukin-37 suppresses tumor growth through inhibition of angiogenesis in non-small cell lung cancer. *Journal of Experimental & Clinical Cancer Research*, Volume 35, pp. 1-10.
- Gerber D, 2008. EGFR Inhibition in the treatment of non-small cell lung cancer. *Drug Development Research*, Volume 69, pp. 359-372.
- Gesthalter YB, Billatos E and Kathuria H, 2017. Lung Cancer. *Genomic and Precision Medicine.*, pp. 165-178.
- Gibson RS, King JC and Lowe N, 2016. A review of Dietary Zinc Recommendation. *Food Nutrition Bulletin*, Volume 37, pp. 443-460.
- Gomez NN, Davicino RC, Biaggio VS, Bianco GA, Alvarez SM, Fischer P, Masnatta L, Rabinovich GA and Gimenez MS, 2006. Overexpression of inducible nitric oxide synthase and cyclooxygenase-2 in rat zinc-deficient lung: involvement of a NF-kappaB dependent pathway. *Nitric Oxide*, Volume 14, pp. 30-38.

Gorrini C, Harris IS and Mak TW, 2013. Modulation of oxidative stress as an anticancer strategy. *Nature Reviews Drug Discovery*, Volume 12, pp. 931-947.

Guachalla LM and Rudolph KL, 2010. ROS induced DNA damage and checkpoint responses: influences on aging?. *Cell Cycle*, Volume 9, p. 4058–4060.

Guo D, Wu C, Jiang, H, Li Q, Wang X and Chen B, 2008. Synergistic cytotoxic effect of different sized ZnO nanoparticles and daunorubicin against leukemia cancer cells under UV irradiation. *Journal of Photochemistry and Photobiology*, Volume 93, p. 119–126.

Gupta NK, Shukla M and Tyagi S, 2016. Knowledge, attituded and practices of biomedical wste management among health care personnel in selectedc primary health care centres in Lucknow. *International Journal of Community Medicine and Public Health*, Volume 3, pp. 309-313.

Haase H and Rink L, 2010. Das essentielle spurenelement zink. *Biologie unserer Zeit*, Volume 40, pp. 314-321.

Haigis MC and Yankner BA, 2010. The aging stress response. *Molecular Cell*, Volume 40, pp. 333-344.

Hainaut P and Pfeifer GP, 2016. Somatic TP53 mutations in the era of genome sequencing. *Cold Spring Harbor Perspectives in Medicine*, Volume 6.

Hajri M, Esteve M, Khoumeri O, Abderrahim R, Terme T, Montana M and Vanelle P, 2016. Synthesis and evaluation of in vitro antiproliferative activity of new ethyl 3-(arylethynyl)quinoxaline-2-carboxylate and pyrido[4,3-b]quinoxalin-1(2H)-one derivatives. *European Journal of Medicinal Chemistry*, Volume 124, pp. 959-966.

Halliwell B and Gutteridge JMC, 1999. Free Radicals in Biology and Medicine. *Oxford University Oxford University*, Volume 2, pp. 1-25.

Hengartner MO, 2000. Apoptosis: corralling the corpses. *Cell*, Volume 104, pp. 325-328.

Huang C-Y, Ger T-R, Wei Z-H and Lai M-F, 2014. Compare Analysis for the Nanotoxicity Effects of Different Amounts of Endocytic Iron Oxide Nanoparticles at Single Cell Level. *PLoS ONE*, Volume 9, p. e96550.

Huanga AM, Lin KW, Lin WH, Wu LH, Chang HC, Ni C, Wang DL, Hsu HY, Su CL and Shih C, 2018. 1-Hydroxy-3-[(E)-4-(piperazine-dium)but-2-enyloxy]-9,10-anthraquinone ditrifluoroactate induced autophagic cell death in human PC3 cells. *Chemico-Biological Interactions*, Volume 281, pp. 60-68.

Indran IR, Tufo G, Pervaiz S and Brenner C, 2011. Recent advances in apoptosis, mitochondria and drug resistance in cancer cells. *Biochimica et Biophysica Acta* , Volume 1807, pp. 735-745.

Jaaks P and Bernasconi M, 2017. The proprotein convertase furin in tumour progression. *International Journal of Cancer*, Volume 141, pp. 654-663.

Jacobson MD, Weil M, and Raff MC, 1997. Programmed cell death in animal development. *Cell*, Volume 88, pp. 347-354.

Jadhavar PS, Kumar D, Purohit P, Pipaliya BV, Kumar A, Bhagat S and Chakraborti AK, 2014. Sustainable Approaches Towards the Synthesis of Quinoxalines. *Springer India*, Volume 13, pp. 412-534.

Jagadeesan A and Sivanantham B, 2012. Zinc: An effective agent in dietary chemoprevention of early stage of prostate cancer. *Basic Research Journal of Medicine and Clinical Sciences* , Volume 1, pp. 05-14.

Jaso A, Zarranz B, Aldana I and Monge A, 2005. Synthesis of New Quinoxaline-2-carboxylate 1,4-Dioxide Derivatives as Anti-Mycobacterium tuberculosis Agents. *Journal of Medicinal Chemistry*, Volume 48, pp. 2019-2025.

John E, Laskow TC, Buchser WJ, Pitt BR, Basse PH, Butterfield LH, Kalinski P and Lotze MT, 2010. Zinc in innate and adaptive tumor immunity. *Journal of Translational Medicine*, Volume 8, p. 118.

Johnstone RW, Ruefli AA and Lowe SW, 2002. Apoptosis: a link between cancer genetics and chemotherapy. *Cell*, Volume 108, pp. 153-164.

Kabanda MM, Murulana LC, Ozcan M, Karadag F, Dehri I, Obot IB and Ebenso EE, 2012. Quantum Chemical Studies on the Corrosion Inhibition of Mild Steel by Some Triazoles and Benzimidazole Derivatives in Acidic Medium. *International Journal of Electrochemical Science* , Volume 7, pp. 5035-5056.

Kailasam SM, Balasubramanian M, Werner K and Subramaniam PR, 2018. Enantioselective approach towards the synthesis of spiro-indeno [1,2-b] quinoxaline pyrrolothiazoles as antioxidant and antiproliferative. *Tetrahedron Letters*, Volume 59, pp. 2921-2929.

Ketter B, Harris JM, Talaska G, Meyer DJ, Pemble SE, Taylor JB, Lang NP and Kadlubar FF, 2009. The human glutathione S-transferase as supergene on susceptibility of lung cancer. *Environmental health perspectives*, Volume 98, p. 87.

Khan A, Gillis K, Clor J and Tyagarajan K, 2012. Simplified evaluation of apoptosis using the Muse cell analyzer. *Postepy Biochem*, Volume 58, pp. 492-496.

Killile AN and Killilea DW, 2007. Zinc deficiency reduces paclitaxel efficacy in LNCaP prostate cancer cells. *Cancer Letters*, Volume 258, pp. 25870-25879.

Kim YS, Morgan MJ, Choksi S and Liu ZG, 2007. NF-induced activation of the Nox1 NADPH oxidase and its role in the induction of necrotic cell death. *Molecular Cell*, Volume 26, pp. 675-687.

Kocdor H, Ates H, Aydin S, Cehreli R, Soyarat F, Kemanli P, Harmanci D, Cengiz H and Kocdor MA, 2015. Zinc supplementation induces apoptosis and enhances antitumor efficacy of docetaxel in non-small-cell lung cancer. *Drug Design, Development and Therapy*, Volume 9, pp. 3899-3909.

Kroemer G, El-Deiry WS, Golstein P, Peter ME, Vaux D, Vandenabeele P, Zhivotovsky B, Blagosklonny MV, Malorni W, Knight RA, Piacentini M, Nagata S and Melino G, 2005. Classification of cell death: recommendations of the Nomenclature Committee on Cell Death. *Cell death and Differentiation*, Volume 12, pp. 1463-1467.

Ku JH, Seo SY, Kwak C and Kim HH, 2012. The role of survivin and Bcl-2 in zinc-induced apoptosis in prostate cancer cells. *Urologic Oncology: Seminars and Original Investigations*, Volume 30, pp. 562-568.

Kumar V, Abbas AK, Fausto N and Aster JC, 2010. Robins and Cotran: pathologic basis of disease. In: 8, ed. *Saunders Elsevier*. Philadelphia: s.n., pp. 25-32.

Labuschagne CF, Zani F and Vousden KH, 2018. Control of metabolism by p53 – Cancer and beyond. *BBA - Reviews on Cancer*, Volume 1870, pp. 32-42.

Lavrik I, Golks A and Krammer PH, 2005. Death receptor signaling. *Journal of Cell Science*, Volume 118, pp. 265-267.

Lee E-J, Oh S-Y and Sung M-K, 2012. Luteolin exerts anti-tumor activity through the suppression of epidermal growth factor receptor-mediated pathway in MDA-MB-231 ER-negative breast cancer cells. *Food and Chemical Toxicology*, Volume 50, pp. 4136-4143.

Lee M-Y, Kim M-A, Kim H-J, Bae Y-S, Kwak J-J, Chung JH and Yun J, 2007. Alkylation agent Methyl Methanesulfonate (MMS) induces a wave of global protein hyperacetylation: Implication in cancer cell death. *Biochemical and Biophysical Research Communications*, Volume 360, pp. 483-489.

Lehner B, Sandner B, Marschallinger J, Lehner C, Furtner T, Couillard-Despres S, Rivera, Francisco J, Brockhoff G, Bauer H-C, Weidner N and Aigner L, 2011. The dark side of BrdU in neural stem cell biology: Detrimental effects on cell cycle, differentiation and survival. *Cell and Tissue Research*, Volume 45, p. 313–328.

Levine AJ, Momand J and Finlay CA, 1991. The p53 tumour suppressor gene. *Nature*, Volume 351, pp. 453-456.

Limbach LK, Wick P, Manser P, Grass RN, Bruinink A and Stark WJ, 2007. Exposure of engineered nanoparticles to human lung epithelial cells: influence of chemical composition and catalytic activity on oxidative stress. *Environmental Science & Technology*, Volume 41, p. 4158–4163.

Liou GY and Storz P, 2010. Reactive oxygen species in cancer. *Free Radical Research*, Volume 44, pp. 479-496.

Maddila S, Momin M, Gorle S, Palakonda L and Jonnalagadda SB, 2015. Synthesis and antioxidant evaluation of novel phenothiazine linked substitutedbenzylideneamino-1,2,4-triazole derivatives. *Journal of the Chilean Chemical Society*, Volume 60, pp. 2919-2923.

Magdalena LC and Tak YA, 2010. Reactive oxygen species, cellular redox systems and apoptosis. *Free Radical Biology and Medicine*, Volume 48, p. 749–762.

Maheswari PU, Barends S, Ozalp-Yaman S, de Hoog P, Casellas H, Teat SJ, Massera C, Lutz M, Spek AL, van Wezel GP, Gamez P and Reedijk J, 2007. Unique ligand-

based oxidative DNA cleavage by zinc(II) complexes of hpyramol and hpyrimol. *Chemistry*, Volume 13, pp. 5213-5222.

Mallavadhani UV , Vanga NR , Jeengar MK and Naidu VG , 2014. Synthesis of novel ring-A fused hybrids of oleanolic acid with capabilities to arrest cell cycle and induce apoptosis in breast cancer cells.. *European Journal of Medicinal Chemistry* , Volume 74, pp. 398-404.

Mallavadhani UV, Vanga NR, Jeengar MK and Naidu VG , 2014. Synthesis of novel ring-A fused hybrids of oleanolic acid with capabilities to arrest cell cycle and induce apoptosis in breast cancer cells. *European Journal of Medicinal Chemistry* , Volume 74, pp. 398-404.

Malumbres M and Barbacid M, 2009. Cell cycle, CDKs and cancer: a changing paradigm. *Nature Review of Cancer*, Volume 9, pp. 153-156.

Mani KS, Murugesapandian B and Kaminsky W, 2018. Enantioselective approach towards the synthesis of spiro-indeno [1,2-b] quinoxaline pyrrolothiazoles as antioxidant and antiproliferative. *Tetrahedron Letters*, Volume 59, pp. 2921-2929.

Maywald M and Rink L, 2015. Zinc homeostasis and immunosenescence. *Journal of Trace Elements in Medicine and Biology*, Volume 29, pp. 24-30.

Minn AJ, Rudin CM, Boise LH and Thompson CB, 1995. Expression of Bcl-XL can confer a multidrug resistance phenotype. *Blood*, Volume 86, pp. 1903-1910.

Minn AJ, Vélez P, Schendel SL, Liang H, Muchmore SW, Fesik SW, Fill M and Thompson CB, 1995. Bcl-x(L) forms an ion channel in synthetic lipid membranes. *Nature*, Volume 385, pp. 353-357.

Miquel C, Borrini F, Grandjouan S, Aupérin A, Viguier J, Velasco V, Duvillard P, Praz F and Sabourin JC, 2005. Role of bax mutations in apoptosis in colorectal cancers with microsatellite instability. *American Journal of Clinical Pathology*, Volume 23, pp. 562-570.

Moding EJ, Kastan MB and Kirsch DG, 2013. Strategies for optimizing the response of cancer and normal tissues to radiation. *Nature Review for Drug Discovery*, Volume 12, p. 526–542.

Mohell N, Alfredsson J, Fransson Å, Uustalu M, Byström S, Gullbo J, Hallberg A, Bykov VJ, Björklund U and Wiman KG, 2015. APR-246 overcomes resistance to cisplatin and doxorubicin in ovarian cancer cells. *Cell Death & Disease*, Volume 18, p. e1794.

Moucheron C, 2009. From cisplatin to photoreactive Ru complexes: targeting DNA for biomedical applications. *New Journal of Chemistry*, Volume 33, pp. 235-245.

Murthi PR, Suresh N, Rani CS, Rao MVB and Pal M, 2015. Pd/C-catalyzed synthesis of (E)-arylmethylideneidolin-3-ol Under Ultrasound: Their initial evaluation as potential anti-proliferation agents. *Letters in Drug Design and Discovery*, Volume 12, pp. 109-116.

Nicco C, Laurent A, Chereau C, Weill B and Batteux F, 2005. Differential modulation of normal and tumor cell proliferation by reactive oxygen species. *Biomedicine & Pharmacotherapy*, Volume 59, pp. 196-174.

Noolvi MN, Patel HM, Bhardwaj V and Chauhan A, 2011. Synthesis and in vitro antitumor activity of substituted quinazoline and quinoxaline derivatives: Search for anticancer agent. *European Journal of Medicinal Chemistry*, Volume 46, pp. 2327-2346.

O'Brien MA and Kirby R, 2008. Apoptosis: a review of pro-apoptotic and anti-apoptotic. *Journal of Veterinary Emergency and Critical Care*, Volume 18, pp. 572-585.

Oktay T, Pornsak S and Crispin R, 2013 . Doxorubicin: an update on anticancer molecular action, toxicity and novel drug delivery systems. *Journal of Pharmacy and Pharmacology*, Volume 65, p. 157–170.

Ott I and Gust R, 2007. Non platinum metal complexes as anti-cancer drugs. *Archives Of Pharmacal Research*, Volume 340, pp. 117-126.

Pallepati P and Averill-Bates DA, 2011. Activation of ER stress and apoptosis by hydrogen peroxide in HeLa cells: protective role of mild heat preconditioning at 40°C. *Biochimica et Biophysica Acta*, Volume 1813, pp. 1987-1999.

Parkin DM, Bray F, Ferlay J and Jema A, 2014. Cancer in Africa. *American Associate for Cancer Research*, Volume 10, pp. 1055-1065.

Patidar AK, Jeyakandan M, Mobyia AK, Selvam G, 2011. Exploring potential of quinoxaline moiety. *International Journal of PharmTech Research*, Volume 3, pp. 386–392.

Pepper C, Hoy T and Bentley DP, 1997. Bcl-2/Bax ratios in chronic lymphocytic leukaemia and their correlation with in vitro apoptosis and clinical resistance. *British Journal of Cancer*, Volume 76, pp. 935-938.

Pereira JA, Pessoa AM, Cordeiro MNDS, Fernandes R, Pruden C, Noronha JP and Vieira M, 2015. Quinoxaline, its derivatives and applications: A State of the Art review. *European Journal of Medicinal Chemistry*, Volume 97, pp. 664-672.

Petersen I, 2011. The morphological and molecular diagnosis of lung cancer. *Deutsches Ärzteblatt International*, Volume 108, pp. 525-531.

Plumb JA, Milroy R and Kaye SB, 1989. Effects of the pH dependence of 3-(4,5-dimethylthiazol-2-yl)-2,5-diphenyl-tetrazolium bromide-formazan absorption on chemosensitivity determined by a novel tetrazolium-based assay. *Cancer research*, Volume 49, pp. 4435-4440.

Quintavalle M, Elia L, Price JH, Heynen-Genel S and Courtneidge SA, 2011. A cell based high-content screening assay reveals activators and inhibitors of cancer cell invasion. *Science Signaling*, p. ra49.

Raffo AJ, Perlman H, Chen MW, Day ML, Streitman JS and Buttyan R, 1995. Overexpression of bcl-2 protects prostate cancer cells from apoptosis in vitro and confers resistance to androgen depletion in vivo. *Cancer Research*, Volume 55, p. 4438.

Reesink-Peters N, Hougardy BM, van den Heuvel FA, Ten Hoor KA, Hollema H, Boezen HM, de Vries EG, de Jong S and van der Zee AG, 2005. Death receptors and ligands in cervical carcinogenesis: an immunohistochemical study. *Gynecological Oncology*, Volume 96, pp. 705-713.

Reinehr R, Becker S, Eberle A, Grether-Beck S and Häussinger D, 2005. Involvement of NADPH oxidase isoforms and Src family kinases in CD95-dependent hepatocyte apoptosis. *Journal of Biological Chemistry*, Volume 280, pp. 27179-27194.

Rhodes N, Heerding DA, Duckett DR, Eberwein DJ, Knick VB, Lansing TJ, McConnell RT, Gilmer TM, Zhang SY, Robell K, Kahana JA, Geske RS, Kleymenova EV, Choudhry AE, Lai Z, Leber JD, Minthorn EA, Strum SL, Wood ER, Huang PS, Copeland RA and Kumar R, 2008. Characterization of an Akt kinase inhibitor with potent pharmacodynamic and antitumor activity. *Cancer Research*, Volume 68, pp. 2366-2374.

Roy K, Wu Y, Meitzler JL, Juhasz A, Liu H, Jiang G, Lu J, Antony S and Doroshow JH, 2015. NADPH oxidases and cancer. *Clinical science*, Volume 128. pp. 863-875.

Sablina AA, Budanov AV, Ilyinskaya GV, Agapova LS, Kravchenko JE and Chumakov PM, 2005. The antioxidant function of the p53 tumor suppressor. *Nature Medicine*, Volume 11, pp. 1306-1313.

Saleh AM, Aljada A, El-Abadelah MM, Sabri SS., Zahra JA, Nasr A and Aziz M.A, 2015. The Pyridone-Annulated Isoindigo (5'-Cl) Induces Apoptosis, Dysregulation of Mitochondria and Formation of ROS in Leukemic HL-60 Cells. *Cellular Physiology and Biochemistry*, Volume 35, pp. 1958-1974.

Sankaran M, Chandraprakash K, Uvarani C and Mohan PS, 2010. Synthesis, antioxidant and toxicological study of novel pyrimido quinoline derivatives from 4-hydroxy-3-acyl quinolin-2-one. *Bioorganic and Medicinal Chemistry Letters*, Volume 20, pp. 7147-7151.

Saraste A and Pulkki K, 2000. Morphologic and biochemical hallmarks of apoptosis. *Cardiovascular Research*, Volume 45, pp. 528-537.

Sardon T, Cottin T, Xu J, Giannis A and Vernos I, 2009. Development and Biological evaluation of a novel Aurora A kinase inhibitor. *ChemBioChem*, Volume 10, pp. 464-478.

Sato T, Machida T, Takahashi S, Iyama S, Sato Y, Kuribayashi K, Takada K, Oku T, Kawano Y, Okamoto T, Takimoto R, Matsunaga T, Takayama T, Takahashi M, Kato and Niitsu Y, 2004. Fas-mediated apoptosome formation is dependent on reactive oxygen species derived from mitochondrial permeability transition in Jurkat cells. *The Journal of Immunology*, Volume 173, pp. 285-295.

Schiller JH, Harrington D, Belani CP, Langer C, Sandler A and Krook J, 2002. Comparison of chemotherapy regimens for advanced non-small cell lung cancer. *New England Journal of Medicine*, Volume 346, pp. 92-98.

Schneider P and Tschopp J, 2000. Apoptosis induced by death receptors. *Pharmaceutica Acta Helvetiae*, Volume 74, pp. 281-286.

Song Y, Leonard SW, Traber MG and Ho E, 2009. Zn deficiency affects DNA damage, oxidative stress, antioxidant defenses, and DNA repair in rats. *Journal of Nutrition*, Volume 139, pp. 1626-1631.

Srivastava S, Banerjee J and Srestha N, 2014. Quinoxaline as a potent heterocyclic moiety. *Journal Of Pharmacy*, Volume 4, pp. 17-27.

Tan J, Wang B and Zhu L, 2009. DNA binding, cytotoxicity, apoptotic inducing activity, and molecular modeling study of quercetin zinc (II) complex. *Bioorganic & Medicinal Chemistry*, Volume 17, pp. 614-620.

Tanga J-Y, Farooqi AA, Ou-Yangd F, Hou M-F, Huangg H-W , Wangg H-R, Lih K-T, Fayyazi S, Shu C-W and Chang H-W, 2018. Oxidative stress-modulating drugs have preferential anticancer effects -involving the regulation of apoptosis, DNA damage, endoplasmic reticulum stress, autophagy, metabolism, and migration. *Seminars in Cancer Biology*, pp. 1-9.

Tariq S, Somakala K and Amir M, 2018. Quinoxaline: An insight into the recent pharmacological advances. *European Journal of Medicinal Chemistry*, Volume 143, pp. 542-557.

Tarnowski BI, Spinale FG and Nicholson JH., 1991. DAPI as a useful stain for nuclear quantitation. *Biotechnic & Histochemistry*, pp. 297-302.

Tessoulin B, Descamps G, Moreau P, Maïga S, Lodé L, Godon C, Marionneau-Lambot S, Oullier T, Le Gouill S, Amiot M, Pellat-Deceunynck C, 2014. PRIMA-1Met induces myeloma cell death independent of p53 by impairing the GSH/ROS balance. *Blood*, Volume 124, pp. 1626-1636.

Tochigi M, Inoue T, Suzuki-Karasaki M, Ochiai T, Ra C andSuzuki-Karasaki Y, 2013. Hydrogen peroxide induces cell death in human TRAIL-resistant melanoma through

intracellular superoxide generation. *International Journal of Oncology*, Volume 42, pp. 863-872.

Trachootham D, Alexandre J and Huang P, 2009. Targeting cancer cells by ROS-mediated mechanisms: a radical therapeutic approach?. *Nature Reviews Drug Discovery*, Volume 8, pp. 579-591.

Tseng CH, Chen YR, Tzeng CC, Liu W, Chou CK, Chiu CC and Chen YL, 2016. Discovery of indeno[1,2-b]quinoxaline derivatives as potential anticancer agents. *European Journal of Medicinal Chemistry*, Volume 108, pp. 258-273.

Tu HY, Huang AM, Teng CH, Hour TC, Yang SC, Pu YS and Lin CN, 2011. Anthraquinone derivatives induce G2/M cell cycle arrest and apoptosis in NTUB1 cells. *Chemico-Biological Interactions*, Volume 19, pp. 5670-5678.

Varley JM, 2003. Germline TP53 mutations and Li-Fraumeni syndrome. *Human Mutation*, Volume 21, pp. 313-320.

Vaux D and Silke J, 2003. Mammalian mitochondrial IAP-binding proteins. *Biochemical and Biophysical Research Communication*, Volume 203, pp. 449-504.

Velagapudi S, Costales M, Vummidi B, Nakai Y, Angelbello A, Tran T, Haniff H, Matsumoto Y, Wang Z, Chatterjee A, Childs-Disney J and Disney M, 2018. Approved Anti-cancer Drugs Target Oncogenic Non-coding RNAs. *Cell Chemical Biology*, Volume 25, pp.1086-1094.

Vijaya K, Sowmyaa pR-R, Arathia BP, Shilpaa S, Shwethaa HJ, Rajub M, Baskaranc V and Lakshminarayana R, 2018. Low-dose doxorubicin with carotenoids selectively alters redox status and upregulates oxidative stress-mediated apoptosis in breast cancer cells. *Food and Chemical Toxicology*, Volume 118, pp. 675-690.

Walton EL, 2016. The dual role of ROS, antioxidants and autophagy in cancer. *Biomedical Journal*, Volume 39, pp. 89-92.

Wang R, Ye F, Zhen Q, Song T, Tan G, Chu W, Zhang Y, Lv B, Zhao X and Liu J, 2016. MicroRNA-148b is a potential prognostic biomarker and predictor of response to radiotherapy in non-small-cell lung cancer. *Journal of Physiology and Biochemistry*, Volume 72, pp. 337-343.

Wang X, 2001. The expanding role of mitochondria in apoptosis. *Genes and Development*, pp. 2922-2033`15.

Waris G and Ahsan H , 2006. Reactive oxygen species: role in the development of cancer and various chronic conditions. *Journal of Carcinogenesis*, Volume 5, pp. 14-14.

Wei BL, Wu SH, Chung MI, Won SJ and Lin CN, 2000. Synthesis and cytotoxic effect of 1,3-dihydroxy-9,10-anthraquinone derivatives,. *European Journal of Medicinal Chemistry*, Volume 35, pp. 1089-1098.

Weili L, Wenzhe W and Mingjian D, 2016. Mir-1244 sensitizes the resistance of non-small cell lung cancer a549 cell to cisplatin. *Cancer Cell International*, Volume 16, pp. 1-7.

WHO, 2016. *World Health Organization*. [Online] Available at: <http://www.who.int/cancer/en/> [Accessed 24 November 2018].

Wistuba II, Brambilla E and Noguchi M, 2018. Classic Anatomic Pathology and Lung Cancer. *IASLC Thoracic Oncology*, Volume 4, pp. 143-163.

Wohlbold L and Fisher RP, 2009. Behind the wheel and under the hood: functions of cyclin- dependent kinases in response to DNA damage. *DNA. DNA Repair (Amst)*, Volume 8, pp. 1018-1024.

World Health Organization, 2008. *The Global: Burden of Disease: 2004 Update*. Geneva: World Health Organization.

Wu H and Zhang J, 2018. Chitosan-based zinc oxide nanoparticle for enhanced anticancer effect in cervical cancer: A physicochemical and biological perspective. *Saudi Pharmaceutical Journal*, Volume 26, p. 205–210.

Yen CY, Hou MF, Yang ZW, Tang JY, Li KT, Huang HW, Huang YH, Lee SY, Fu TF, Hsieh CY, Chen BH and Chang HW, 2015. Concentration effects of grape seed extracts in anti-oral cancer cells involving differential apoptosis, oxidative stress, and DNA damage. *MC Complementary and Alternative Medicine*, Volume 15, p. 94.

Yoshihiro S-K, Miki S-K, Mayumi Uand Toyoko O, 2014. Depolarization Controls TRAIL-Sensitization and Tumor-Selective Killing of Cancer Cells: Crosstalk with ROS. *Frontiers in Oncology*, Volume 4, pp. 1-14.

Zhang HY , 2005. Structure-activity relationships and rational design strategies for radical-scavenging antioxidants. *Current Computer-Aided Drug Design*, Volume 1, p. 257–273.